Studies on the role of platelet serotonin in platelet function, hemostasis, thrombosis and stroke

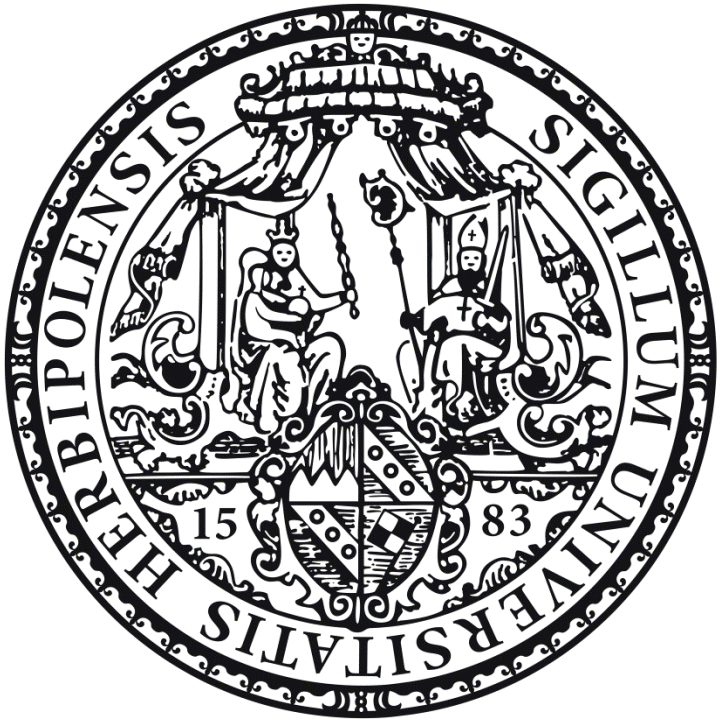

Studien zur Rolle des Serotonins aus Thrombozyten für die Thrombozytenfunktion, Hämostase, Thrombose und Schlaganfall

Doctoral thesis for a doctoral degree
at the Graduate School of Life Sciences,
Bayerische Julius-Maximilians-Universität Würzburg,
Section Biomedicine

Submitted by
Karen Wolf
from Bad Kissingen

Würzburg 2016

Submitted on :_____

Office stamp

Members of the *Promotionskomitee*:

Chairperson:	Prof. Dr. Thomas Dandekar
Primary Supervisor:	Prof. Dr. Bernhard Nieswandt
Supervisor (Second):	Prof. Dr. Christoph Kleinschnitz
Supervisor (Third):	Prof. Dr. Alma Zernecke-Madsen

Date of Public Defense: _____

Date of Receipt of Certificates: _____

Table of contents

Summary

Platelet activation and aggregation are important processes in hemostasis resulting in reduction of blood loss upon vessel wall injury. However, platelet activation can lead to thrombotic events causing myocardial infarction and stroke. A more detailed understanding of the regulation of platelet activation and the subsequent formation of thrombi is essential to prevent thrombosis and ischemic stroke. Cations, platelet surface receptors, cytoskeletal rearrangements, activation of the coagulation cascade and intracellular signaling molecules are important in platelet activation and thrombus formation. One such important molecule is serotonin (5-hydroxytryptamin, 5-HT), an indolamine platelet agonist, biochemically derived from tryptophan. 5-HT is secreted from the enterochromaffin cells into the gastrointestinal tract (GI) and blood. Blood-borne 5-HT has been proposed to regulate hemostasis by acting as a vasoconstrictor and by triggering platelet signaling through 5-HT_{2A} receptor. Although platelets do not synthetize 5-HT, they take it up from the blood and store it in their dense granules which are secreted upon platelet activation. To identify the molecular composite of the 5-HT uptake system in platelets and elucidate the role of platelet released 5-HT in thrombosis and ischemic stroke, 5-HT transporter knock-out mice (*5Htt*$^{-/-}$) were analyzed in different *in vitro* and *in vivo* assays and in a model of ischemic stroke. In *5Htt*$^{-/-}$ platelets, 5-HT uptake from the blood was completely abolished and agonist-induced Ca^{2+} influx through store operated Ca^{2+} entry (SOCE), integrin activation, degranulation and aggregation responses to glycoprotein (GP) VI and C-type lectin-like receptor 2 (CLEC-2) were reduced. These observed *in vitro* defects in *5Htt*$^{-/-}$ platelets could be normalized by the addition of exogenous 5-HT. Moreover, reduced 5-HT levels in the plasma, an increased bleeding time and the formation of unstable thrombi were observed *ex vivo* under flow and *in vivo* in the abdominal aorta and carotid artery of *5Htt*$^{-/-}$ mice. Surprisingly, in the transient middle cerebral artery occlusion model (tMCAO) of ischemic stroke *5Htt*$^{-/-}$ mice showed nearly normal infarct volumes and a neurological outcome comparable to control mice. Although secreted platelet 5-HT does not appear to play a crucial role in the development of reperfusion injury after stroke, it is essential to amplify the second phase of platelet activation through SOCE and thus plays an important role in thrombus stabilization.

To further investigate the role of cations, granules and their contents and regulation of integrin activation in the process of thrombus formation, genetically modified mice were analyzed in the different *in vivo* thrombosis models. Whereas *Tph1*$^{-/-}$ mice (lacking the

enzyme responsible for the production of 5-HT in the periphery), *Trpm7^{KI}* (point mutation in the kinase domain of Trpm7 channel, lacking kinase activity) and *Unc13d$^{-/-}$/Nbeal2$^{-/-}$* mice (lacking α-granules and the release machinery of dense granules) showed a delayed thrombus formation *in vivo*, *MagT1$^{y/-}$* mice (lacking a specific Mg^{2+} transporter) displayed a pro-thrombotic phenotype *in vivo. Trpm7$^{fl/fl\text{-}Pf4Cre}$* (lacking the non-specific Mg^{2+} channel) and *RIAM$^{-/-}$* mice (lacking a potential linker protein in integrin “inside-out” signaling) showed no alterations in thrombus formation upon injury of the vessel wall.

Zusammenfassung

Thrombozytenaktivierung und Aggregation sind wichtige Schritte der Hämostase, die zur Reduktion des Blutverlustes bei Gefäßwandverletzung führen. Jedoch kann die Aktivierung von Thrombozyten zur Thrombose führen, wodurch Herzinfarkt und Schlaganfall entstehen kann. Ein besseres Verständnis der Regulierung der Thrombozytenaktivierung und die darauf folgende Thrombusbildung sind notwendig, um Thrombose und Hirninfarkte zu vermeiden. Kationen, Thrombozyten-Oberflächenrezeptoren, Zytoskelett-Reorganisation, Aktivierung der Koagulationskaskade und intrazellulare Signalmoleküle sind wichtig in der Thrombozytenaktivierung und Thrombusbildung. Solch ein wichtiges Molekül ist Serotonin (5-hydroxytryptamin, 5-HT), ein Indolamin-Thrombozyten-Agonist, welcher aus Tryptophan synthetisiert wird. 5-HT wird aus den Enterochromaffinzellen in den Gastrointestinaltrakt (GI) und das Blut abgegeben. 5-HT aus dem Blut wirkt als Regulator der Hämostase durch die Wirkung als Vasokonstriktor und die Auslösung der Thrombozyten-Signalwege durch den 5-HT_{2A} Rezeptor. Thrombozyten synthetisieren kein 5-HT, sondern nehmen es aus dem Blut auf und speichern es in den dichten Granula, die nach der Thrombozyten-Aktivierung freigesetzt werden. Um die molekulare Zusammensetzung des 5-HT Aufnahmesystems in Thrombozyten zu identifizieren und die Rolle des 5-HT aus Thrombozyten in Thrombose und ischämischem Schlaganfalls zu klären, wurde eine 5-HT Transporter-defiziente Mauslinie (*5Htt*$^{-/-}$) in verschiedenen *in vitro* und *in vivo* Untersuchungen und im Model des ischämischen Schlaganfalls analysiert. In *5Htt*$^{-/-}$ Thrombozyten ist die Aufnahme von 5-HT aus dem Blut vollständig geblockt und Agonisten-induzierter Ca^{2+} Fluss durch Speicher-abhängigen Ca^{2+} Einstrom (SOCE), Integrinaktivierung, Degranulierung und Aggregation abhängig von Glykoprotein (GP) VI und *C-type lectin-like receptor 2* (CLEC-2) waren reduziert. Diese *in vitro* beobachteten Defekte in *5Htt*$^{-/-}$ Thrombozyten konnten durch Zugabe von 5-HT normalisiert werden. Zudem wurden reduzierte 5-HT Werte im Plasma, eine erhöhte Blutungszeit und die Bildung von instabilen Thromben *ex vivo* unter Fluss und *in vivo* in der abdominalen Aorta und der Carotis von *5Htt*$^{-/-}$ Mäusen beobachtet. Überraschenderweise zeigten die *5Htt*$^{-/-}$ Mäuse nach transientem Verschluss der A. cerebri media (tMCAO), einem Modell des ischämischen Schlaganfalls, ein normales Infarktvolumen und einen unveränderten neurologischen Endzustand im Vergleich zu Kontrollmäusen. Obwohl sekretiertes 5-HT aus Thrombozyten keine wesentliche Rolle in der Entwicklung eines Reperfusionsschadens nach einem Schlaganfall spielt, ist es essentiell in der Verstärkung

der zweiten Phase der Thrombozytenaktivierung durch SOCE und spielt eine wichtige Rolle in der Thrombusstabilität.

Um die Rolle von Kationen, Granula und deren Bestandteile und der Regulierung in der Integrinaktivierung im Prozess der Thrombusbildung zu untersuchen, wurden genetisch veränderte Mäuse in den verschiedenen *in vivo* Thrombosemodellen getestet. Während *Tph1*$^{-/-}$ Mäuse (denen das Enzym zur Produktion von 5-HT in der Peripherie fehlt), *Trpm7*^{KI} (Punktmutation in der Kinasedomäne des Trpm7 Kanals, Fehlen der Kinase Aktivität) und *Unc13d*$^{-/-}$*/Nbeal2*$^{-/-}$ Mäuse (denen die α-Granula und die Freisetzungsmaschinerie der dichten Granula fehlt) und keine oder eine verlangsamte Thrombusbildung zeigten, wiesen *MagT1*$^{y/-}$ Mäuse (denen der spezifische Mg^{2+}-Transporter fehlt) einen prothrombotischen Phänotyp auf. *Trpm7*$^{fl/fl\text{-}Pf4Cre}$ Mäuse (denen der nicht spezifische Mg^{2+} Kanal fehlt) und *RIAM*$^{-/-}$ Mäuse (denen ein potentielles Linker Protein im Integrin "*inside-out*" Signal fehlt) zeigten keine Veränderung in der Thrombus Bildung nach Verletzung der Gefäßwand.

1. Introduction

1.1. Platelet production

Platelets are small, discoid anucleate cells with a size of 3-4 µm in humans and 1-2 µm in mice. In healthy humans, the number of platelets ranges between 150,000-450,000 platelets per µL, whereas the platelet count in mice is approximately 1,000,000 platelets per µL blood.[1,2] The lifespan of platelets is restricted to 10 days in humans and to about 5 days in mice,[3] with most circulating platelets never becoming activated. Aged, dysfunctional or pre-activated platelets are cleared in the liver and spleen by phagocytosis.[4] Platelets are produced by their polyploid precursor cells, the megakaryocytes (MKs), in the bone marrow (BM). The exact mechanism of platelet formation from MKs is still not fully understood. According to the current model, mature MKs reside in the vicinity of sinusoidal vessels into which they form and release proplatelets into the circulation where final platelet formation takes place.[5-7]

Due to the lack of a nucleus, platelet protein synthesis is limited. Nevertheless, platelets contain MK-derived messenger RNA (mRNA) and the translational machinery for *de novo* protein synthesis.[8] Furthermore, platelets enclose numerous cell organelles like granules and structures such as the bilamellar plasma membrane (PM) with several channels of the open canalicular system (OCS). This OCS is a source from which the surface area of the membrane can be increased upon platelet activation and shape change from a discoid (Figure 1A) to a spherical (Figure 1B) morphology.[9] In addition platelets contain a dense tubular system (DTS) originated from the endoplasmatic reticulum (ER) of MKs, glycogen stores, mitochondria and three types of granules (α-granules, dense granules and lysosomes), see Figure 1C.

Circulating platelets survey vascular integrity, thus playing a major role in hemostasis. Upon injury, platelets can adhere to exposed subendothelial extracellular matrix (ECM), leading to their activation, the release of secondary mediators and local production of thrombin, resulting in recruitment and activation of further platelets and the formation of a hemostatic plug. This process is important to seal vascular injuries, to minimize blood loss and to prevent infections. On the other hand, uncontrolled platelet activation in diseased vessels can lead to thrombotic vessel occlusion. Myocardial infarction (MI) and stroke, triggered by thrombus embolization are severe diseases and the major cause of death and morbidity worldwide.[10] Therefore, understanding of the regulation of platelet activation via inhibitory and activatory mechanisms is essential to

design improved therapeutic approaches for the prevention of uncontrolled platelet activation.

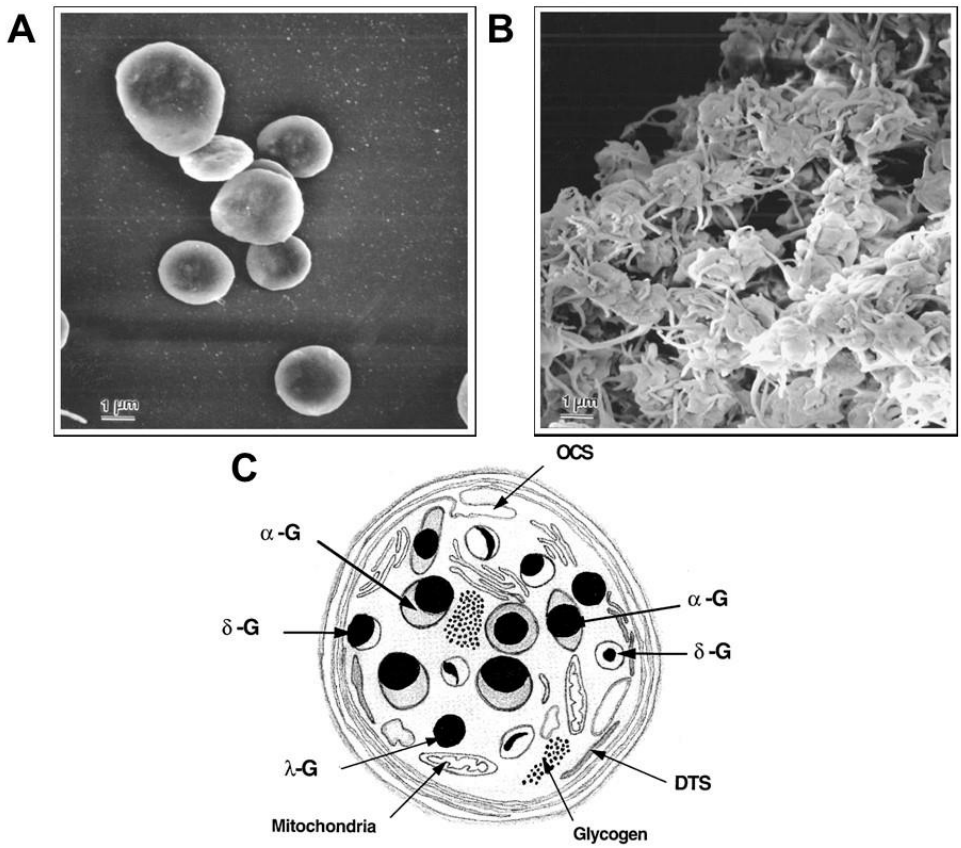

Figure 1: Platelet shape and content. (A) Platelet morphology in resting conditions and (B) upon platelet activation. (C) Schematic picture of a platelet containing open canalicular system (OCS) and dense tubular system (DTS), mitochondria and the three major granule types. The α-granules (α-G), dense granules (δ-G) and lysosomes (λ-G). (Images A+B kindly provided by Christian Gachet, image C is taken from: Rendu and Brohard-Bohn, Platelets 2001)[11]

1.2. Platelet granules

There are three major granules found in platelets, α-granules, dense granules and lysosomes (Figure 1C).[12]

The α-granules contain around 300 distinct molecules, like adhesion molecules and coagulation factors, such as von Willebrand factor (vWF), fibronectin, thrombospondin-1, fibrinogen, plasminogen, coagulation factors (factor V, VII, XI and XII) as well as plasma proteins, angiogenic factors, anti-angiogenic factors, growth factors, proteases, necrotic factors (e.g. TNFs) and other cytokines.[12] Several adhesion molecules like GPIIb/IIIa and P-selectin are known to be prominent on the α-granule membrane. The α-granules originate from precursor granules in the trans-Golgi apparatus of MKs. The contents of these granules are important at sites of vessel wall injury, playing a

significant role in hemostasis, inflammation, antimicrobial host defense, wound healing, angiogenesis, malignancy and atherosclerosis.[13,14]

Dense granules contain small inorganic molecules like 5-HT, adenosine di-or triphosphate (ADP, ATP) and polyphosphates. Most of the molecules are derived from MKs and packaged into granules destined for future platelets during biosynthesis. It is hypothesized that some proteins, such as fibrinogen and factor V are endocytosed from the blood stream by MKs and platelets and then transported to the granules.[12,13]

Lysosomes store glycohydrolases which are needed for degradation of glycoproteins, glycolipids and glycosaminoglycans. In addition, they contain cathepsin (cathepsin D and E) and lysosomal membrane proteins. The release of lysosomal enzymes plays an important role in the final step of granule secretion and platelet activation in a forming clot and is hypothesized to contribute to remodeling the site of damage.[15,16]

1.3. Platelet activation and thrombus formation

Platelet activation and thrombus formation requires ligand-receptor binding, the activation of signaling and the release of granule contents at sites of vascular injury. Platelet activation can be divided into three major steps: the tethering and adhesion of platelets, platelet activation and finally platelet aggregation and thrombus growth (Figure 2).[17]

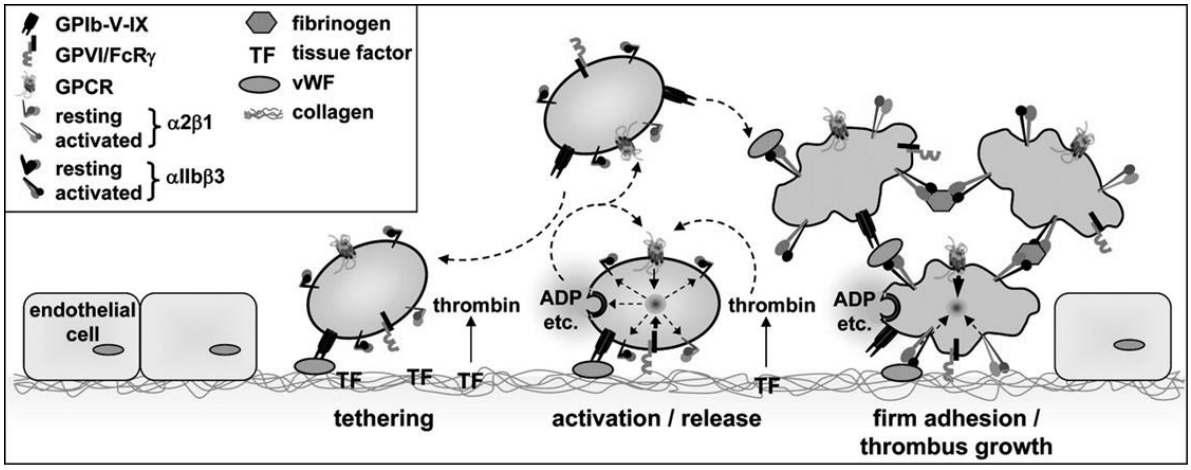

Figure 2: Platelet adhesion and activation at sites of vascular injury leading to stable thrombus formation. Platelet tethering on the injured vessel wall is mediated via GPIb-vWF interactions, enabling platelets to stay in close contact with the ECM. This interaction allows the binding of collagen in the ECM by its receptor on platelets, GPVI, triggering intracellular signaling and, resulting in Ca^{2+}-mobilization, phosphatidylserine (PS) exposure, cytoskeletal rearrangement, mobilization of α-and dense granules, the release of "second wave" mediators and the "inside-out" activation of integrins. All these processes together lead to the recruitment of further platelets into the growing thrombus. (Image is taken from: Vargo-Szabo *et al.*, ATVB 2008.)[17]

Another major regulator of thrombus formation are the prevailing rheological conditions in the vessel at the site of an injury.

1.4. Vessel wall and fluidity in thrombus formation

The prevailing blood flow conditions in the vessel are an important determinant of platelet tethering in the process of thrombus formation. Blood flow is variable in blood vessels depending on the location within the vessel lumen, due to the shearing effects of adjacent fluid layers and their distance to each other. The highest blood flow is found in the center of the vessel.[18] The shear rate depends on the vessel size and can range from 500 s^{-1} to 10,000 s^{-1} in venules or arterioles, whereas in stenosed vessels a shear rate of >20,000 s^{-1} can be reached.[18-21] There are different adhesion mechanisms known in platelets, operating at different shear rates.

At shear rates around 10,000 s^{-1}, platelets can adhere via GPIbα to collagen-bound, immobilized vWF on the ECM without the activation of αIIbβ3, which has been shown to be sufficient to trigger thrombus formation under these conditions.[22] In veins and large arteries with low shear rates <500 s^{-1}, the interaction between the GPIb complex and vWF plays a minor role.[23]

At shear rates of >1,000 s^{-1}, as found in small arteries, arterioles and stenosed arteries, the initial tethering starts with platelets adhering to the ECM via interactions between the receptor complex GPIb-V-IX and collagen-bound vWF.[21-25]

These interactions are transient and do not mediate firm adhesion, but maintain the close contact between platelets and the surface of the ruptured vessel wall, containing different molecules like laminin, fibronectin and collagen. “Rolling” of circulating platelets enables the interaction of the immunoglobulin-like receptor GPVI and the thrombogenic ECM protein collagen as the second phase of thrombus formation. The major collagen receptor GPVI binds collagen with a low affinity, which is sufficient to induce intracellular signaling, resulting in integrin activation. In addition, platelet activation leads to a rise of cytosolic Ca^{2+} concentration, cytoskeletal rearrangements, mobilization of α- and dense granules, the release of “second wave” mediators, like ADP, ATP and 5-HT [26-28] and thromboxane A_2 (TxA_2) and the exposure of negatively charged procoagulant phosphatidylserine (PS) on the platelet surface. At the same time, exposed tissue factor (TF) triggers local thrombin generation. Thrombin and the released agonists can act in an autocrine and paracrine way on G protein-coupled receptors (GPCR; G_q, $G_{12/13}$, G_i), inducing signaling cascades downstream of the receptors, full

platelet activation and recruitment of additional circulating platelets. The “final common pathway” of platelet activation, is the conformational change of integrins, most notably αIIbβ3, from a low-affinity to their high-affinity, active state.[29] This “inside-out” activation results in firm platelet adhesion, aggregation and thrombus growth.[17] Besides the major αIIbβ3 integrin (ligand: fibrinogen), platelets express other integrins, namely αvβ3 (ligand: vitronectin), α2β1 (ligand: collagen), α5β1 (ligand: fibronectin) and α6β1 (ligand: laminin).[30] The binding between integrin αIIbβ3 and fibrinogen leads to the bridging of activated platelets and thus the formation and stabilization of the thrombus. Additionally, integrin αIIbβ3 is important in the formation of stable platelet aggregates by binding to several ligands other than fibrinogen, such as vWF, fibronectin, thrombospondin and vitronectin.[29] Upon ligand binding, integrins undergo “outside-in” signaling. The binding triggers a clustering of the integrin, leading to increased ligand affinity and the activation of downstream signals resulting in granule secretion. The secretion of the granule contents induces platelet spreading and leads to the retraction of the blood clot, a process which is important in facilitating wound healing by bringing wound edges into closer proximity.[31,32]

1.5. Signaling pathways in platelet activation

Platelet activation can occur through two principal pathways depending on the inducing stimulus. The first is initiated by ligand binding to the (hem)Immunoreceptor tyrosine-based activation motif (ITAM)-bearing receptors, like GPVI and CLEC-2. The second is initiated by soluble agonists such as ADP, thrombin, TxA_2 and 5-HT which trigger platelet activation via different GPCRs and by “inside-out” and “outside-in” signaling of the different integrins, expressed on the surface of platelets (Figure 3).[30,31,33]

1.5.1. (hem)ITAM signaling during platelet activation

The ITAM consists of two tyrosine residues with the highly conserved consensus sequence Yxx(L/I) separated by 6-12 other amino acids. This motif can be found in several cells of the immune system including Fc-receptors (FcR) and T and B cell receptors (TCR, BCR). Upon ligand binding the receptor is clustered and phosphorylation of the ITAM tyrosine occurs, leading to a signaling cascade involving several kinases, adapter proteins and effector molecules. There are only two (hem)ITAM-bearing receptors expressed in mouse platelets, GPVI and CLEC-2, whereas human platelets express one further receptor: the FcγRIIA.[34] In CLEC-2 only “the half” of this sequence is present, which is why the signaling motif in the cytoplasmic tail of the receptor is

referred to as the (hem)ITAM. The endogenous CLEC-2 ligand podoplanin is not known to be expressed in the vasculature and thus other hypothesized vascular ligands for CLEC-2 remain to be identified. The activation of the (hem)ITAM signaling pathway leads to the activation of phospholipase C (PLC)γ2 resulting in the cleavage of phosphatidyl-inositol-4,5-bisphospate (PIP_2) to diacylglycerol (DAG), which further activates protein kinase C (PKC) and promotes inositol-3,4,5-trisphosphate (IP_3) production.

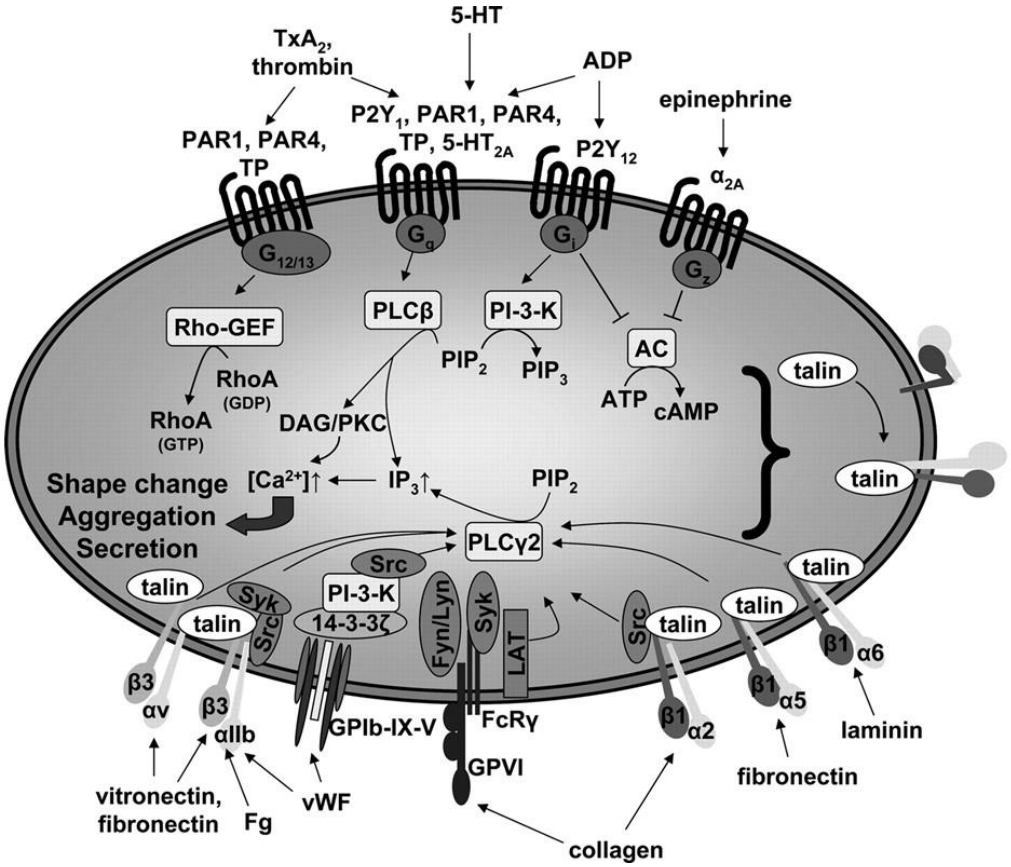

Figure 3: Major platelet signaling pathways. Thrombin, epinephrine and "second wave" mediators, like ADP, TxA_2, and 5-HT can couple heterotrimeric G proteins (G_q, $G_{12/13}$, G_i), leading to the activation of downstream signaling. Ligand binding to receptors like GPVI and CLEC-2 lead to the activation of PLCγ2. Both pathways culminate in integrin activation, Ca^{2+} mobilization, platelet shape change, aggregation and secretion. PI_3K, phosphatidylinositol-3-kinase; PIP_2, phosphatidylinositol-4,5-bisphosphate; PIP_3, phosphatidylinositol-3,4,5-trisphosphate; IP3, inositol-3,4,5-trisphosphate; AC, adenylate cyclase; DAG, diacylglycerol; PLC, phospholipase C; CLEC-2: C-type lectin like receptor 2; PAR, protease-activated receptor; ADP, adenosine diphosphate; GDP, guanosine diphosphate; GTP, guanosine triphosphate; GEF, guanine nucleotide exchange factor; RhoA, Ras homolog gene family member A; Fg, fibrinogen; TF, tissue factor; TxA_2 , thromboxane A_2 ; vWF, von Willebrand factor; LAT, linker for activation of T cells; Syk, spleen tyrosine kinase; SFK, Src family kinase. (Image taken from: Stegner and Nieswandt, J Mol Med 2011)[24]

Activation of these signaling molecules leads to the mobilization of Ca^{2+} from intracellular stores and then Ca^{2+} entry through channels in the PM, a process called SOCE.

The whole (hem)ITAM signaling pathway culminates in integrin activation, platelet shape change, aggregation and secretion (Figure 3, Figure 4).

1.5.2. GPVI/FcRγ-chain complex and ITAM-signaling

The major platelet collagen binding receptor is GPVI, a 62-kDa type I transmembrane receptor of the Immunoglobulin (Ig) superfamily non-covalently associated with the ITAM-bearing FcRγ-chain. This receptor is exclusively expressed on MKs and platelets. Ligand binding induces phosphorylation of the ITAM via Src family tyrosine kinases (SFK), followed by the recruitment and activation of spleen tyrosine kinase (Syk), thus initiating the assembly of the linker for activation of T cells (LAT) signalosome. This further leads to the activation of effector proteins, like PLCγ2, phosphatidylinositol-3,4,5-trisphosphate (PI_3K) and small GTPase, resulting in Ca^{2+} mobilization, integrin activation, degranulation and platelet aggregation (Figure 3, Figure 4).

1.5.3. Platelet activation through GPCRs

Many different ligands including amines, lipids, peptides, ions, nucleotides or proteases can amplify further platelet activation via GPCRs (seven-transmembrane containing receptors coupled to G-proteins: G_q, $G_{12/13}$, G_i).[35] GPCRs play a major role in the second phase of thrombus formation, as their signaling pathways can act as a part of a positive-feedback loop, amplifying platelet activation and recruiting more platelets to a growing thrombus. The binding of ligands released from platelet granules, damaged endothelial cells or the binding of mediators produced after cell activation induces the activation of the G protein signaling pathways which culminate in the activation of PLCβ (via G_q coupled receptors), the activation of the PI_3K/Akt signaling (via G_i coupled receptors) and the stimulation of Rho-GTPases (via $G_{12/13}$ coupled receptors) (Figure 3). Examples of such ligands are ADP/ATP and 5-HT released from dense granules, interacting with the receptors $P2Y_1$/$P2Y_{12}$ and $5\text{-}HT_{2A}$ respectively. TxA_2, which is produced by the metabolism of arachidonic acid (AA) by cyclooxygenase and thromboxane synthase enzymes, is released upon platelet activation, binds to thromboxane-prostanoid receptors (TP) α and β to promote plug formation.[24,35] The major platelet agonist thrombin is an important protease for the stability of the platelet-rich plug by cleavage of plasma fibrinogen into fibrin. Upon activation of the coagulation cascade via the intrinsic and the extrinsic pathway, prothrombin is cleaved to thrombin.[24,35]

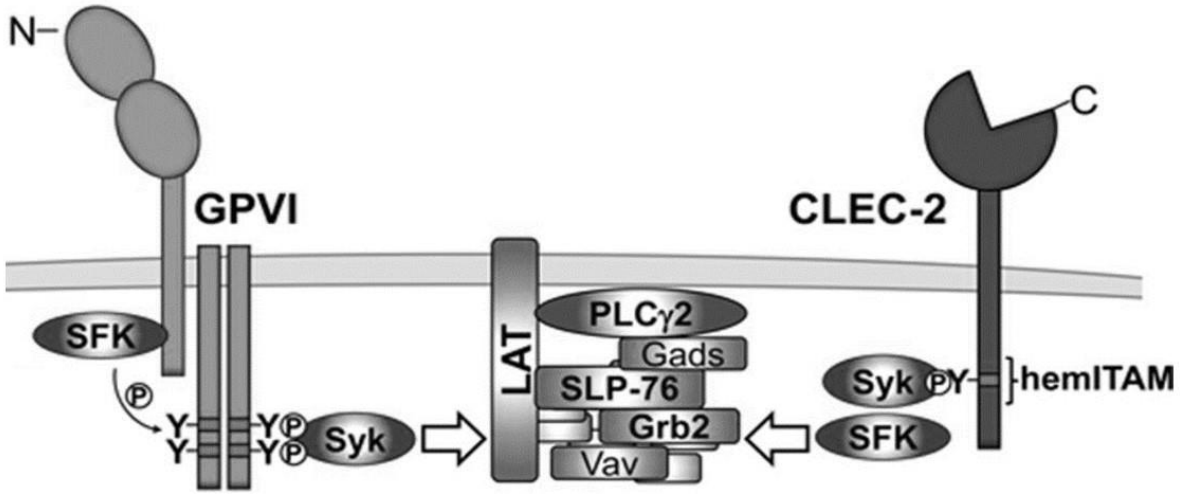

Figure 4: GPVI and CLEC-2 signaling in platelets. Ligand binding (GPVI: collagen, CLEC-2: unknown in vasculature) induces phosphorylation of the ITAM, which leads to the activation of a powerful downstream signaling cascade. Src family tyrosine kinase (SFK); spleen tyrosine kinase (Syk); linker for activation of T cells (LAT); phospholipase (PL) Cγ2; SH2 domain-containing leukocyte protein of 76 kDa (SLP-76); growth factor receptor-bound protein 2 (Grb2); Grb2-related adapter protein 2 (Gads); Vav proteins. (Image taken from Stegner *et al.,* ATVB 2014)[36]

1.6. Serotonin (5-HT), an important indolamine in the brain and platelets

Serotonin (5-hydroxytrytamine, 5-HT; MW 176.2) is a small indolamine which is best known as a monoamine neurotransmitter in the brain. 5-HT was first described in the early 1930's by Dr. Vittorio Erspamer in enterochromaffin cells of the gut from which Dr. Erspamer isolated 5-HT and noted it caused contraction in smooth muscle cells in rat uterus.[37] This contraction causing substance was first named enteramine and later re-named to 5-HT.[38] Only 5 % of 5-HT is synthesized in the brain (in the Raphe nuclei), whereas 95 % is produced by the enterochromaffin cells of the GI, mast cells and monocytes/macrophages.[39] 5-HT is synthesized (Figure 5) from the essential amino acid L-tryptophan (TRP) to 5-hydroxytryptophan (5-HTP) by the enzyme L-tryptophan hydroxylase (TPH) 1 in the brain and TPH2 in the periphery. The activity of these TPH enzymes is the rate limiting step in the production of 5-HT. Whilst its chemical precursors can pass across the blood-brain-barrier, 5-HT cannot, thereby effectively isolating the brain from pool of 5-HT generated in the periphery. 5-HT is metabolized in cells, such as neurons by two different monoamine oxidases (MAO) A and B, the products of this breakdown are then excreted by the kidney. 5-HT itself can also be metabolized via a different mechanism to melatonin as depicted in Figure 5.[40-42]

5-HT is involved in diverse biological processes. In the brain it regulates several complex behavioral networks, which control (for example) mood, perception, reward, anger, aggression, appetite, memory, sexuality and attention. In the periphery (where most 5-HT is produced), 5-HT regulates heart development, heart rate, valvulopathy, pain, nociception, early embryonic development, local vasoconstriction or vasodilation, vascular resistance, blood pressure, hemostasis, platelet function and many processes more.[43,44]

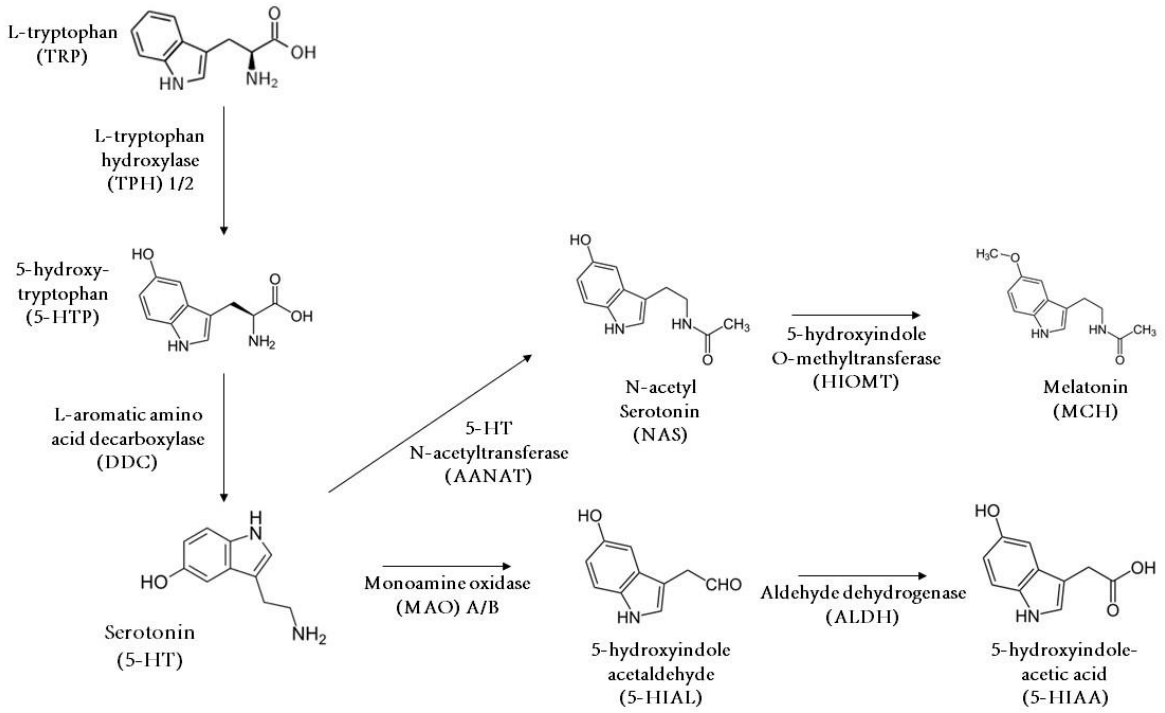

Figure 5: 5-HT biosynthesis and degradation. 5-HT is synthesized from tryptophan through hydroxylation by tryptophan hydroxylase 1 or 2, depending on the site of synthesis, to 5-hydrosytryptophan. The product is decarboxylated by L-aromatic amino acid decarboxylase to 5-HT. 5-HT itself can be deaminated by monoamine oxidase A or B to 5-hydroxyindole acetaldehyde and then dehydrogenised via the aldehyde dehydrogenase to 5-hydroxyindole-acetic acid, which can be secreted by the kidney. 5-HT is also the precursor for melatonin. 5-HT N-acetyltransferase synthesizes N-acetyl 5-HT via the 5-hydroxyindole O-methyltransferase to produce melatonin. (Modified from Berumen *et al*., Scientific World J. 2012 and Hickman *et al.,* Mol Cell 1999)[41,45]

As it is involved in the regulation of so many important functions, alterations in 5-HT concentration in the body are associated with many different diseases. These are as diverse as the functions of 5-HT and include irritable bowel syndrome, restless legs syndrome, sudden infant death syndrome, autism, headache, insomnia, anxiety, depression, anorexia, schizophrenia, Parkinson's and Alzheimer's disease, pulmonary hypertension and MI.[43,46,47]

After its synthesis in enterochromaffin cells of the GI, 5-HT is released into the blood-stream. 5-HT can then bind to its different receptors expressed throughout the body (Figure 6). There are 17 serotonin receptors, belonging to 7 different receptor subfamilies: 5-HT_1 (A-F, P, S), 5-HT_2 (A-D), 5-HT_3, 5-HT_4, 5-HT_5, 5-HT_6 and 5-HT_7.[48] All receptors belong to the GPCR superfamily with the exception of 5-HT_3, which belongs to the nicotinic acetylcholine receptor superfamily and is a ligand-gated ion channel.[41] In addition to binding its cognate receptors 5-HT can also be taken up from the circulation into cells via the 5-HT transporter (5Htt). After uptake 5-HT can then be stored in cellular vesicles/granules via the action of vesicular monoamine transporter (VMAT) 1/2 which is expressed in neurons, neuroendocrine cells and platelets. In platelets 5-HT is stored in the dense granules where it can reach concentrations of up to 65 mM[49].

1.6.1. 5-HT in neurons

In neurons, 5-HT can be released into the synaptic cleft upon firing and then bind to different postsynaptic receptors (5-HT_{1A-F}, 5-HT_{2A-C}, 5-HT_{3-7}), inducing signaling propagation between neurons. The presynaptic neurons also express 5-HT receptors: 5-HT_{1A} and 5-HT_{1B} which are thought to decrease the amount of 5-HT released into the synaptic cleft and therefore also the subsequent firing rate at the presynapsis.[44,50] 5-HT receptor stimulation or 5-HT itself can trigger desensitization, internalization and receptor recycling in the presynaptic neuron.[44] 5-HT triggers effector signals downstream of postsynaptic receptors. Binding of 5-HT to 5-HTR_1 couples the $G_{i/o}$ protein alpha subunit, leading to the inhibition of adenylate cyclase (AC) and the subsequent reduction of cyclic adenosine-monophosphate (cAMP). Upon binding to 5-HT_2, PLCβ is activated via the coupling of $G_{q/11}$ protein alpha. Activation of this receptor-G protein unit leads to the formation of IP_3 and DAG and further mobilization of Ca^{2+}. The ionotropic, cation-specific ligand-gated ion channel 5-HTR_3 triggers no second messenger signal. This receptor instead influences the activation of 5-HTR_2 by depolarization of the postsynaptic membrane. The receptors 5-$HTR_{4,6,7}$ couple G_s protein alpha upon 5-HT binding, leading to activation of AC and the increase of cAMP. The activation of all these signaling cascades via the different receptors triggers potassium channels, protein kinases and the mobilization of Ca^{2+}, leading to the release of neurotransmitter from central serotonergic, noradrenergic and dopaminergic neurons.[51]

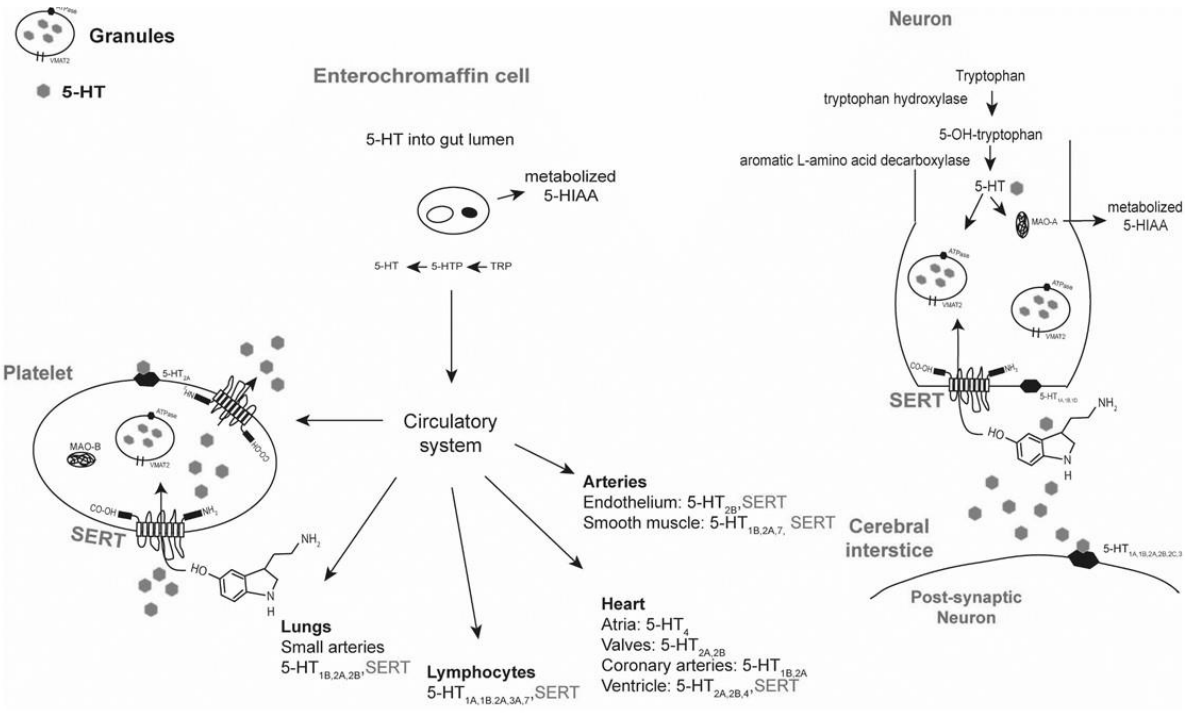

Figure 6: 5-HT biosynthesis and receptor distribution in brain and periphery. Serotonin (5-HT), serotonin transporter (SERT), monoamine oxidase (MAO), 5-hydroxyindole acetic acid (5-HIAA), 5-hydroxytryptophan (5-HTP), tryptophan (TRP), vesicular monoamine transporter (VMAT). (Modified from Yubero-Lahoz *et al.,* Curr. Med. Chem. 2013)[52]

1.6.2. 5-HT in platelets

Upon platelet activation, stored 5-HT can be released from the dense granules. 5-HT can then bind to the 5-HT_{2A} receptor expressed on platelets, inducing G_q-signaling via PLCβ, PKC and mobilization of Ca^{2+} to further amplify platelet activation (Figure 7). There are several 5-HT receptors expressed on lymphocytes, the endothelium and smooth muscle cells of arteries, all of which may then be influenced by platelet released 5-HT.[52] 5-HT can also activate another process in platelets, termed serotonylation, in particular of small GTPases downstream of the G_q-receptor. Mobilized Ca^{2+} activates tissue transglutaminase (TG) and factor XIIIa. TG mediates the transamidation of small GTPases, like cytoplasmic Ras homolog gene family member A (RhoA) and Rab4. Serotonylation blocks the inactivation of both molecules.

A complex consisting of Ca^{2+} and calmodulin (CaM) can activate guanine exchange factors (GEFs), which trigger the exchange of guanosine di- (GDP) to triphosphate (GTP) on RhoA and Rab4 and thus induces activation of the respective protein. These two active molecules are involved in cytoskeleton rearrangement, exocytosis of α- and dense granules and their contents. Some of these contents, like fibrinogen and FV are also known to be serotonylated. These pro-coagulant molecules are exposed on the

platelet surface, and are used to mark a subpopulation of highly activated, pro-coagulant platelets, called the collagen and thrombin-activated (COAT) platelets. These COAT platelets are highly PS-positive with low integrin activity and are thought to facilitate coagulation via promotion of thrombin generation.[49,53]

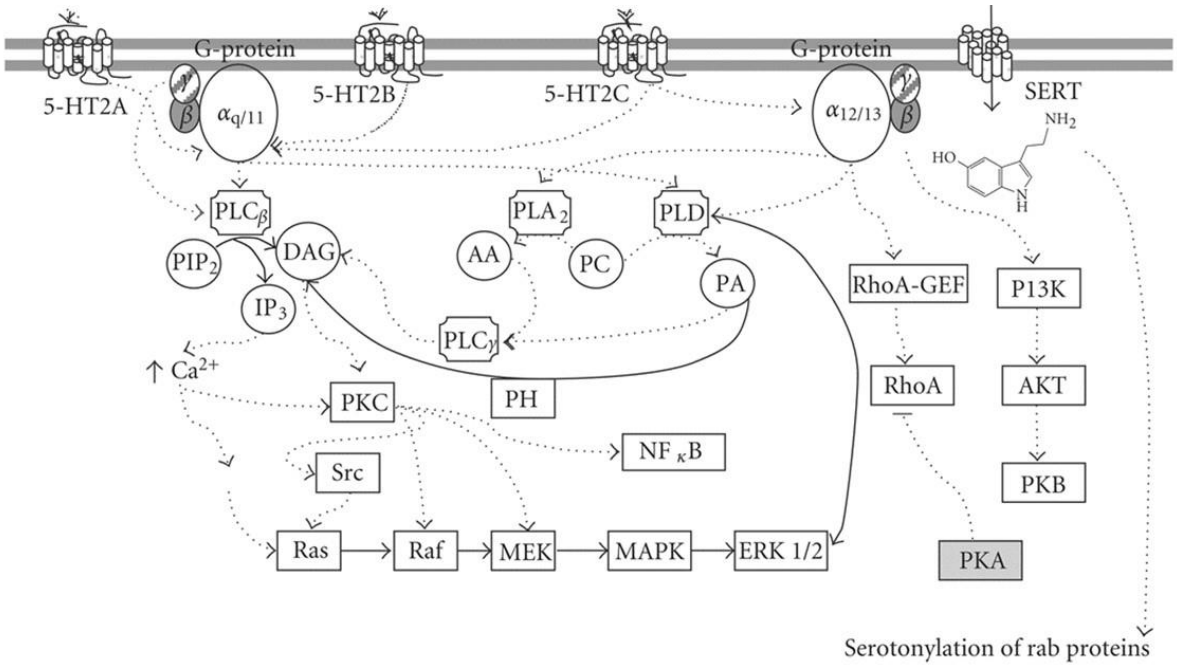

Figure 7: 5-HT receptor signaling in neurons. Signaling pathways downstream of the the 5-HT transporter and the different 5-HT receptors 2A, B and C. Phospholipase C (PLC) β/γ; diacylglycerol (DAG); inositol 1,4,5-triphosphate (IP_3); phophatidylinositol 4,5-bisphosphate (PIP_2); protein kinase B/C (PK B/C); extracellular signal-regulated kinases 1 and 2 (ERK1/2); phospholipase A_2 (PLA_2); arachidonic acid (AA); phophatidylcholine (PC); phophatidic acid (PA); phospholipase D (PLD); mitogen-activated protein kinase (MEK); mitogen-activated protein kinase (MAPK); phosphohydrolase enzyme (PH); protein kinase A (PKA); 5-HT transporter (SERT); Ras homolog gene family member A (RhoA); RhoA-guanosine exchange factor (RhoA-GEF); phosphatidylinositol-3-kinase (PI_3K); nuclear factor-kappaB (NFκB) and proteins: Src, Ras, Raf, AKT. (Image taken from Berumen *et al.,* Scientific World J 2012)[41]

1.6.3. Serotonin transporter (5Htt)

Besides the above mentioned 5-HT receptors, a 5-HT transporter (SERT, 5Htt, 5-Htt) also exists encoded by the gene *SLC6A4* and composed of 14 exons.[46] The transporter has 12 transmembrane domains (Figure 8A+B) with 630 amino acids. In humans, alternative promotors and differential splicing results in several mRNA species or splice variants, which can regulate gene expression.[46] The splice variants vary in their length and interestingly are associated with depression, suicide, bipolar disorders, anxiety disorders, substance-abuse disorders, autism, neurodegenerative disorders, eating disorders and attention-deficit/hyperactivity disorder.[46] 5Htt is the major trans-

porter for the uptake of 5-HT, besides the dopamine transporter (DAT), the noradrenaline transporter (NET) and the organic transporter (OCT) 1/3.[54,55] The 5-HT transport machinery is targeted by several antidepressant drugs, like the selective serotonin reuptake inhibitors (SSRIs), which are commonly used to treat patients with psychiatric disorders. The 5-HT transporters are thought to be able to compensate for one another where they are co-expressed. For example a recent publication demonstrated that 5-HT can be taken up in the vena cava independently of 5Htt expression.[56]

5Htt is highly expressed on neurons, endothelial cells, mast cells, natural killer cells, dendritic cells, B cells and platelets,[57] but also in the intestine, vasculature and immune system.[56] In the brain, this 5-HT transporter is important for the clearance of 5-HT in the synaptic cleft and subsequent storage in neuronal cells for later release upon stimulation.

In platelets, 5Htt is thought to mediate the uptake of 5-HT from the circulation, after which it is stored and then released upon platelet activation. This release of 5-HT from platelets is known to support the recruitment of other platelets to forming thrombi due to the expression of the 5-HT receptor 5-HT_{2A} on platelets. In addition to recruiting new platelets to a growing thrombus 5-HT can also act in an autocrine fashion amplifying a positive feedback loop via 5-HT_{2A} (the only 5-HT receptor on platelets) which synergizes with other important activatory platelet signals.

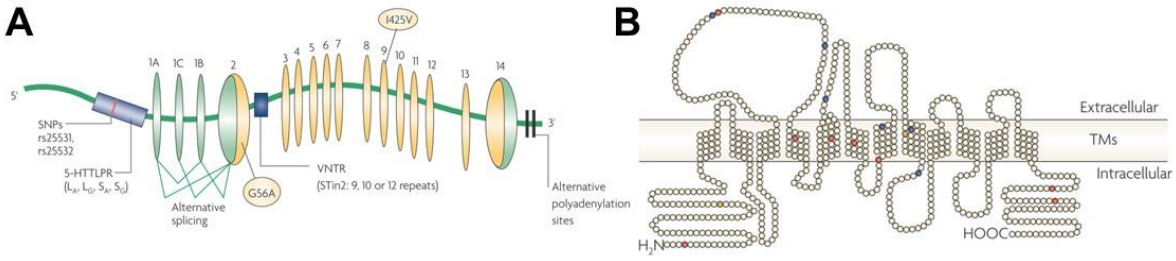

Figure 8: 5-HT transporter gene and protein.(A) Scheme of the gene locus of 5HTT in humans. Serotonin-transporter-gene-linked polymorphic region (5-HTTLPR), variable number of tandem repeats (VNTR), variable number of tandem repeats (SNPs). (B) Schematic illustration of the 5HTT transporter. Transmembrane segments (TMs). (Images taken from Murphy and Lesch, Nature Reviews 2008)[46]

1.6.4. Selective serotonin reuptake inhibitors (SSRI)

Many people suffer from psychiatric disorders during their lifetime,[58] and the increased frequency of diagnosis over time has intensified the research for new drugs for the treatment of these diseases. The first antidepressant monoamine oxidase inhibitors (MAOIs) and tricyclic antidepressants (TCAs) were developed in the early 1950,[59,60]

followed by the development of SSRIs in the late 1970s.[59] SSRIs are commonly used for the treatment of patients with severe depressive and anxiety disorders. SSRIs act in the same manner as TCAs however without the side-effects on other neuroreceptors.[61] The SSRIs were produced to selectively inhibit the uptake of 5-HT via the 5Htt transporter in the brain, whilst having minimal side-effects on proteins like DAT and NET, that can also transport 5-HT.[62] SSRIs modulate the allosteric region of the transporter, leading to a conformational change and thus blocking of the uptake of 5-HT.[62] The uptake of 5-HT into neurons is important for the clearance of the synaptic cleft, preventing firing rates and overstimulation of receptors.[63] This uptake and the later release is blocked upon treatment with SSRIs, like fluvoxamine, fluoxetine, nortriptyline, citalopram and escitalopram.[64] The different SSRIs vary in kinetic characteristics, being competitive to mixed competitive/non-competitive inhibitors. Two different binding sites on 5Htt have been identified, a low-affinity allosteric site, mediating the dissociation of SSRIs from their high-affinity site, which induces the blockade of 5-HT uptake.[63] As there is no difference between 5Htt transporter expressed in brain and on platelets, the platelet serotonergic system mimics the presynaptic serotonergic system, and therefore platelets have been used to study the effects and changes on 5Htt upon SSRI treatment.[63] Several studies reported side-effects of SSRI during treatment related to hemostasis, including an increase in bleeding risk,[65,66] 5-HT syndrome,[61] reducing incidence of MI[64] and reduction of thrombotic events.[64]

1.7. Platelet activation and divalent cations

1.7.1. Ca^{2+} is essential for platelet activation

Ca^{2+} is a second messenger in virtually all cells and regulates multiple cellular functions such as exocytosis, gene transcription, cell motility, cell cycle and apoptosis.[67] There are two mechanisms leading to an increase of cytoplasmic Ca^{2+} concentration: 1.) is the uptake of Ca^{2+} from outside a cell via Ca^{2+} channels in the PM, 2.) the release of Ca^{2+} from intracellular Ca^{2+} stores. It is reported that Ca^{2+} is stored in mitochondria, the ER, in the DTS, in lysosomes, the Golgi apparatus, in secretory granules, like dense granules and in the nuclear envelope.[68-71] The main channels for Ca^{2+} influx are voltage-gated Ca^{2+} channels, receptor-operated Ca^{2+} (ROC) channels and store-operated Ca^{2+} (SOC) channels, which mediate SOCE across the PM.[67,72,73]

Ca^{2+} is known to be a major signaling molecule in platelet activation, regulating cytoskeletal rearrangement, aggregation, firm adhesion and granule secretion.[74] The Ca^{2+}

store release in platelets is in the DTS and release from this store is regulated by IP_3 via its IP_3 receptor (IP_3R), forming a Ca^{2+} channel. The channel activity is mediated by the binding of IP_3 to the N-terminus of the IP_3R, a region, which also contains an inhibitory domain for the binding of IP_3. The pore unit is located in the C-terminus of the receptor, regulating Ca^{2+} influx.[75] On platelets and other cells three different isoforms of IP_3R are present, IP_3R1, IP_3R2 and IP_3R3. The most important isoforms in platelets are IP_3R1 and IP_3R2.[76]

In resting platelets, Ca^{2+} pumps and exchangers in the store and cell PM ensure that the intracellular Ca^{2+} concentration stays at a constant level. Upon stimulation, PLC isoforms are activated, resulting in the hydroxylation of PIP_2 into IP_3 and DAG. The production of DAG leads to the activation of the ROC channel canonical transient receptor potential channel (TRPC) 6 in the PM and further induces receptor-operated Ca^{2+} entry (ROCE). Concomitantly, Ca^{2+} store depletion is mediated by the production of IP_3. The changes in store Ca^{2+} concentrations are detected via stromal interaction molecule (STIM) 1 which upon Ca^{2+} depletion from the store activates the SOC channel, Ca^{2+} release-activated channel (CRAC) protein (Orai)1, inducing SOCE.[77]

1.7.2. Platelet activation and Mg^{2+}

Besides Ca^{2+}, Mg^{2+} has also been identified as an important divalent cation in several physiological processes. Cellular Mg^{2+} is bound to ATP, due to its high binding affinity to polyphosphate-containing molecules, like DNA, RNA and ATP. The remaining 5 % of Mg^{2+} circulates and can act as a second messenger like Ca^{2+}. Mg^{2+} is important for the proliferation of T cells and their stimulation via the TCR leads to an increase in intracellular Mg^{2+}, where it plays an important role in T cell function and development.[78] It is also known that Mg^{2+} has an effect on cellular metabolism, bioenergetics and Ca^{2+} channel activity.[79] Hypomagnesia is associated with impaired glucose tolerance, diabetes mellitus, obesity, insulin resistance and decreased insulin secretion.[80] Conversely hypermagnesia is associated with vasospastic angina.[79]

Several channels and transporters for Mg^{2+} have been identified. They are located in mitochondria, the Golgi apparatus and the PM. The most important known channels essential for Mg^{2+} influx and homeostasis belong to the group of transient receptor potential cation channel superfamily M (TRPM), TRPM6 and TRPM7.

1.7.3. Divalent cations and 5-HT

The binding of 5-HT to its receptor induces mobilization of cytosolic Ca^{2+}, leading to platelet activation and other cellular processes.[81,82] In addition to this mobilization of cytosolic Ca^{2+} is also known to regulate 5-HT uptake kinetics. In human platelets, the rise of cytoplasmic Ca^{2+}-levels without the initiation of exocytosis induces a reduction in 5-HT transport into the cytoplasm and the release of 5-HT.[83] In a separate study rabbit platelets activated in the presence of the extracellular calcium chelator ethylene glycol tetraacetic acid (EGTA) had a decrease in 5-HT transport.[84] In line with this, treatment of human platelets with the membrane permeant calcium chelator BAPTA-AM lead to a reduction of 5-HT transport in the presence of extracellular Ca^{2+}.[83] Both publications show that Ca^{2+} is important in the uptake process of 5-HT. It is hypothesized that 5Htt activity is modulated by phosphorylation. Interestingly, 5Htt has multiple consensus sites for PKC and it has been shown that the activity of PKC is important for the internalization of the transporter suggesting a link between intracellular Ca^{2+} levels and 5-HT uptake.[85-88]

1.8. Arterial thrombosis models in mice

MI, stroke and peripheral arterial occlusion are the major causes of mortality and morbidity worldwide.[89] Thus, platelet activation and thrombus formation are the focus of intense research to understand the process of thrombosis and to avoid inappropriate platelet activation. Murine models of occlusive arterial thrombosis enable the testing of new drugs, like anticoagulants, antiplatelet or fibrinolytic agents.[90] The possibility to delete or mutate (knock-out/in), block or inhibit a potential target *in vivo* with their short reproduction time makes mice a perfect model for this type of research.[91] A further advantage of this model is that thrombi formed in mice are histologically similar to those formed in humans upon vessel wall injury.[91]

There are several arterial thrombosis models known in mice. Models of venous thrombosis recapitulate stasis and coagulation activation in the venous system. Endothelial layer disruption and the subsequent activation of platelets, leading to thrombus formation are central features of arterial thrombus formation. The major focus in these models are the changes in thrombosis upon blocking or mutation of receptors or their ligands (activators/inhibitors), interaction partners or signaling molecules, to develop new drugs.[92] Endothelial damage in the arterial system is most often induced by laser,

mechanical, electrical or (photo-)chemical injury. The severity of the injury and thrombosis progression are monitored via the blood flow or by intravital microscopy allowing real-time analysis of the processes of thrombosis.[90,92]

1.8.1. Thrombosis after chemical injury of arteries

Arteries can be injured via the topical application of a ferric chloride ($FeCl_3$) drop or with a $FeCl_3$ saturated filter paper for a few minutes, depending on the model and the chosen vessel. Thrombus formation is observed via intravital microscopy or blood flow is measured by a Doppler flow probe to detect time to vessel occlusion. The applied $FeCl_3$ diffuses through the vessel wall, from the media to the intima and then the endothelium.[90,93] Currently it is thought that this $FeCl_3$ induces the generation of reactive oxygen species,[93] leading to vessel wall injury, the denudation of the endothelial surface and the exposure of the pro-coagulant subendothelial matrix. Pro-coagulant proteins, such as collagen and TF, then mediate adherence and activation of platelets via receptors and the activation of the coagulation cascade, resulting in the generation of thrombin[94] and subsequently lead to the formation of a thrombus.[90,93] However, the mechanism of $FeCl_3$-induced injury is still not entirely understood. Several groups have investigated $FeCl_3$-induced endothelial injury by scanning electron microscopy and transmission electron microscopy.[95] In contrast to other data, illustrating the denudation of the endothelial layer, a recent study has suggested that the endothelial layer remains intact implying that collagen and produced TF are not exposed upon $FeCl_3$ injury.[95] Another publication stated that $FeCl_3$ damages all layers of the vessel, besides the internal elastic lamina, thereby leading to the exposure of only basement membrane components.[94] The structure and function of important adhesive proteins, like fibrinogen, vWF and collagen, were shown to be affected upon $FeCl_3$ treatment *in vitro*.[94]

1.8.2. Mechanical injury of the abdominal aorta

There are several approaches to induce a mechanical injury of the aorta, such as firm compression with forceps, introduction of a guide wire into the vessel or the injury of the vessel via rotation[96] or ligation with a filament.[97] To analyze the formation of an occlusive thrombus, a Doppler flow probe is used to detect the blood flow over time.[98] Thrombus formation in these mechanical thrombosis models is due to the exposure of collagen and is strongly dependent on ITAM-signaling.[96]

1.8.3. Genetically modified mice assessed by *in vivo* thrombosis models

A complex activation machinery is required for physiological platelet function, including soluble agonists and enzymes, ions, transporters, adapter proteins, proteins involved in cytoskeletal rearrangement, surface receptors, proteins essential for vesicle mobilization and granule release. To understand the role of such players in the process of thrombosis, genetically modified mice lacking individual proteins were analyzed in the different thrombosis models.

1.8.3.1. Tryptophan hydroxylase 1 (Tph1)

Tph1$^{-/-}$ mice lack peripheral 5-HT in the circulation and in platelets, due to the lack of the enzyme that hydroxylyses tryptophan to 5-HT in the periphery.[99] This mouse line was generated to detect alterations due to the lack of 5-HT in the body, whereas in the brain, 5-HT is still produced by Tph2. The lack of 5-HT in the periphery in humans is associated with impulsive behavior and aggression,[100] irritable bowel syndrome,[101] sudden infant death syndrome,[102] anxiety disorders[103] and many other diseases.

It is published that peripheral 5-HT plays a major role in several processes, like hemostasis, the immune system and in many others.[104] This led to the investigation of the *Tph1*$^{-/-}$ mice and their comparison to the *5Htt*$^{-/-}$ mice. The lack of 5-HT in this mouse model is associated with decreased neutrophil recruitment to inflammatory sites, mild anemia, cardiopathy and diabetes.[105] It is known that these mice have other deficits in liver regeneration, in regulation of pulmonary arterial pressure, in erythropoiesis and in hemostasis.[104]

1.8.3.2. Unc13d/Nbeal2

The release of platelet granule contents is important for platelet activation. The secretion of the different granules is regulated by SNARE proteins expressed on granule and plasma membranes and is dependent on $[Ca^{2+}]_i$.[106] The soluble N-ethylmaleimide-sensitive-factor attachment receptor (SNARE) complex consists of numerous proteins including members of the Munc13 protein family.[106] The whole complex is essential for granule fusion with the PM which ultimately results in the release of the granule contents.[106] Munc13-4 deficiency in mice results in abolished dense granule secretion and up to a 60 % reduction of α-granule secretion. General blood parameters and the surface expression of the major platelet glycoproteins are normal in these mice. However,

due to the lack of granule content secretion, tail bleeding times are increased and the mice are protected from thrombosis.[106,107]

One member of the BEACH-WD40 domain protein family is Neurobeachin-like 2 (NBEAL2), a 302 kDa protein.[108] The proteins of this BEACH domain family are reported to be associated with protein trafficking, (others with this function include Nbeal1, Lyst and Lrba).[108] *NBEAL2,* in contrast to neurobeachin, is not expressed in brain tissue, but is present in MKs and platelets.[108] Mice lacking this protein are devoid of α-granules in MKs and platelets reflecting the human storage pool disease Gray Platelet Syndrome (GPS) in which *NBEAL2* is found to be deleteriously mutated.[108-110] *NBEAL2*$^{-/-}$ mice display a moderate thrombocytopenia, with an increased platelet size. Upon stimulation with collagen or collagen-related peptide (CRP) platelet aggregation was reduced compared to *Wt*. In line with the lack of alpha granules, P-selectin expression was reduced compared to *Wt* upon activation with GPCR-, GPVI- and CLEC-2-specific agonists. Furthermore, the mice were protected in different thrombosis models and had increased tail bleeding times.[108,109]

1.8.3.3. Transient receptor potential cation channel, subfamily M, member 7 (TRPM7)

TRPM7 is a non-selective cation channel, permeable to Ca^{2+}, Mg^{2+}, Mn^{2+} and Zn^{2+}. The channel consists of six transmembrane domains with a pore forming loop (Figure 9). The assembly of three channels is required to form an active channel.[111] This channel also functions as an enzyme, due to the carboxy-terminal serine/threonine kinase domain and was therefore initially termed a “chanzyme”. The receptor is regulated by external pH and by Mg^{2+}, as well as Zn^{2+}, Mn^{2+}, Ca^{2+} and polyvalent cations, like neomycin and spermin.[78,112] The receptor can be regulated by acidification and activated by cytoplasmic alkalinization.[112] It is widely expressed in humans, with a high copy number in immune cells, cardiac and smooth muscle cells.[112] The channel is important in embryonic development, shown by the lethality of a constitutive knock-out mouse line.[113,114]

The kinase domain of TRPM7 in the intracellular C-terminal tail resembles the myosin II heavy chain kinases, a member of the α-kinase family.[115] TRPM7 is reported to interact with myosin II and actin filaments *in vitro* in mammalian cells.[116] The kinase has been proposed to be essential for the ion channel activity, but this is controversially discussed. It has been shown that the kinase activity does not affect channel current

amplitudes or channel sensitivity to Mg^{2+}.[117] On the other hand it was also published that the kinase activity is important in channel activity and Mg^{2+} uptake.[112] The kinase domain seems to indirectly regulate the channel activity, but this is also controversially discussed.[118]

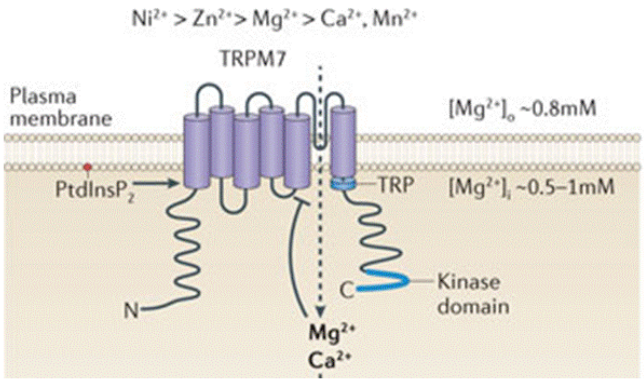

Figure 9: Structure of the TRPM7 channel. The channel is a non-selective permeable cation channel for Ca^{2+} and Mg^{2+}, which can also act as an enzyme through its carboxy-terminal serine/ threonine kinase domain. Mg^{2+} can inhibit the channel activity through an unknown mechanism. Transient receptor potential cation channel M7 (TRPM7), Phosphatidylinositol-4,5-bisphosphate (PtdInsP2). (Picture taken from Feske *et al.*, Nature Reviews 2012)[78]

1.8.3.4. Magnesium transporter 1 (MagT1)

MagT1 is the magnesium transporter 1 protein, a ~70 kb X-linked gene, consisting of 10 exons encoding a 335 amino acid protein in humans.[119] MagT1 is a highly conserved, widely expressed transporter in immune and epithelial cells in humans and its expression upon low extracellular Mg^{2+} levels is up-regulated in these cells. MagT1 is a voltage-dependent transporter located in the PM and the four transmembrane regions are highly selective to Mg^{2+} over Ca^{2+}, Zn^{2+}, Ni^{2+} and other cations (Figure 10A).[78,120] MagT1 consists of five transmembrane domains and an intracellular amino terminus.[78] MagT1 is known to be important in TCR signaling. Upon stimulation of the TCR, MagT1 enables the influx of Mg^{2+}, which further activates PLCγ1, leading to the production of IP_3 and the release of Ca^{2+} (Figure 10B).[119,121] Levels of cytosolic free Mg^{2+} levels and uptake are reduced in knockdown studies, but supplementation of Mg^{2+} or mammalian mRNA can rescue the defects, like early development arrest.[122] MagT1 is associated with the disease X-linked immunodeficiency with magnesium defect, Epstein-Barr virus and neoplasia disease (XMEN). Current data showed that XMEN patients have a mutation in the MagT1 transporter, leading to a loss of the MagT1 expression at the mRNA level.

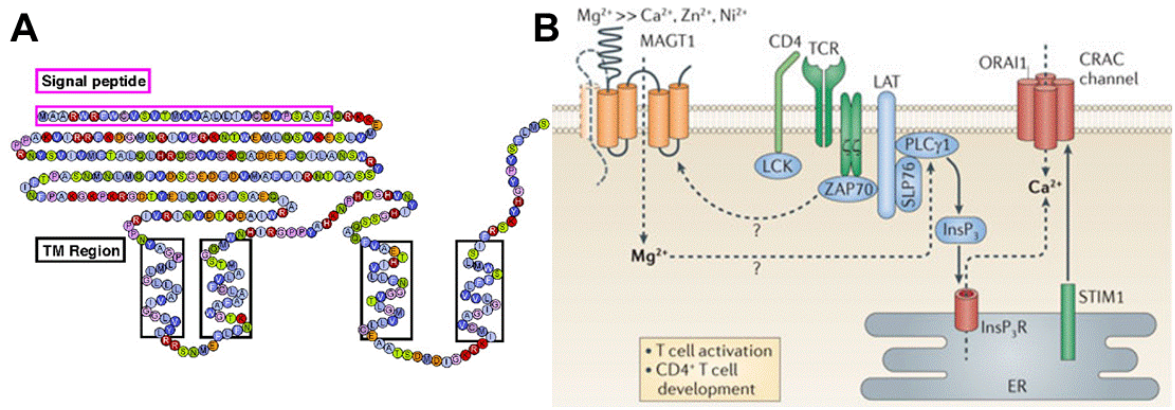

Figure 10: Structure of the MagT1 channel. (A) Secondary structure of the Mg^{2+} transporter protein 1 (MagT1). Indicated are the transmembrane helices (TM) in rectangles and the signal peptides in the beginning of the sequence (Picture taken from Zhou and Clapham, PNAS 2009)[122]. (B) MagT1 opens upon stimulation of the T cell receptor (TCR) leading to an increase in intracellular Mg^{2+} concentrations, PLCγ1 activation and Ca^{2+} influx via SOCE. Endoplasmatic reticulum (ER), inositol-1,4,5-triphosphate ($InsP_3$), inositol-1,4,5-triphosphate receptor ($InsP_3R$), linker for activation of T cells (LAT), stromal interaction molecule (STIM) 1, ξ-chain-associated protein kinase of 70 kDa (ZAP70), cluster of differentiation (CD) 4, Calcium release-activated channel (CRAC) protein (ORAI) 1, proteins: LCK, SLP76. (Picture taken from Feske *et al.*, Nature Reviews 2012)[78]

1.8.3.5. Rap1 guanosine triphosphate (GTP) interacting adaptor molecule (RIAM)

RIAM is a member of the Mig-10/RIAM/lamellipodin family. RIAM was thought to be an important mediator in αIIbβ3 integrin activation downstream of the thrombin receptors (protease-activated receptor (PAR)1 in humans or PAR4 in mice). Binding of thrombin to the PAR receptor stimulates the generation of IP_3 and DAG.[123] Subsequent increase of cytosolic Ca^{2+}, the activation of calcium diacylglycerol guanine nucleotide exchange factor I (CalDAG-GEFI) and PKC leads to the conversion of Rap to its active form RAP1-GTP. The activation of this molecule leads to the recruitment of RIAM and its binding partner talin 1 to the PM.[123] The head of talin 1 subsequently binds to the β3 integrin tail, leading to integrin adopting its high-affinity state and so inducing the activation of αIIbβ3 integrin (Figure 11).[123,124] Watanabe *et al.*[125] and Han *et al.*[126] showed a major role of RIAM in αIIbβ3 integrin activation by knockdown of the protein in CHO cells.

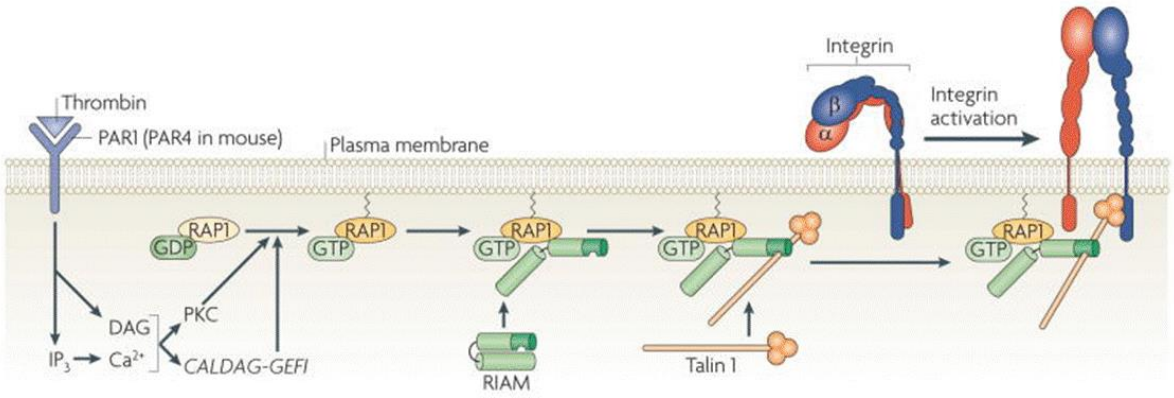

Figure 11: RIAM in "inside-out" activation of integrins. Activation cascade of αIIbβ3 integrin upon binding of thrombin to PAR in Chinese hamster ovary cells, leading to the generation of IP_3 and DAG. IP_3 further stimulates the increase of cytosolic Ca^{2+}, which together with DAG activates CALDAG-GEFI and PKC. These molecules are responsible for the conversion of RAP1 from its inactive to its active form. The active protein recruits RIAM and its binding partner talin 1 to the PM. This recruitment leads to the binding of talin to the β3 integrin tail and the activation of the integrin. (Picture taken from Shattil *et al.*, Nature Reviews 2010)[123]

2. Aim of the study

The aim of this study was to identify the role of platelet stored 5-HT in platelet activation, thrombosis, hemostasis and in the tMCAO model of ischemic stroke. As a first part of the study, *5Htt*$^{-/-}$ mice, lacking the transporter for the uptake of 5-HT in platelets, were analyzed *in vitro* and *in vivo* to detect the role of 5-HT in the process of platelet activation and thrombosis.

The effects of long-term treatment of depressed patients with SSRIs is mimicked by the *5Htt*$^{-/-}$ mouse strain. The SSRIs block uptake of 5-HT to increase the amount of 5-HT in the presynaptic cleft and the firing rate of the neurons. As a side effect, SSRIs also block the uptake of 5-HT in the periphery, such as in platelets. The mouse strain was analyzed in different *in vivo* models of hemostasis and ischemic stroke to test the role of 5-HT in this processes.

In the second part of this thesis, genetically modified mouse strains were analyzed in different *in vivo* thrombosis models, namely *Unc13d*$^{-/-}$/*Nbeal2*$^{-/-}$, *Tph1*$^{-/-}$, *MagT1*$^{y/-}$, *Trpm7*$^{fl/fl\text{-}Pf4Cre}$, *Trpm7*^{KI} and *RIAM*$^{-/-}$ mice.

3. Materials and Methods

3.1. Materials

3.1.1. Chemicals and reagents

If not listed otherwise chemicals and reagents were purchased from Sigma-Aldrich (Steinheim, Germany), AppliChem (Darmstadt, Germany) and Roth (Karlsruhe, Germany). Other chemicals are listed in the table below. Primers for genotyping were purchased from Metabion (Planegg-Martinsried, Germany). CRP was generously provided by Dr. Steve Watson (University Birmingham, UK). Rhodocytin (Rhd) was kindly provided by Johannes Eble (University Hospital Frankfurt, Germany). Annexin-A5-DyLight488 was kindly provided by Jonathan F. Tait (Medical Center Washington, USA).

Table 1: Used chemicals and reagents.

Name	company
10x Taq Buffer (+KCl, -$MgCl_2$)	Fermentas (St. Leon-Rot, Germany)
6x loading dye solution	Fermentas (St. Leon-Rot, Germany)
Acetic acid	Roth (Karlsruhe, Germany)
Adenosindiphosphate (ADP)	Sigma-Aldrich (Steinheim, Germany)
Agarose	Roth (Karlsruhe, Germany)
Alexa Fluor488	Molecular Probes (Eugene, USA)
Ammonium persulfate (APS)	Roth (Karlsruhe, Germany)
Apyrase (grade III)	Sigma-Aldrich (Steinheim, Germany) GE Healthcare (Amersham, England)
Bovine serum albumin (BSA)	AppliChem (Darmstadt, Germany) Sigma-Aldrich (Steinheim, Germany
Bromophenol blue	Sigma-Aldrich (Steinheim, Germany)
Calcium chloride	Roth (Karlsruhe, Germany)
Convulxin (CVX)	Enzo Life Sciences (Lörrach, Germany)
Deoxynucleotide triphosphates (dNTP) mix	Fermentas (St. Leon-Rot, Germany)
Dimethyl sulfoxide (DMSO)	Sigma-Aldrich (Steinheim, Germany)
Dry milk, fat free	AppliChem (Darmstadt, Germany)
DyLight-488	Pierce (Rockford, USA)
Ellagic acid	Sigma-Aldrich (Steinheim, Germany)
Enhanced chemiluminescence (ECL) detection substrate	MoBiTec (Göttingen, Germany)

Eosin	Roth (Karlsruhe, Germany)
Ethylene glycol tetraacetic acid (EGTA)	Sigma-Aldrich (Steinheim, Germany)
Ethylenediaminetetraacetic acid (EDTA)	AppliChem (Darmstadt, Germany)
Eukitt® quick-hardening mounting medium	Sigma-Aldrich (Steinheim, Germany)
Fentanyl	Janssen-Cilag GmbH (Neuss, Germany)
Fibrillar collagen type I (Horm)	Nycomed (Munich, Germany)
Fibrillar collagen type I	Sigma-Aldrich (Steinheim, Germany)
Flumazenil	Delta Select GmbH (Dreireich, Germany)
Fluorescein isothiocynate (FITC)	Molecular Probes (Oregon, USA)
Forene® (isoflurane)	Abott (Wiesbaden, Germany)
Fura-2 acetoxymethyl ester	Invitrogen (Karlsruhe, Germany)
Gene Ruler DNA Ladder Mix	Fermentas (St. Leon-Rot, Germany)
Giemsa 20x	Sigma-Aldrich (Steinheim, Germany)
Glucose	Roth (Karlsruhe, Germany)
Hematoxylin	Sigma-Aldrich (Steinheim, Germany)
N-2-Hydroxyethylpiperazine-N'-2-ethanesulfonic acid (HEPES)	Roth (Karlsruhe, Germany)
Heparin-sodium-500	Ratiopharm (Ulm, Germany)
Human fibrinogen	Sigma-Aldrich (Steinheim, Germany)
Igepal®CA-630	Sigma-Aldrich (Steinheim, Germany)
Indomethacin	Alfa Aesar (Karlsruhe, Germany)
Integrilin® (Eptifibatide)	Millennium Pharmaceuticals Inc. (Cambridge, USA)
Iron-III-chloride hexahydrate ($FeCl_3 \cdot 6H_2O$)	Roth (Karlsruhe, Germany)
Magnesium chloride ($MgCl_2$)	Fermentas (St. Leon-Rot, Germany)
Medetomidine (Dormitor)	Pfizer (Karlsruhe, Germany)
Midazolam (Dormicum)	Roche (Grenzach-Wyhlen, Germany)
Midori Green™	Biozym Scientific (Oldenburg, Germany)
Naloxon	Delta Select GmbH (Dreireich, Germany)
Page Ruler® Prestained Protein Ladder	Fermentas (St. Leon-Rot, Germany)
Paraformaldehyde (PFA)	Roth (Karlsruhe, Germany)
Phenol/chloroform/isoamyl alcohol	AppliChem (Darmstadt, Germany)
Pluronic F-127	Invitrogen (Karlsruhe, Germany)
PPP-reagent	Thrombinoscope (Düsseldorf, Germany)
Polyvinylidene difluoride (PVDF) membrane	Thermo Fisher (Darmstadt, Germany)
Prostacyclin (PGI_2)	Calbiochem (Bad Soden, Germany)

Protease inhibitor cocktail	Sigma-Aldrich (Steinheim, Germany)
Proteinase K	Fermentas (St. Leon-Rot, Germany)
R-phycoerythrin (PE)	EUROPA (Cambridge, UK)
Serotonin	Sigma-Aldrich (Steinheim, Germany)
Sodium azide	Sigma-Aldrich (Steinheim, Germany)
Sodium citrate	AppliChem (Darmstadt, Germany)
Sodium dodecyl sulfate (SDS)	Sigma-Aldrich (Steinheim, Germany)
Sodium hydroxide	AppliChem (Darmstadt, Germany)
Sodiumhydrogenphosphate	Roth (Karlsruhe, Germany)
Sodium orthovanadate	Sigma-Aldrich (Steinheim, Germany)
SPHERO™ AccuCount Particles, 5.05 µm	Spherotech (Lake Forest, USA)
SYBR Select Master Mix	Life Technologies (Carlsbad, USA)
Taq Polymerase	Fermentas (St. Leon-Rot, Germany)
Tetramethylethylenediamine (TEMED)	Roth (Karlsruhe, Germany)
Thrombin (20 U/mL) (100 U/mL)	Roche Diagnostics (Mannheim, Germany) Sigma-Aldrich (Steinheim, Germany)
Thrombin calibrator	Thrombinoscope (Düsseldorf, Germany)
Thrombin substrate (fluorescently labeled)	Thrombinoscope (Düsseldorf, Germany)
Triton X-100	Sigma-Aldrich (Steinheim, Germany)
Tween 20®	Roth (Karlsruhe, Germany)
U46619	Alexis Biochemicals (San Diego, USA)
Water, nuclease free	Roth (Karlsruhe, Germany)
Xylol	Sigma-Aldrich (Steinheim, Germany)
β-mercaptoethanol	Roth (Karlsruhe, Germany)

3.1.2. ELISA

Table 2: Used ELISA assays.

IP-One ELISA assay	Cisbio (Codolet, France)
Serotonin ELISA Fast Track	Labor Diagnostika Nord (Nordhorn, Germany)
Serotonin Research ELISA	Labor Diagnostika Nord (Nordhorn, Germany)
5-HIAA ELISA kit	Labor Diagnostika Nord (Nordhorn, Germany)
Melatonin ELISA kit	Enzo Life Sciences AG (Lausen, Austria)

3.1.3. Kits

Table 3: Used Kits.

QIAquick Gel Extraction Kit	Qiagen (Hilden, Germany)
NucleoSpin® RNA kit	Macherey-Nagel (Düren, Germany)
cDNA Reverse Transcription kit	Life Technologies (Carlsbad, USA)

3.1.4. Antibodies

3.1.4.1. Commercially available antibodies

Table 4: Used purchased antibodies.

Antibody	Host organism	Manufacturer
Anti-phosphotyrosine (4G10)	Mouse	Merck Millipore (Billerica, USA)
Anti-β-actin	Rabbit	Sigma-Aldrich (Steinheim, Germany)
Anti-SERT	Rat	Santa Cruz (Dallas, USA)
Anti-rabbit IgG-HRP	Goat	Cell Signalling (Cambridge, UK)
Anti-rat IgG-HRP	Goat	Dianova (Hamburg, Germany)
Anti-mouse IgG-HRP	Rat	DAKO (Hamburg, Germany)

3.1.4.2. Homemade monoclonal antibodies (mAb)

Self-made antibodies, are listed below. All antibodies were available unlabeled, FITC-/PE/Cy5-labeled or labeled with DyLight-488.

Table 5: Used homemade mAbs.

Antibody	Clone	Isotype	Antigen	Reference
EDL-1	57B10	IgG2a	β3	[127]
MWReg30	5D7	IgG1	αIIbβ3	[128]
DOM2	89H11	IgG2a	GPV	[129]
INU1	11E9	IgG1κ	CLEC-2	[130]
JAQ1	98A3	IgG2a	GPVI	[131]
JON/A	4H5	IgG2b	αIIbβ3	[132]
JON6	14A3	IgG2b	αIIbβ3	unpublished
LEN1	12C6	IgG2b	α_2	[133]
p0p4	15E2	IgG2b	GPIbα	[127]
p0p6	56F8	IgG2b	GPIX	[129]
ULF1	97H11	IgG2a	CD9	[127]
WUG1.9	5C8	IgG1	P-selectin	[134]
-	α-fibrinogen Cy5	-	Fibrinogen	[135]

3.1.5. Buffers and solutions

If not indicated otherwise, all buffers were prepared and diluted using $aqua_{bidest.}$ pH was adjusted with HCl or NaOH. All used buffers are listed below.

Table 6: Used buffers and media.

Buffer	Components
2x lysis buffer	300 mM NaCl, 20 mM TRIS, 2 mM EGTA, 2 mM EDTA, pH 7.5; 2 % Igepal, 2 mM Na_3VO_4, 10 mM NaF
4x SDS sample buffer	20 % β-mercaptoethanol, 20 % TRIS buffer, 40 % glycerol, 4 % SDS, 0.04 % bromophenol blue
50x TAE buffer, pH 8.0	0,2 M TRIS, 5.7 % acetic acid, 10 % (0.5 M) EDTA
50x alkaline lysis buffer, pH 12 (HOT Shot)	1.25 M NaOH, 10 mM EDTA
50x neutralizing solution, pH 5 (HOT Shot)	2 M TRIS-HCL
Blocking buffer (Western blot)	5 % BSA or fat-free dry milk in TBS-T
Decalcification buffer, pH 7.4	1 mM EDTA in PBS
FACS buffer	PBS, 0.1 % BSA, 0.02 % NaN_3
Heparin buffer	20 U/mL heparin in TBS
IP-buffer	15 mM TRIS/HCl (pH 8.0), 155 mM NaCl, 1 mM EDTA, 0.005 % NaN_3
Laemmli buffer for SDS-PAGE, pH 8.3	40 mM TRIS, 0.95 M glycine, 0.5 % SDS
Lysis buffer (DNA isolation)	100 mM TRIS base, 5 mM EDTA, 200 mM NaCl, 0.2 % SDS, add 100 µg/mL Proteinase K (20 mg/mL)
Phosphate buffered saline (PBS), pH 7.14	127 mM NaCl, 2.7 mM KCl, 1.5 mM KH_2PO_4, 8 mM Na_2HPO_4
Separating gel buffer, pH 8.8	1.5 M TRIS/HCl
Sodium citrate buffer, pH 7.0	0.129 M sodium citrate in NaCl
Stacking gel buffer, pH 6.8	0.5 M TRIS/HCl
Stripping buffer, pH 2.0	62.5 mM TRIS, 2 % SDS, 100 mM β-mercaptoethanol
TE buffer, pH 8.0	10 mM TRIS base, 1 mM EDTA
Transfer buffer (Semi-dry western blot)	50 mM TRIS ultra, 40 mM glycine, 20 % methanol
TRIS buffer, pH 6.8	13 % TRIS
TRIS-buffered saline (TBS), pH 7.3	137 mM NaCl, 20 mM TRIS

Tyrode's-HEPES buffer with Ca^{2+}, pH 7.4	137 mM NaCl, 2.7 mM KCl, 12 mM $NaHCO_3$, 0.43 mM NaH_2PO_4, 2 mM $CaCl_2$, 1 mM $MgCl_2$, 5 mM HEPES, 0.35 % BSA, 0.1 % glucose
Washing buffer (Western blot) (TBS-T)	0.1 % Tween 20® in TBS buffer

3.1.6. Animals

Mice lacking the *5Htt* gene were kindly provided by Prof. K. Lesch (Department of Neurology, University Würzburg) and were bred in our animal facility. *Tph1*$^{-/-}$ mice were kindly provided by Dr. Daniel Dürschmied (Heart Center, Freiburg University). *Trpm7*$^{fl/fl\text{-}Pf4Cre}$ (knock-out of the channel) and *Trpm7*^{KI} mice were kindly provided by Prof. Dr. T. Gudermann and Dr. V. Chubanov (Walther-Straub Institute for Pharmacology and Toxicology, LMU München). *Trpm7*^{KI} mice have a tyrosine to arginine mutation in an amino acid residue of the kinase domain, leading to the inactivation of the kinase activity.

Table 7: Mice used in this work.

Genotype	Background	Publication
5Htt$^{-/-}$	C57BL/6J	[136]
Tph1$^{-/-}$	C57BL/6J	[137]
MagT1$^{y/-}$	C57BL/6N	unpublished
Trpm7^{KI}	C57BL/6	[117]
Trpm7$^{fl/fl\text{-}Pf4Cre}$	C57BL/6	[113]
RIAM$^{-/-}$	C57BL/6	[124]
Unc13d$^{-/-}$*/Nbeal2*$^{-/-}$	C57BL/6J	unpublished

3.2. Methods

3.2.1. Animals

Animal studies were approved by the district government of Lower Franconia (Bezirksregierung Unterfranken). Experiments were performed using 5- to 12- week old littermates from *5Htt*$^{+/-}$ breeding pairs. Mice were anesthetized with a combination of midazolam/ medetomidine/ fentanyl (5/0.5/0.05 mg/kg body weight) administered by i.p. or by isoflurane inhalation.

3.2.2. Mouse genotyping

3.2.2.1. Isolation of genomic DNA from mouse ear samples

3.2.2.1.1. Phenol/chloroform isolation

To obtain murine genomic DNA, samples from ear punching were incubated at 56°C with constant shaking at 1,400 rpm in 500 µL lysis buffer containing 0.1 mg/mL Proteinase K for 2-3 h. By the addition of 500 µL phenol/chloroform/isoamyl alcohol (25:24:1) cellular proteins and lipids were removed. Samples were mixed well and centrifuged for 10 min at 10,000 rpm in an Eppendorf 5417R tabletop centrifuge at room temperature (RT). After centrifugation the upper phase was transferred into a new tube containing 500 µL isopropanol to precipitate the DNA. The nucleic acids were spun down by centrifugation at 14,000 rpm at 4°C for 10 min. The pellet was washed and dehydrated by adding 500 µL 70 % ethanol with a direct centrifugation of 15 min at 14,000 rpm at 4°C. To remove the remaining ethanol, the DNA was dried for 30 min at 37°C and the DNA pellet was dissolved in 50 µL TE buffer at 37°C and 600 rpm for 30 min. 1 µL of the sample was used per PCR reaction.

3.2.2.1.2. HOT Shot method

Alternatively the HOT Shot method was used for genotyping. Ear punching samples were incubated at 96°C with constant shaking at 1,400 rpm in 100 µL 1x alkaline lysis buffer for 2-3 h. After the samples were cooled to RT, 100 µL of 1x neutralization buffer was added. 1 µL of the solution was directly used for PCR reaction.

3.2.2.2. Detection of 5Htt allele by PCR

PCR was used to genotype the mice. The PCR mix (Table 8) with the indicated primers (Table 10) and the genomic DNA were mixed and cycled with the indicated PCR program (Table 9). Resulting band sizes after electrophoresis through a 2 % agarose gel were analyzed, the *Wt*-allele showed a band size of 227 bp, whereas the *Ko*-allele resulted in a band size of 272 bp. Heterozygous mice were detected by the appearance of both bands.

Table 8: PCR mix for *5Htt Wt/Ko/Het*:

1.0 µL	DNA sample (of HOT SHOT sample)
2.5 µL	10x Taq buffer (+KCl, -$MgCl_2$)
2.5 µL	$MgCl_2$ [25 mM]
0.5 µL	dNTPs [25 nM each]
0.05 µL	5HTTex2F.
0.05 µL	5HTTi2R.
0.05 µL	5HTTNeoF
0.2 µL	Taq-Polymerase (0.5 U/mL)
18.15 µL	H_2O

Table 9: PCR program for *5Htt Wt/Ko/Het*:

Step	Temperature [°C]	Time [s]	Repeats [cycles]
Denaturation	96	180	1
Denaturation	94	30	40
Annealing	62	30	40
Elongation	72	30	40
Elongation	72	300	1
Cooling	22	∞	1

Table 10: Primer list for 5Htt loci.

Primer name	Primer sequence
5HTTex2F.	5'-gcg ttt tcc cta cat atg cta cca g-3'
5HTTi2R.	5'-aag cct cgc aca gcc tac ctt ag-3'
5HTTNeoF	5'-cag ctc att cct ccc act cat ga-3'

3.2.2.3. Agarose gel electrophoresis

A 2 % agarose gel was used for the detection of genotyping PCR products. After cooling to approximately 60°C, 5 µL Midori green per 100 mL were added and the molten gel was poured into a tray with a comb. The gel was positioned in an electrophoresis chamber after solidification of the gel. PCR reactions were mixed with 5 µL 6x sample loading buffer and 20 µL were loaded into the slots. The separation of the DNA bands was done by electrophoresis (130 V for 30 min). The size of the bands was determined by comparison to a 1 kb DNA ladder and bands were visualized under UV light.

3.2.3. Quantitative PCR

Mice were sacrificed and livers collected in liquid nitrogen and cut into small pieces. These samples were used for quantitative PCR. The assay was performed in the Medical Clinic and Policlinic II at the University hospital of Würzburg in collaboration with Dr. Heike Hermanns and Donata Dorbath. RNA isolation from liver tissue was carried out using the NucleoSpin® RNA kit (Machery-Nagel) according to the manufacturer's instructions. For cDNA synthesis, 1 µg of total RNA was reverse-transcribed with the High-Capacity cDNA Reverse Transcription Kit (Life Technologies). Quantitative real-time PCR was performed on a ViiA™7 Real-time PCR System using the SYBR Select Master Mix (Life Technologies) and the primers (Table 11) located in distinct exons of the gene. Relative mRNA expression was calculated by the comparative ΔΔCt-Method normalized to the housekeeping gene ribosomal protein, large, P0 (RPLP0). All primers had melting temperatures of 58-60 °C according to the Primer Express 3.0 software (Life Technologies).

Table 11: Primer list for factor V and X.

Primer name	Primer sequence (Microsynth AG)
F7-forward	5'-tcc gct act ggg gaa aca tc-3'
F7-reverse	5'-gct cat ccc atc ctt ctc a-3'
F10-forward	5'-cac ctg ctc gga ggg att t-3'
F10-reverse	5'-cgg cag agt ttc cga aca aa-3'

3.2.4. *In vitro* analyses of platelet function

3.2.4.1. Platelet preparation and platelet washing

Mice were bled under isoflurane anesthesia from the retroorbital plexus into 300 µL heparin (20 U/mL) up to 1 mL. An additional 300 µL of heparin were added to the samples. Blood was centrifuged (Eppendorf centrifuge 5415C) for 6 min at 800 rpm at RT. The buffy coat und supernatant were transferred to a new tube containing 300 µL heparin. Samples were centrifuged for 6 min at 800 rpm at RT to obtain platelet-rich plasma (PRP). To prepare washed platelets, PRP was transferred to a new tube containing PGI_2 (0.1 µg/mL) and apyrase (0.02 U/mL) and centrifuged at 2,800 rpm for 5 min at RT. The platelet pellet was washed twice with Tyrode's-HEPES buffer containing 0.02 U/mL apyrase and 0.1 µg/mL PGI_2. Platelet numbers were determined by taking a 1:10 dilution of the platelet suspension. Measurement was performed with a

Sysmex KX-21N automated hematology analyzer (Sysmex Deutschland GmbH, Germany). Finally, the platelet pellet was resuspended in Tyrode's-HEPES buffer containing 0.02 U/mL apyrase and incubated for 30 min at 37°C.

3.2.5. Fluorescence-activated cell sorting (FACS) analyses

3.2.5.1. Platelet counting

For determination of platelet count and size, 50 µL blood were drawn from the retro-orbital plexus of anesthetized mice and collected in a tube containing 300 µL heparin (20 U/mL). 1 mL of Tyrode's-HEPES buffer containing 2 mM Ca^{2+} was added to the different samples and 50 µL were used for FACS measurements. Platelets were gated on the basis of a double positive signal, using the fluorophore-conjugated antibodies 14A3-PE (α-αIIbβ3) and 89H11-FITC (α-GPV). Samples were mixed well and incubated for 15 min at RT. The reaction was stopped by the addition of 500 µL 1x PBS and a defined number of fluorescently labeled beads (AccuCount fluorescent particles, 5.2 µm) were added and samples were measured with a FACSCalibur (BD Bioscience, USA) flow cytometer. FACS settings were set to the indicated values shown in Table 13 to Table 15. The platelet count was calculated as described in Table 12.

Table 12: Calculation for platelet count.

$$\frac{A}{B} \times \frac{C}{D} = \text{Number of cells per µL}$$

A = number of events for the test samples
B = number of fluorescent particles events
C = number of fluorescent particles per 50 µL
D = volume of test sample initially used in µL

Table 13: Detector/Amps

Parameter	Detector	Voltage
P1	FSC	E01
P2	SSC	299
P3	FL1	630
P4	FL2	518
P5	FL3	150

Table 14: Threshold

Value	Parameter
253	FSC-H
52	SSC-H
52	FL1-H
52	FL2-H
52	FL3-H

Table 15: Compensation

Value	Parameter
FL1	2.4 % of FL2
FL2	7.0 % of FL1
FL2	0 % of FL3
FL3	0 % of FL2
FL1	2.4 % of FL2

3.2.5.2. Glycoprotein expression

50 µL heparinized blood was taken from anesthetized mice into 300 µL heparin (20 U/mL). The samples were centrifuged at 2,800 rpm for 5 min at RT. Samples were washed twice by the addition of 1 mL Tyrode's-HEPES buffer and centrifuged at 2,800 rpm for 5 min at RT. The final pellet was dissolved in 750 µL Tyrode's-HEPES

buffer containing 2 mM Ca^{2+} and 50 µL was used for each FACS tube. The samples were incubated with specific FITC-labeled mAbs for the respective glycoproteins for 15 min at RT, stopped with 500 µL 1x PBS and analyzed on a FACSCalibur (BD Bioscience, USA).

3.2.5.3. Integrin activation and P-selectin exposure

Blood was washed as described in section 3.2.4.1 and resuspended in 750 µL Tyrode's-HEPES buffer containing 2 mM Ca^{2+} and 50 µL were used for each FACS tube. The samples were activated with the indicated agonists and concentrations and the platelets were labeled with 4H5-PE (integrin activation) and 5C8-FITC (P-selectin expression) in the presence or absence of 10 µM 5-HT. The samples were mixed and incubated for 7 min at 37°C and 7 min at RT. The samples were measured on a FACSCalibur (BD Bioscience, USA) after stopping the reaction with 500 µL 1x PBS.

3.2.5.4. Phosphatidylserine (PS) exposure

Washed platelets (5×10^5 platelets per µL) were diluted 1:10 with Tyrode's-HEPES buffer containing 2 mM Ca^{2+}. Platelets were activated with respective agonists and concentrations. PS-exposure was determined using fluorophore-conjugated antibody Annexin-A5-DyLight488 and 4H5-PE for 15 min at 37°C. The samples were analyzed with a FACSCalibur (BD Bioscience, USA) flow cytometer after stopping the reaction with Tyrode's-HEPES containing 2 mM Ca^{2+}.

3.2.5.5. Collagen and thrombin activated (COAT) platelets

Washed platelets (5×10^5 platelets per µL) were diluted 1:10 in Tyrode's-HEPES buffer containing 2 mM Ca^{2+}. The platelets were activated with respective agonists and concentrations. COAT platelets were determined using fluorophore-conjugated antibody Annexin-A5-DyLight488 and 4H5-PE for 15 min at 37°C. The samples were analyzed on a FACSCalibur (BD Bioscience, USA) flow cytometer after stopping the reaction with Tyrode's-HEPES containing 2 mM $CaCl_2$.

3.2.5.6. Microparticle (MP) formation

Washed platelets (5×10^5 platelets per µL) were diluted 1:10 in Tyrode's-HEPES buffer containing 2 mM Ca^{2+}. Activation of the platelets to form microparticles was obtained by the addition of respective agonists and concentrations. Microparticle formation was determined using fluorophore-conjugated antibodies Annexin-A5-DyLight488 and

14A3-PE for 15 min at 37°C. The reaction was stopped by the addition of 500 µL Tyrode's-HEPES buffer containing 2 mM Ca^{2+} and measured on a FACSCalibur (BD Bioscience, USA).

3.2.5.7. Platelet fibrinogen binding

Washed platelets (5×10^5 platelets per µL) were diluted 1:10 in Tyrode's-HEPES buffer containing 2 mM Ca^{2+}. The binding of fibrinogen following platelet activation with the indicated agonists was determined using fluorophore-conjugated antibodies Annexin-A5-DyLight488 and α-fibrinogen-Cy5 for 15 min at 37°C. The reaction was stopped by the addition of 500 µL Tyrode's-HEPES buffer containing 2 mM Ca^{2+} and measured on a FACSCalibur (BD Bioscience, USA).

3.2.6. Aggregometry

For the measurement of platelet aggregation, washed platelets were used (see 3.2.4.1). 50 µL of washed platelets with the concentration of 5×10^7 platelets per µL, were diluted with 110 µL Tyrode's-HEPES buffer containing Ca^{2+} and 70 µg/mL fibrinogen, except for thrombin measurements. After 30 s of starting the measurement platelets were activated with 1.6 µL of different agonists (100x concentrated) in the presence or absence of 10 µM 5-HT. Aggregation was measured by a four-channel aggregometer (APACT4, Laborgeräte und Analysensysteme, Hamburg) for 10 min. Calibration of the channels was performed by platelet-poor plasma (PPP) to set aggregation to 100 %, whereas PRP was set as 0 % aggregation. Thrombin measurements were performed without fibrinogen, whereas ADP measurements were performed with PRP analog to the other measurements.

3.2.7. Intracellular calcium measurements

Washed platelet pellet was resuspended in Tyrode's-HEPES buffer and was labeled with fura-2 AM (5 µM) in the presence of pluronic F-127 (0.2 µg/mL) for 20 min at 37°C. Extracellular dye was removed by centrifugation for 5 min at 2,800 rpm and the pellet was resuspended in Tyrode's-HEPES buffer containing 1 mM Ca^{2+}. Activation of platelets was performed under stirring conditions with the respective agonist concentration in the presence or absence of 5-HT. Fluorescence was measured with an LS 55 fluorimeter (PerkinElmer, USA) with excitation at 340 and 380 nm and emission at 509 nm. Each measurement was calibrated using Triton X-100 and EGTA.

3.2.8. Static adhesion of platelets on human fibrinogen

Coverslips were coated with fibrinogen (100 µg/mL, F4883, Sigma Aldrich) and blocked with 1 % BSA/PBS. After washing with Tyrodes's-HEPES buffer, washed platelets (3×10^5 platelets/µL) were either unstimulated or activated with 0.01 U/mL thrombin (10602400001, Roche). At the respective time point platelet spreading was stopped by addition 4 % PFA/PBS and pictures taken with a Zeiss Axiovert 200 inverted microscope (60x/0.60 NA objective) equipped with a CoolSNAP EZ camera (Visitron) and analyzed off line using ImageJ software. Four different stages of platelet spreading were evaluated: stage 1 – roundish; stage 2 – filopodia only; stage 3 – filopodia and lamellipodia; stage 4 – fully spread.

3.2.9. Platelet adhesion under flow conditions

Cover slips were coated with 100 µL of 200 µg/mL HORM collagen (fibrillar type I collagen) over night at 37°C. Cover slips were blocked with 300 µL 1 % BSA/PBS for at least 30 min. Mice were bled in 300 µL 20 U/mL heparin up to 1 mL. 800 µL of heparinized blood were diluted with 400 µL Tyrode's-HEPES buffer containing 2 mM Ca^{2+}. Platelets were labeled with 56F8-DyLight488 and were incubated for 5 min at 37°C. Blood was filled into a 1 mL syringe and was placed in a pulsion-free pump system. Blood was perfused with a shear rate of 1,000 s^{-1} (7.53 mL/h) over the collagen coated coverslips in the presence or absence of 5-HT (co-infusion) in the flow chamber. Aggregate formation in the flow chamber was recorded in real time and after the experiment had finished bright-field and fluorescence images were taken with a Zeiss Axiovert 200 inverted microscope (40x/0.60 objective) equipped with a CoolSNAP-EZ camera (Visitron) and analyzed off-line using ImageJ with respect to surface coverage and thrombus volume.

3.2.10. PS-exposure under flow conditions

Cover slips were coated with 100 µL of 200 µg/mL HORM collagen and dried over night at 37°C. Cover slips were blocked with 300 µL of 1 % BSA/PBS for at least 30 min at 37°C. Mice were bled in 300 µL 20 U/mL heparin up to 1 mL. 800 µL of blood-heparin mixture were added to 400 µL Tyrode's-HEPES buffer with 2 mM Ca^{2+}, additional 5 U/mL heparin and 250 ng/mL Annexin-A5-DyLight488. Blood was filled into a 1 mL syringe and placed in a non-pulsing pump apparatus. Blood was perfused with a shear rate of 1,000 s^{-1} (7.53 mL/h) over the collagen coated coverslips in the flow chamber. Aggregate formation in the flow chamber was recorded in real time. The

chamber was then washed with Tyrode's-HEPES buffer containing 2 mM Ca^{2+} and 5 U/mL heparin. Afterwards bright-field and fluorescence images were taken with a Zeiss Axiovert 200 inverted microscope (40x/0.60 NA objective) equipped with a CoolSNAP-EZ camera (Visitron) and analyzed off-line using ImageJ. Covered surface area and procoagulant index were analyzed.

3.2.11. Clot retraction

Mice were bled into 100 µL sodium citrate (0.129 M) up to 1 mL. Blood was centrifuged at 1,800 rpm for 7 min. The upper phase was transferred into a new tube and the lower phase containing the erythrocytes was kept at 37°C. Samples were again centrifuged at 800 rpm for 5 min. The upper phase was transferred to a new tube. Samples were centrifuged at 2,800 rpm for 5 min at RT. The supernatant (PPP) was pooled and kept at 37°C. The platelet pellets were resuspended in Tyrode's-HEPES containing 0.02 U/mL apyrase and 0.1 µg/mL PGI_2. Platelet samples diluted 1:10 in 1x PBS were analyzed with a Sysmex KX-21N automated hematology analyzer. The platelet samples were centrifuged at 2,800 rpm for 5 min at RT. The platelet pellet was adjusted to 3 x 10^5 platelets per µL with 250 µL of the pooled plasma. Samples were pipetted into an aggregometry cuvette without a stirrer containing 20 mM $CaCl_2$, 1 µL of red blood cells and 4 U/mL thrombin. Samples were mixed shortly and incubated in a cell culture incubator at 37°C with 5 % CO_2. Pictures were taken at 0, 15, 30, 45, 60 min and then every half an hour up to 4 h.

3.2.12. Western blotting

3.2.12.1. Western blotting of platelet lysates

Platelet lysates were prepared from washed platelets, washed in Tyrode's-HEPES buffer without BSA. The platelet pellet (1 x 10^6 platelets per µL) was lysed in a calculated volume of IP-buffer containing protease inhibitors (1:100) and 1 % Igepal for 30 min on ice. Subsequently, samples were centrifuged at 14,000 rpm for 10 min at 4°C. The supernatant was transferred into a new reaction tube and mixed with 4x SDS sample buffer without or with β-mercaptoethanol for non-reducing/reducing conditions. The samples were boiled at 95°C for 5 min.

Samples were loaded into 10 % acrylamide gels and run for 2-3 h at 20 mA per gel. Afterwards the semi-dry transfer method was used for 1 h with 0.8 mA/cm^2 to transfer the proteins from the gel to a PVDF membrane. The membrane was afterwards

blocked with either 5 % BSA or 5 % milk dissolved in 1x TBS-T for 1 h. The membrane was incubated with the primary antibody at the indicated concentration over night at 4°C. The membrane was washed afterwards with 1x TBS-T for 1 h. Subsequently the membrane was incubated with the secondary antibody diluted in 1x TBS-T. The membrane was washed and then incubated with ECL solution.

3.2.12.2. Western blotting of tyrosine phosphorylation

Platelet lysates for tyrosine phosphorylation were prepared from washed platelets, washed in Tyrode's-HEPES buffer without BSA. Platelets from several mice were pooled and resuspended in Tyrode's-HEPES buffer to obtain 1×10^6 platelets per µL. 10 µM indomethacin, 5 mM EDTA and 2 U/mL apyrase were added to the platelet suspension to prevent aggregation. The platelet suspension was transferred to an aggregometry cuvette and 50 µL were transferred to a tube containing 50 µL of 2x lysis buffer and kept on ice (resting). The respective agonist was added to the cuvette and at the indicated time points (15, 30, 60, 120 and 300 s) 50 µL were transferred to a tube containing 50 µL of 2x lysis buffer. Samples were then vortexed and incubated on ice. Subsequently samples were centrifuged at 14,000 rpm at 4°C for 5 min to pellet cell debris. The supernatant was transferred to a new tube and was mixed with 4x SDS reducing buffer and denaturated for 10 min at 70°C. Gel preparation and semi-dry blotting was as for the previously described Western blotting conditions. After blotting, the membrane was blocked in 5 % BSA in TBS-T for 1 h at RT followed by the incubation with the primary α-phosphotyrosine antibody 4G10 (1:1,000) over night at 4°C. The following day, the membrane was washed in TBS-T for 1 h and incubated for 1 h at RT with the secondary rabbit anti-mouse IgG-HRP antibody (1:2,500). The membrane was afterwards washed in TBS-T and then incubated with ECL solution to detect proteins.

3.2.13. Preparation of mouse plasma

Mice were bled into 100 µL of sodium citrate (0.129 M) up to 1 mL. The blood was centrifuged twice for 5 min at 14,000 rpm at RT to obtain PPP. PPP was then stored or directly used for analyses. PPP was diluted 1:3 in 0.9 % NaCl solution for the measurement of plasma factor levels. The assays were performed in the central laboratory at the University hospital of Würzburg in collaboration with Dr. Sabine Herterich.

3.2.14. ELISA

3.2.14.1. IP_1 ELISA

Platelets were washed with Tyrode's-HEPES buffer without phosphate and Ca^{2+} and were resuspended in Tyrode's-HEPES buffer without phosphate, containing 2 mM Ca^{2+}, 50 mM Li^{+}, 10 µM indomethacin and 2 U/mL apyrase with a concentration of 8 x 10^5 platelets per µL. 80 µL of the platelet suspension were pipetted into different tubes and activated with different agonists (20x concentrated) for 5 min at 450 rpm and 37°C. The reaction was stopped by addition of 10 % lysis reagent from the ELISA kit (Cisbio) and incubated for 30 min at 37°C without shaking. 50 µL of the lyzed platelets were used for the IP_1 ELISA assay according to the manual (Cisbio, Codolet, France).

3.2.14.2. Serotonin ELISA Fast Track

Released platelet 5-HT was measured with washed platelets (5 × 10^5 platelets per µL) in Tyrode's-HEPES buffer. Platelets were activated for 5 min by using the respective agonists and concentrations in the presence of 50 mM $CaCl_2$ and 100 µg/mL fibrinogen (except for thrombin). Samples were shortly centrifuged and the supernatant was collected. 5-HT concentration and release was assessed by ELISA (Serotonin ELISA Fast Track, LDN) according to the manufacturer's recommendation.

3.2.14.3. Serotonin Research ELISA

Heparinized whole blood with 5 mM EDTA was centrifuged twice at 2,400 g for 10 min to obtain PPP. Degradation of 5-HT in the plasma samples was inhibited by the addition of 1 % 5-HT stabilizer from the ELISA kit. Plasma 5-HT content was analyzed by an ELISA (Serotonin Research ELISA, LDN) according to the manual of the manufacturer.

3.2.14.4. 5-HIAA ELISA

At midday, urine was collected from mice and used for the commercial ELISA (5-HIAA ELISA kit, LDN GmbH & Co. KG). 5 HIAA concentrations in the urine samples were analyzed according to the manufacturer's instructions.

3.2.14.5. Measurement of melatonin in blood plasma

At midday, anesthetized mice were bled into 5 mM EDTA and plasma was obtained by centrifugation twice at 4°C for 10 min. Melatonin was extracted from the plasma and samples were diluted with 250 µL of 1x stabilizer and used for the ELISA (Melatonin

ELISA Kit, Enzo Life Sciences Inc.). The melatonin concentration in the extracted plasma samples was analyzed according to the manufacturer's instructions.

3.2.15. Thrombin generation

Mice were bled into 50 µL 0.129 M sodium citrate with non-heparinized capillaries and tubes were filled up with citrate to reach 10 % sodium citrate in the blood-citrate mixture. PPP preparations were pooled from 2 mice with the same genotype if necessary. To activate platelets, the samples were incubated with CRP (20 µg/mL) for 10 min at 37°C. After stimulation, samples (4 vol) were transferred to a polystyrene 96-well plate already containing 1 vol of thrombin calibrator, 5 pM PPP reagent (Thrombinoscope BV, 5 pM tissue factor, 4 µM phospholipids) or ellagic acid (Sigma Aldrich). The coagulation reaction was started by adding 1 vol fluorescent thrombin substrate (2.5 mM Z-GGR-AMC, 20 mM HEPES, 140 mM NaCl, 200 mM $CaCl_2$, and 6 % BSA). The thrombin generation was measured according to the calibrated automated thrombogram method.[138,139] The data were analyzed using the Thrombinoscope Software (Thrombinocscope BV). Samples were run in duplicate. Thrombin generation assay was performed by Sarah Beck and Tano Marth.

3.2.16. Sample preparation for histology

3.2.16.1. Samples for hematoxylin/eosin staining

Spleens and bones were taken out and were fixed in 4 % PFA/PBS over night at 4°C. Bones were then decalcified for 4 days in 10 % EDTA/PBS with a daily buffer change and then stored in 1x PBS until further proceeding. Samples were dehydrated in an automated tissue processor (Leica ASP200S) and embedded in paraffin. Three µm Sections were cut with a Microm Cool Cut HM 355 (Microm GmbH, Neuss) and were transferred to slides and dried over night at 37°C.

3.2.16.2. Samples for neutrophil staining

Brains were taken out after 24 h of the reperfusion injury and were embedded in Tissue Freezing Medium® and immediately frozen in liquid nitrogen (done in collaboration with Dr. Peter Kraft and Dr. Michael Schuhmann in the group of Prof. Guido Stoll and Prof. Christoph Kleinschnitz, Department of Neurology, University of Würzburg, Germany).

3.2.16.3. Hematoxylin/eosin staining of paraffin sections

The paraffin section were deparaffinized twice for 5 min in Xylol. Afterwards the samples were dehydrated in a graded ethanol series (100 %, 90 %, 80 % and 70 %) for 2 min each and then washed with deionized H_2O. The slides were then stained for 25 s in hematoxylin and subsequently washed with running water for 5 min. Afterwards the samples were stained with 0.05 % eosin, containing 1-2 drops of 100 % acetic acid and washed with deionized water. Samples were rehydrated in a graded ethanol series (70 %, 80 %, 90 % and 100 %) for 2 min each. Samples were then twice deparaffinized in Xylol for 5 min. Slides were dried and then embedded with 2 drops of Eukitt solution, covered with a cover slip and dried over night. Five slices per animal were analyzed to count the number of MKs in bone and spleen.

3.2.16.4. Neutrophil staining in brain sections

Cryo-embedded brains from mice with a 60 min ischemia induced reperfusion injury were cut into 10 µm-thick sections. Immunostaining of leukocytes on brain slides was performed according to the description of Schumann *et al.*[140] with Ly6B.2 antibody (rat anti-mouse, MCA771G, AbD Serotec, 1:500). Five slices per animal were analyzed to count the total number of infiltrated leukocytes in the ipsilesional hemisphere at a 10 fold magnification.

3.2.17. *In vivo* analyses of murine platelet function

3.2.17.1. Tail bleeding time

Mice were anesthetized by an i.p. injection of a combination of midazolam/medetomidine/fentanyl (5/0.5/0.05 µg/g body weight). 1-2 mm of the tail tip was amputated with a scalpel and every 20 s the blood drops were absorbed onto filter paper without contact to the wound site until the formation of a stable hemostatic plug (Figure 12). The time to complete arrest of bleeding was determined. The experiment was stopped at the latest after 20 min to prevent excessive blood loss. Anesthesia was antagonized by the injection of antidote antisedan/anexate/narcanti (5/0.1/0.4 µg/µL in 0.9 % NaCl).

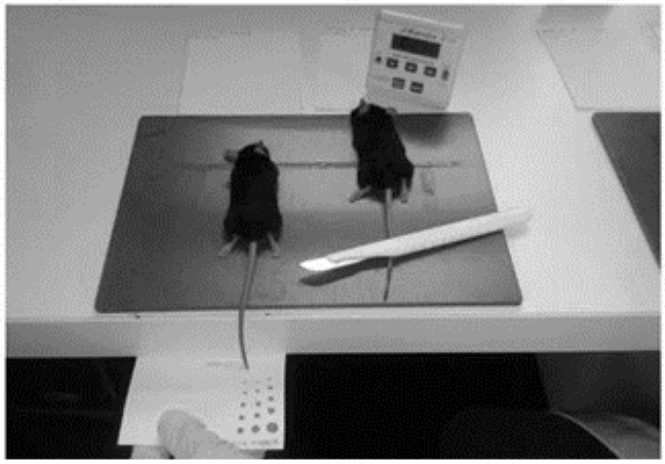

Figure 12: Tail bleeding time assay with filter paper. One mm of the tail tip was amputated and blood drops were collected with filter paper without touching the wound site. The time to formation of a stable hemostatic plug was determined.

3.2.17.2. Intravital microscopy of thrombus formation after $FeCl_3$-induced injury of mesenteric arterioles

Anesthetized 4-5 weeks old mice with a body weight of 15-20 g were used for the model of $FeCl_3$-induced injury of mesenteric arterioles. After midline abdominal incision, the mesentery was exteriorized carefully. Arterioles with a diameter of 35-60 µm and free of fat tissue were immobilized on a Petri-dish using gauze saturated with 0.9 % NaCl. The injury of the arterioles was induced by application of a filter paper (3 mm^2 triangular) soaked with 20% $FeCl_3$. Adhesion, aggregation and thrombus formation of fluorescently labeled platelets (56F8-DyLight488; anti-GPIX Ig derivate) was monitored until complete occlusion occurred (blood flow stopped for > 1 min) or for a maximum of 40 min after induction of thrombus formation (Figure 13A). Images were recorded with a Zeiss Axiovert 200 inverted microscope (10x/0.60 NA objective, Zeiss, Germany) equipped with a CoolSNAP-EZ camera (Visitron, Germany).

3.2.17.3. Intravital microscopy of thrombus formation after mechanical injury of the abdominal aorta

Mice were anesthetized and placed on a heating pad. The abdominal cavities were opened with a longitudinal incision. An ultrasonic flow probe (0.5 PSB 699; Transonic Systems, USA) was placed around the abdominal aorta. Thrombus formation was induced by firm compression of the aorta with a forceps for approximately 15 s. Blood flow was monitored for 30 min or until complete occlusion occurred (no blood flow for > 3 min, see Figure 13B).

3.2.17.4. Carotid artery thrombosis model

The right carotid artery of anesthetized mice was exposed through a vertical midline incision in the neck. The ultrasonic flow probe (0.5 PSB 699; Transonic Systems) was placed around the carotid artery and blood flow was measured. The injury of the vessel was induced by topical application of a saturated filter paper (0.5 x 1 mm) with 6-10 % $FeCl_3$ for 1.5-2 min. Blood flow was monitored for 30 min or until complete occlusion occurred (no blood flow for > 3 min, see Figure 13C).

3.2.17.5. Transient middle cerebral artery occlusion (tMCAO) model of ischemic stroke in mice

Mice were anesthetized by isoflurane inhalation and tMCAO was performed as previously described[141] using the intraluminal filament (6021PK10; Doccol Corporation USA) technique. The filament was advanced through the right carotid artery to reduce cerebral blood flow in the middle cerebral artery. The filament was removed after 1 h to allow reperfusion (Figure 13D, 1st image). The extent of infarction was assessed 24 h after reperfusion on 2,3,5-triphenyltetrazolium chloride (TTC)-stained brain sections (Figure 13D, 2nd image). 24h after reperfusion the Bederson test was scored (Figure 13D, 3rd image), motor function and coordination were graded using the grip test (Figure 13D, 4th image).[142] These experiments were carried out in collaboration with Dr. Peter Kraft and Dr. Michael Schuhmann in the group of Prof. Guido Stoll and Prof. Christoph Kleinschnitz, Department of Neurology, University Hospital of Würzburg, Germany.

3.2.18. Data analyses

The presented results are mean ± standard deviation (SD) from at least three independent experiments per group. Differences between control and *Ko* mice were statistically analyzed using the Student's t-test. For a test of independence, the two tailed Fisher's test for control versus the respective group was used. P values < 0.05 were considered statistically significant (*p < 0.05; **p < 0.01; ***p < 0.001).

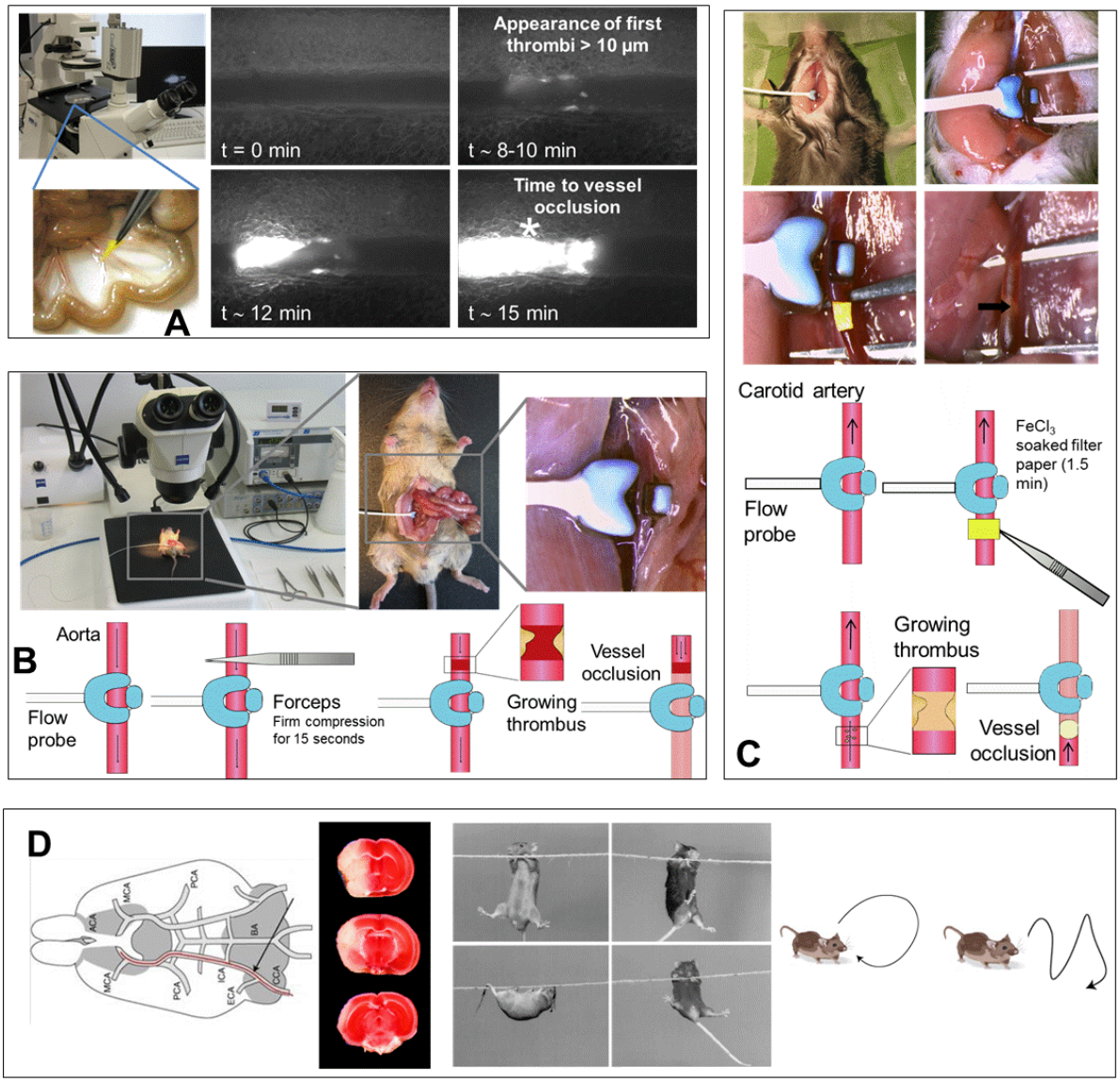

Figure 13: *In vivo* thrombosis models and tMCAO. (A) Model of the mesenteric artery injury by $FeCl_3$. Exteriorized intestine of a mouse under the microscope (left). Mesentery artery injured with a $FeCl_3$ soaked filter paper (lower panel). Representative images upon injury of a mesentery artery with $FeCl_3$ at the indicated time points. Stable vessel occlusion is shown by a star (right). (B) Mechanical injury of the abdominal aorta. Images of the anesthetized mouse with a flow probe placed around the abdominal aorta. Mechanical injury of the abdominal aorta with a forceps and the following occlusion of the vessel by the growing thrombus. (C) Injury of the carotid artery with a $FeCl_3$ saturated filter paper. Pictures and schematic images of the injury of the carotid artery with $FeCl_3$. The vessel was injured by topical application of a soaked filter paper with $FeCl_3$. (D) tMCAO model in mice. The filament is advanced through the right carotid artery to reduce cerebral blood flow in the middle cerebral artery (1st image). The brain sections were stained 24 h after tMCAO with TTC-staining to detect brain infarct size (2nd image). Motor function and coordination were determined by the grip test (3rd image) and neurological status was scored with the Bederson score (4th image).[141]

4. Results

4.1. *In vitro* and *in vivo* characterization of *5Htt*$^{-/-}$ mice

4.1.1. Unaltered platelet count and volume in *5Htt*$^{-/-}$ mice

5Htt$^{+/-}$ (*Het*) mice were intercrossed to obtain *5Htt*$^{-/-}$ (*Ko*) and the respective littermate *Wt* control mice. Genotyping was performed by PCR on genomic DNA isolated from ear pieces. Figure 14A shows PCR products in *5Htt*$^{+/+}$ mice (*Wt)*, *5Htt*$^{+/-}$ (*Het)* and *5Htt*$^{-/-}$ mice. The offspring (*5Htt*$^{+/+}$, *5Htt*$^{+/-}$ and *5Htt*$^{-/-}$) were healthy and born at a normal Mendelian ratios, indicating that 5Htt is dispensable for embryonic development.

Platelet count (Figure 14B) and size (Figure 14C) were analyzed by flow cytometry and a blood cell analyzer (Sysmex cell counter KX 21N, Sysmex Deutschland GmbH, Germany) and no obvious differences in *5Htt*$^{-/-}$ mice compared to *Wt* controls were observed. These results indicated that the lack of 5Htt is dispensable for platelet production.

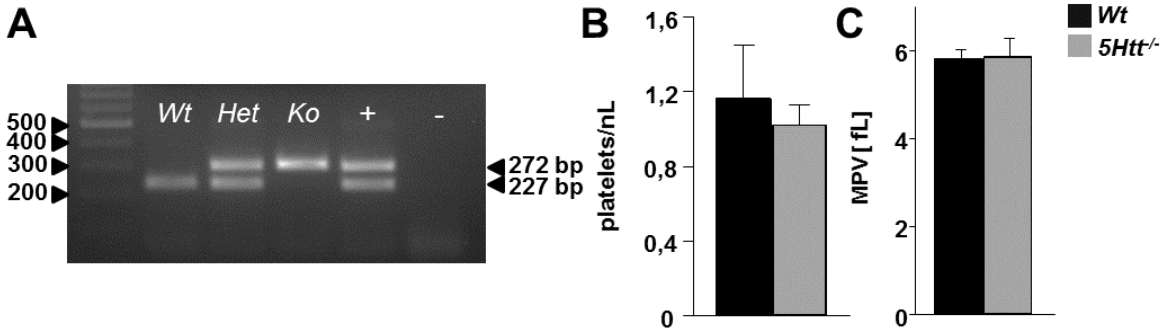

Figure 14: *5Htt*$^{-/-}$ platelets display normal platelet count and size. (A) Genotyping of *5Htt*$^{+/+}$ (*Wt*), *5Htt*$^{+/-}$ (*Het*) and *5Htt*$^{-/-}$ (*Ko*) mice by PCR, visualized on a 2 % agarose gel. DNA of *Het* mice served as positive and water as negative control. (B) Similar platelet count and (C) size in *5Htt*$^{-/-}$ and *Wt* mice. Values are mean ± SD. (Wolf *et al.*, PlosOne, 2016)[143]

5Htt is an important transporter in the plasma membrane of platelets for the uptake of 5-HT. To test whether the absence of this transporter has an effect on the expression levels of major glycoproteins on the cell surface, flow cytometric analyses were performed. The levels of the major glycoproteins were similar in *Wt* and *5Htt*$^{-/-}$ samples (Figure 15), indicating that the lack of the transporter and platelet 5-HT do not influence major surface glycoprotein expression.

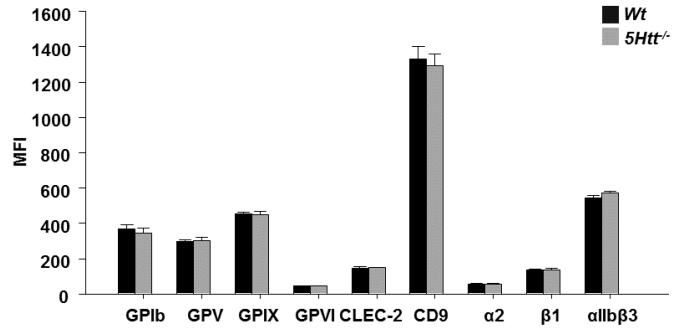

Figure 15: Glycoprotein expression is unaltered in *5Htt*$^{-/-}$ mice. Diluted whole blood was stained with fluorophore labeled antibodies directed against platelet glycoproteins and platelets were analyzed by flow cytometry. Values are mean fluorescence intensity (MFI) ± SD.

4.1.2. Unaltered hematological parameters in *5Htt*$^{-/-}$ mice

Since the *5Htt*$^{-/-}$ mice were a constitutive knock-out mouse line and to rule out any effects of 5Htt on general hematopoiesis, blood samples from *Wt* and *5Htt*$^{-/-}$ mice were analyzed with an automated cell counter to measure basic blood parameters. The analyses showed no differences in white (WBC) and red blood cell (RBC) count, as well as in hemoglobin content (HGB) and hematocrit values (HCT), between *Wt* and *5Htt*$^{-/-}$ samples.

Table 16: *5Htt*$^{-/-}$ mice exhibit normal hematological parameters. Blood cell distribution was determined with a whole blood analyzer. White blood cell (WBC), red blood cell (RBC), hemoglobin (HGB) and hematocrit (HCT), not significant (n.s.).

Genotype	WBC [x10^3 per µL]	RBC [x10^6 per µL]	HGB [g/dL]	HCT [%]
Wt	8.5±2.2	8.6±0.4	13.3±0.8	46.3±3.1
5Htt$^{-/-}$	8.0±1.2	8.4±1.0	13.0±0.9	44.6±4.9
significance	n.s.	n.s.	n.s.	n.s.

4.1.3. *5Htt*$^{-/-}$ alters plasma and platelet 5-HT levels and its metabolites

To test whether 5Htt represents the only route for 5-HT uptake in platelets, 5-HT release from the cells upon stimulation (Figure 16A) was analyzed. Measurement of the 5-HT concentration in blood plasma and platelets was performed by a 5-HT-ELISA. Secreted platelet 5-HT was below the levels of detection in both resting and activated *5Htt*$^{-/-}$ platelets as was the total 5-HT concentration in platelet lysates (Figure 16A). Surprisingly, the concentration of 5-HT in the blood plasma was also significantly reduced in *5Htt*$^{-/-}$ mice (Figure 16B). These results demonstrated that the 5-HT transporter 5Htt is essential for 5-HT uptake in platelets. This appears to be in sharp contrast

to neurons, in which alternative compensatory 5-HT uptake mechanisms exist, such as DAT, NET and OCT1/3.[54] Additionally, we found that the 5-hydroxyindolacetic acid (5-HIAA) concentration, an important metabolite product of 5-HT, was increased in the urine of *5Htt*$^{-/-}$ mice (Figure 16C), whereas the melatonin concentration was normal in the *5Htt*$^{-/-}$ blood plasma (Figure 16D).

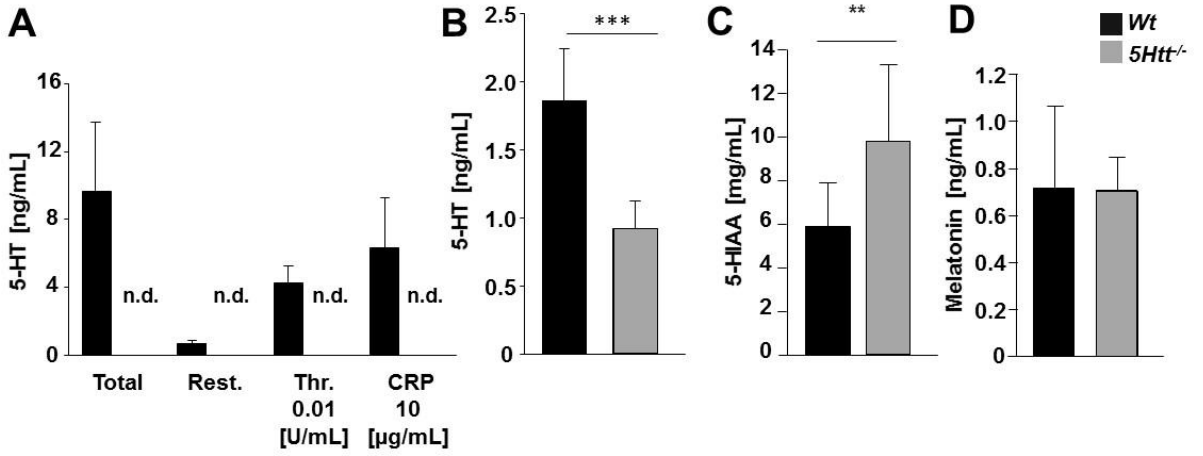

Figure 16: 5-HT content and levels of metabolites. (A) 5-HT content and release was determined by ELISA. Washed platelets were stimulated with indicated agonists. Thrombin (Thr), collagen-related peptide (CRP) and resting (Rest.), n.d.: not detectable. (B) Citrate-anticoagulated blood was centrifuged to obtain PPP and 5-HT levels were measured with a highly sensitive ELISA. (C) 5-HIAA and (D) melatonin level in urine or plasma samples of *Wt* and *5Htt*$^{-/-}$ mice. (Wolf *et al.*, PlosOne, 2016)[143]

4.1.4. Secreted platelet 5-HT is required for maximal platelet responses to (hem)ITAM signaling

5-HT is considered to be a “weak agonist” of platelets due to its inability to induce platelet aggregation by itself, but it is known to synergize with other signaling pathways and to potentiate aggregation responses of other platelet agonists.[144] Furthermore, it has been shown that 5HTT itself directly interacts with integrin αIIbβ3, indicating a functional crosstalk between them.[145] To study the consequence of abolished 5Htt function and the loss of platelet stored 5-HT on platelet activation, αIIbβ3 integrin activation and P-selectin surface exposure in response to different agonists were monitored by flow cytometry. The contribution of platelet 5-HT or 5Htt to GPCR mediated platelet activation was not altered as *5Htt*$^{-/-}$ platelet responses to thrombin, ADP and U46619 were comparable to *Wt* platelets (Figure 17A). In contrast, αIIbβ3 integrin activation and P-selectin surface exposure in response to agonists operating via the (hem)ITAM coupled receptors GPVI and CLEC-2 were significantly reduced in *5Htt*$^{-/-}$ platelets revealing a specific role for 5-HT and/or 5HTT in GPVI and CLEC-2 mediated platelet activation (Figure 17A).

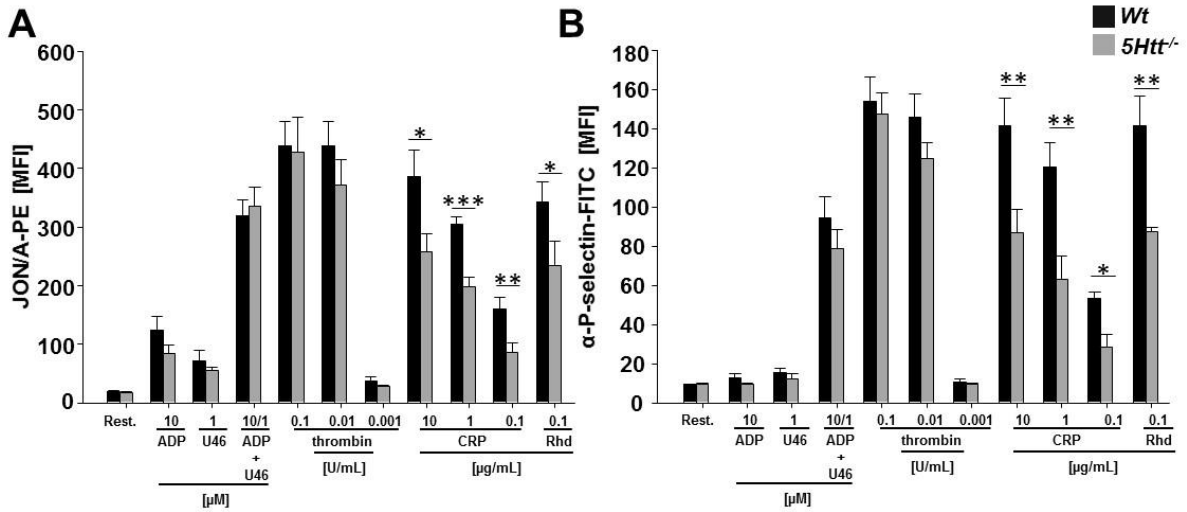

Figure 17: Integrin αIIbβ3 activation and degranulation in *5Htt*$^{-/-}$ platelets. Flow cytometric analyses of (A) integrin activation and (B) degranulation, measured by P-selectin exposure on the platelet surface. Washed blood was incubated for 15 min at RT with indicated agonist and measured with a FACSCalibur. Results are MFI ± SD. Resting (Rest), adenosine-diphosphate (ADP), U46619 (stable TxA_2 analog, U46), collagen-related peptide (CRP), rhodocytin (Rhd). * p<0.05, ** p<0.01. (Wolf *et al.*, PlosOne, 2016)[143]

4.1.5. PS-exposure and microparticle (MP) formation as well as COAT platelet generation is unaltered in *5Htt*$^{-/-}$ mice

It has recently been shown that SSRI treatment of platelets reduces the formation of COAT platelets and MP formation.[146-150] COAT platelets are defined as highly activated, PS-positive platelets with low levels of activated integrins, due to pronounced integrin closure. The respective gating strategy for the analysis of COAT platelets is depicted in Figure 18A+B. In contrast to previous publications,[147,149,151] the formation of COAT platelets was unaltered in *Wt* and *5Htt*$^{-/-}$ mice (Figure 19B). MP formation was assessed by flow cytometry. Briefly, platelets (Figure 18D, ellipse) and platelet-derived particles (like MPs; Figure 18D, rectangle) were stained with 14A3-PE (anti-GPIIb/IIIa) and Annexin-A5-DyLight488. MPs were defined as double positive for both staining's (Figure 18E). MP formation was found to be normal in *5Htt*$^{-/-}$ mice (Figure 20B) thus excluding the possible role of 5-HT in these processes.

To test whether the 5-HT transporter or 5-HT itself regulates procoagulant activity of platelets, PS exposure was determined by Annexin-A5 staining. The percentage of Annexin-A5 positive cells shown by flow cytometry was similar in *Wt* and *5Htt*$^{-/-}$ mice. However, upon stimulation with Rhd less *5Htt*$^{-/-}$ platelets were PS-positive compared with *Wt* controls (Figure 19A).

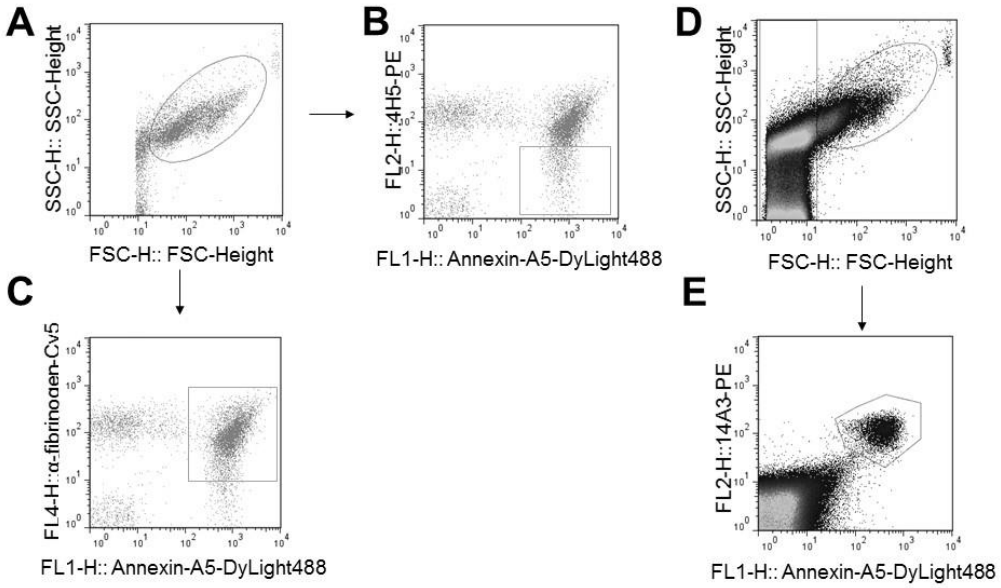

Figure 18: Gating strategy for COAT platelets, MP formation and fibrinogen binding. Flow cytometric analyses of washed blood. Platelets were stained with the indicated antibodies. (A) Gating strategy of platelets. (B) Platelets were stained with 4H5-PE and Annexin-A5-DyLight488 to measure COAT platelets, Annexin-A5 single positive cells determined COAT platelets in this approach. (C) Gating strategy for fibrinogen binding. Platelets were stained with α-fibrinogen-Cy5 antibody and Annexin-A5-DyLight488. Double positive cells determined COAT platelets in this approach. (D) Gating strategy for MP formation. (upper panel). Platelets are gated based on their FSC/SCC and dual positive characteristics Events that fell outside of the platelet gate whilst maintaining dual positivity for 14A3-PE and Annexin-A5-DyLight488 were counted as platelet derived MP (lower panel).

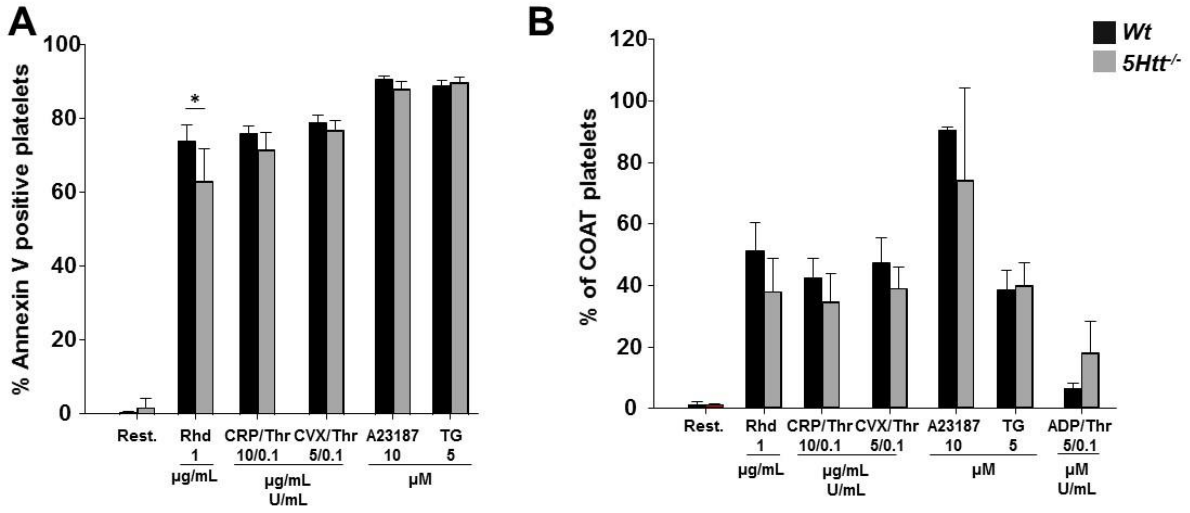

Figure 19: PS-exposure, COAT platelets and MP formation in *5Htt*$^{-/-}$ mice. Flow cytometric analyses of *Wt* and *5Htt*$^{-/-}$ platelets. (A) Washed platelets were stained with JON/A-PE and Annexin-A5-DyLight488 and activated with the indicated concentrations of agonists. (B) COAT platelets were analyzed by staining of washed platelets with 14A3-PE and Annexin-A5-DyLight488. Values are mean ± SD. * $p<0.05$.

4.1.6. Unaltered fibrinogen binding and MP formation in *5Htt*$^{-/-}$ platelets

5-HT has been proposed to act as a linker between FV and fibrinogen derived from α-granules, thus stabilizing the binding of the molecules and to other platelets via serotonylation.[147,151]

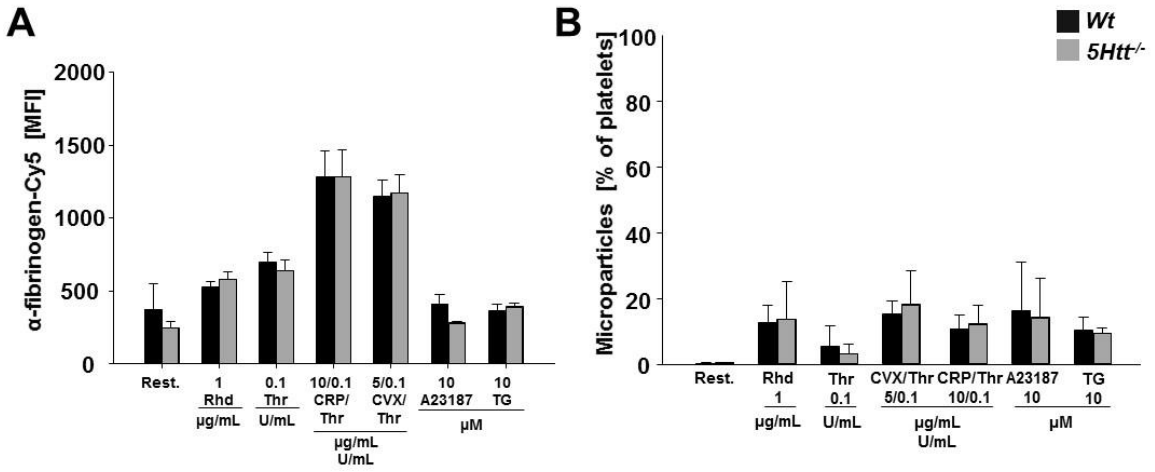

Figure 20: Unaltered fibrinogen binding and MP formation in *5Htt*$^{-/-}$ mice. Flow cytometric analyses of *Wt* and *5Htt*$^{-/-}$ platelets. (A) Washed platelets were stained with Annexin-A5-DyLight488 and α-fibrinogen-Cy5 and activated with the indicated agonists to measure fibrinogen binding. (B) Washed platelets were stained with 4H5-PE and Annexin-A5-DyLight488 to detect formed MPs. The platelets were activated with the indicated agonists. Results show mean or MFI ± SD. (Wolf *et al.*, PlosOne, 2016)[143]

To test whether fibrinogen binding was reduced in the absence of platelet-derived 5-HT, fibrinogen binding was analyzed in activated platelets by flow cytometry. No difference in fibrinogen binding in *Wt* and *5Htt*$^{-/-}$ platelets was measured (Figure 20A).

4.1.7. Reduced aggregation of *5Htt*$^{-/-}$ platelets upon stimulation with GPVI or CLEC-2 agonists

Previous studies have shown defects in platelet aggregation of *5Htt*$^{-/-}$ platelets upon activation with high dose of several agonists, such as ADP and thrombin.[145] Furthermore, hyperreactive platelets were observed upon infusion of 5-HT into *Wt* mice[53] indicating an important role for 5-HT in platelet aggregation. Similar to the effects on integrin activation and degranulation, defects in the ability of *5Htt*$^{-/-}$ platelets to form stable aggregates were also observed. Aggregation responses were slightly reduced upon activation of platelets with different GPCR agonists, such as ADP, the TxA_2 analog U46619 and thrombin. The aggregation responses to GPVI or CLEC-2 specific agonists were markedly reduced, comparable to the activation responses found in flow cytometry experiments (Figure 21).

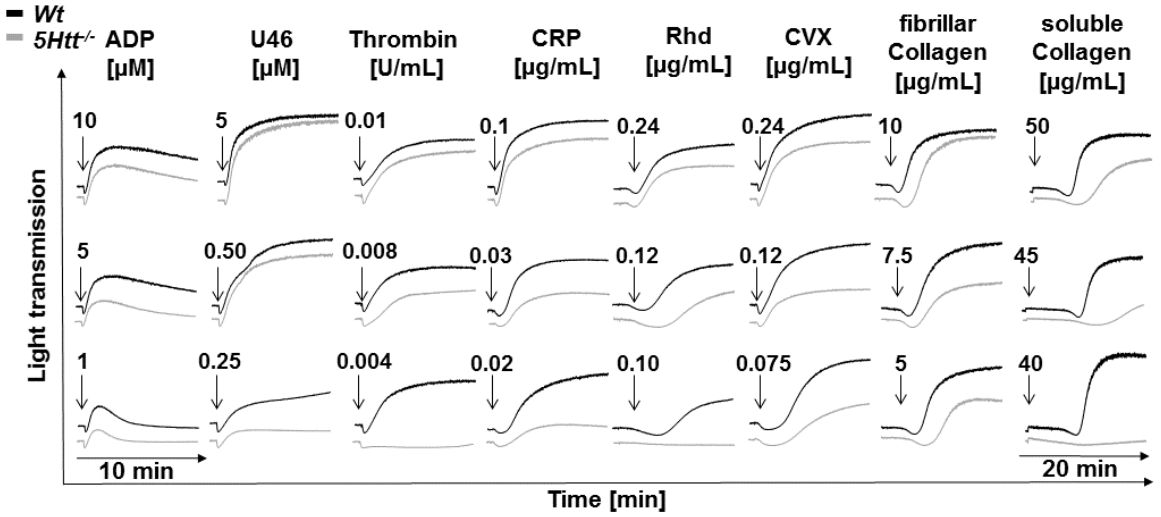

Figure 21: Reduced aggregation of *5Htt*$^{-/-}$ platelets upon stimulation with different agonists. Washed platelets were activated with the indicated agonists. Light transmission was recorded with a Fibrintimer 4-channel aggregometer and the addition of the agonists is indicated by an arrow. Aggregometry measurements upon activation with ADP were performed in PRP, whereas all others were performed with washed platelets. (Wolf *et al.*, PlosOne, 2016)[143]

4.1.8. Unaltered tyrosine phosphorylation in *5Htt*$^{-/-}$ platelets

Changes in protein tyrosine phosphorylation and PLCγ2 activity after GPVI or CLEC-2 stimulation were unaltered in *5Htt*$^{-/-}$ platelets, as assessed by Western blotting (Figure 22A+B) and inositol monophosphate (IP_1) ELISA (Figure 22C), respectively.

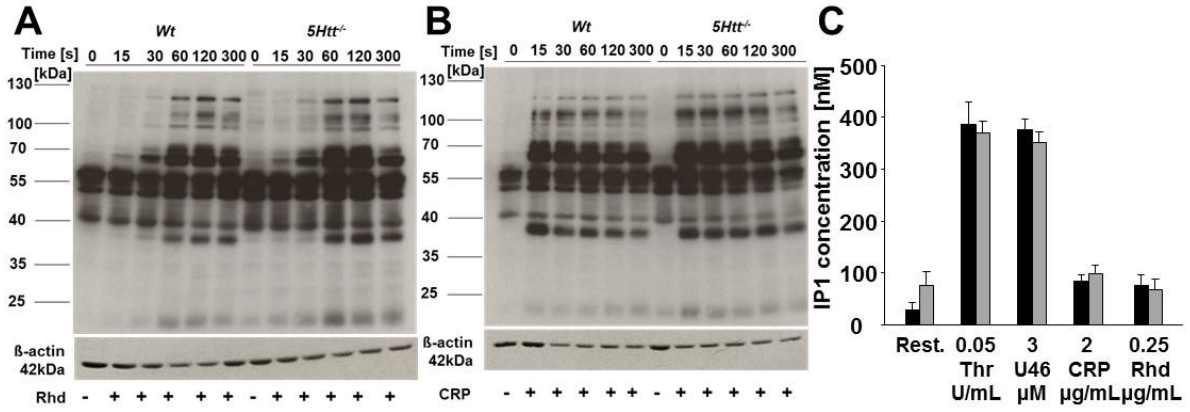

Figure 22: Tyrosine phosphorylation assay of *Wt* and *5Htt*$^{-/-}$ platelets. Washed platelets were stimulated with 1 µg/mL CRP or 2 µg/mL Rhd for the indicated times, in the presence of "second wave" inhibitors (apyrase, EDTA and indomethacin). Western blot of whole cell lysates was performed and the membrane was probed with the anti-phosphotyrosine antibody 4G10 (1:1,000). A-Actin (1:2,500) served as loading control. (C) Washed platelets were activated with the indicated agonists in the presence of 2 mM Ca^{2+}, 50 mM Li^{+}, 100 µg/mL fibrinogen (not included when thrombin was used) and "second wave" inhibitors. The activation was stopped by the addition of 10 % lysis reagent and the supernatant was used for the IP_1 ELISA according to the manual. (Wolf *et al.*, PlosOne, 2016)[143]

Therefore, we concluded that the defects in response to (hem)ITAM stimulation were downstream of the initial (hem)ITAM signaling cascade.

4.1.9. Unaltered tyrosine phosphorylation without inhibitors of the "second wave" mediators in *5Htt*$^{-/-}$ platelets

Apyrase is a scavenger of ADP,[152] whereas EDTA chelates extracellular cations, such as Ca^{2+}[153] and indomethacin is an inhibitor of cyclooxygenase, which is important for the production of TxA_2.[154] In the presence of all these "second wave" inhibitors, the feedback loops provided by ADP, TxA_2 and Ca^{2+} mobilization are blocked. To test if the feedback loop is important, Western blot analyses of tyrosine phosphorylation were repeated in the absence of apyrase, EDTA and indomethacin and in the presence of integrillin (GPIIb/IIIa inhibitor) to prevent platelet aggregation. Western blotting of tyrosine phosphorylation upon stimulation with CRP in the presence (Figure 22B) or absence of the inhibitors of the "second wave" (Figure 23) showed no difference, indicating that the feedback loops provided by these "second wave" mediators are functional in *5Htt*$^{-/-}$ platelets.

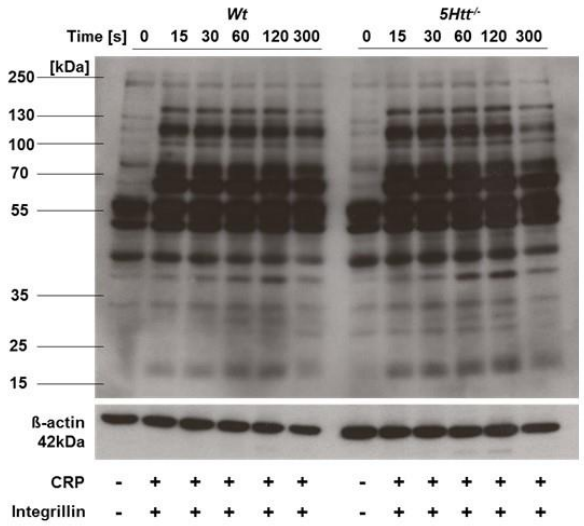

Figure 23: Tyrosine phosphorylation assay of *Wt* and *5Htt*$^{-/-}$ platelets in the absence of "second wave" inhibitors. Washed platelets were stimulated with 1 µg/mL CRP for the indicated times, in the absence of "second wave" inhibitors (apyrase, EDTA and indomethacin). Western blot of whole cell lysates were performed and the membrane was probed with the anti-phosphotyrosine antibody 4G10 (dilution: 1:1,000). A-Actin (dilution: 1:2,500) served as loading control.

4.1.10. 5-HT potentiation of (hem)ITAM signaling is mediated by SOCE

A key factor in platelet integrin activation and degranulation is a sustained increase in cytoplasmic Ca^{2+} levels. 5-HT binds $5HT_{2A}$ on the platelet surface which activates the Gq-PLCβ pathway and subsequent Ca^{2+} mobilization and PKC activation. Given that the initial signaling cascade downstream of (hem)ITAM containing receptors, including

PLC activity (Figure 22C) and IP_3 dependent Ca^{2+} store depletion (Figure 24A) was unaffected in *5Htt*$^{-/-}$ platelets, Ca^{2+} influx after activation was assessed (Figure 24B). In line with the functional defects observed in *5Htt*$^{-/-}$ platelets, GPVI and CLEC-2 induced Ca^{2+} influx was significantly reduced in these cells (Figure 24B). Surprisingly, ADP and U46619 mediated Ca^{2+} responses were also affected, whereas thrombin and 5-HT mediated Ca^{2+} influx were similar to *Wt* platelets (Figure 24B).

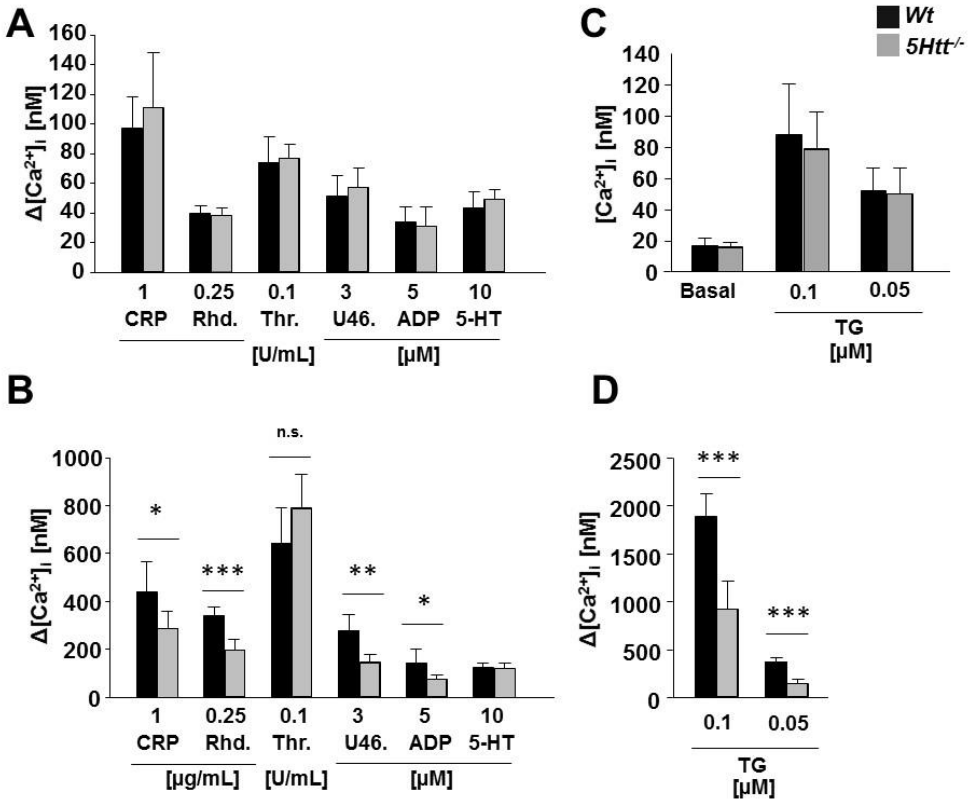

Figure 24: The lack of *5Htt* leads to alterations in Ca^{2+} signaling. Washed platelets were labeled with fura-2 AM in the presence of pluronic F-127 for 20 min at 37°C. Excess dye was removed by centrifugation and the platelet pellet was resuspended in Tyrode's-HEPES buffer containing Ca^{2+}. Platelets were activated with the indicated agonists in the presence of 0.5 µM EGTA for store release (A) or for Ca^{2+} influx (B) under stirring conditions. (C) Fura2-labeled platelets were incubated with the indicated concentrations of thapsigargin to analyze TG-induced SOCE. (D) Reduced TG induced SOCE in *5Htt*$^{-/-}$ platelets. Fluorescence was measured with a LS 55 fluorimeter.* p<0.05, ** p<0.01, *** p<0.001. (Wolf *et al.*, PlosOne, 2016)[143]

4.1.11. *5Htt*$^{-/-}$ platelets mediate accelerated clot retraction *in vitro*

Platelet aggregation requires integrin "inside-out" and "outside-in" activation of integrins to enable the interaction with the respective ligands and downstream signaling. "Inside-out" signaling is triggered by increases in intracellular Ca^{2+} concentrations and describes the shift of integrins from a low to a high-affinity state for their ligands. The binding of a ligand to the integrin leads to clustering of the integrins and the initiation of signaling cascades into the platelet in a process termed "outside-in" signaling.[31] Clot

retraction, (the contraction and consolidation of a formed thrombus) is reliant on the "outside-in" signaling of the αIIbβ3 integrin. Upon binding to fibrin (generated from fibrinogen cleavage by thrombin) a reorganization of the platelet cytoskeleton is initiated and as this occurs the integrin links the contractile cytoskeleton to the fibrin fibers thus providing the pulling forces necessary to contract and stabilize a thrombus.[155 32]

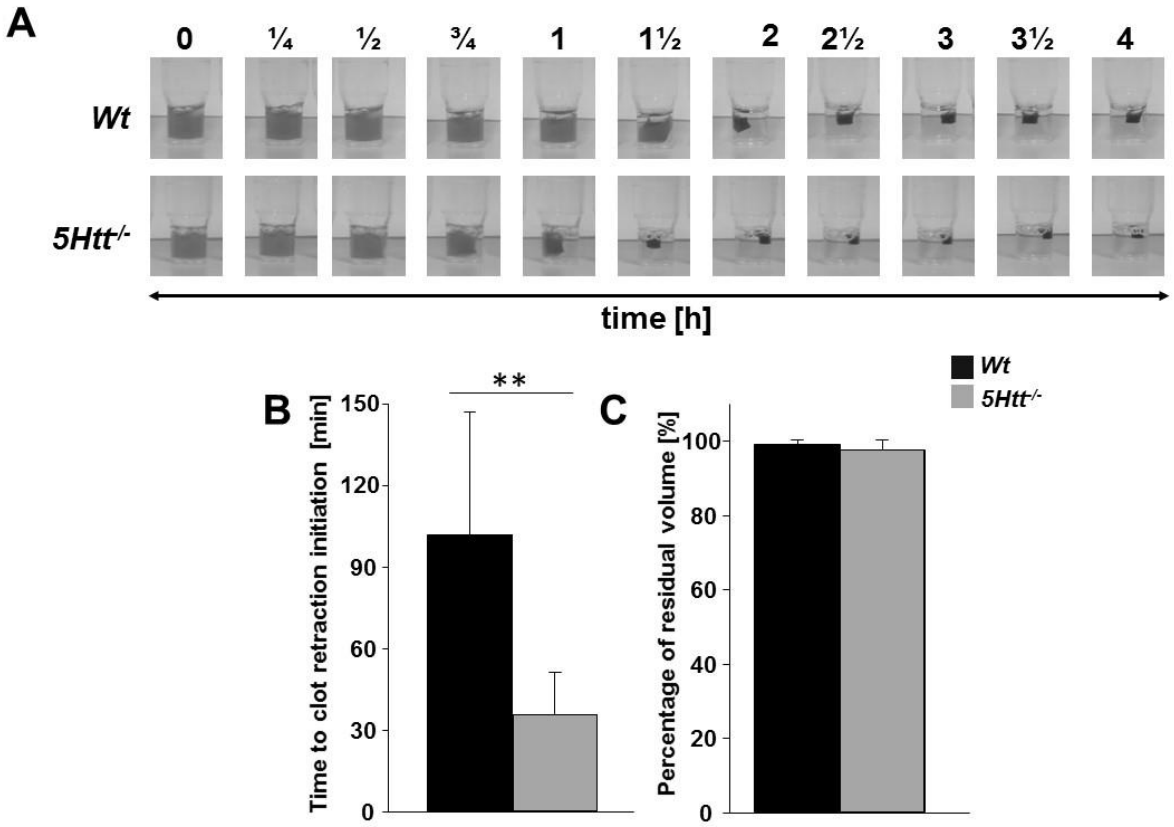

Figure 25: Accelerated clot retraction in 5*Htt*$^{-/-}$ mice. Clot retraction of *Wt* and *5Htt*$^{-/-}$ PRP in the presence of 4 U/mL thrombin and 20 mM $CaCl_2$. (A) Representative images were taken at the indicated time points. (B) Time to initiation of clot retraction and (C) percentage of residual volume were analyzed in *Wt* and *5Htt*$^{-/-}$ PRP. ** p<0.01.

An *in* vitro clot formation and retraction assay was used to test whether the lack of *5Htt* and platelet stored 5-HT has an effect on this process. *Wt* and 5*Htt*$^{-/-}$ PRP in the presence of thrombin (4 U/mL) and 20 mM Ca^{2+} were monitored over 4 h (Figure 25A). In this assay, *5Htt*$^{-/-}$ platelets formed and retracted a similar clot, in terms of size and weight, which resulted in the same residual plasma volume after 4 h (Figure 25C). Within the observation time period however, an accelerated clot retraction was noted in *5Htt*$^{-/-}$ samples as compared to *Wt,* with *Wt* platelets initiating retraction at 83 ± 41 min and *5Htt*$^{-/-}$ platelets at 32 ± 13 min (Figure 25B).

4.1.12. Unaltered spreading of *5Htt*$^{-/-}$ platelets

Similar to clot retraction, platelet spreading requires functional integrin “outside-in” signaling to coordinate and direct the generation of filo- and lamellipodia. In the presence of 5*Htt*$^{-/-}$ platelets clot retraction was accelerated, indicating that integrin “outside-in” signaling may be altered in these platelets. Therefore to have a direct analysis of the platelets themselves platelets from *Wt* and *5Htt*$^{-/-}$ mice were allowed to spread on a fibrinogen coated surface in the presence (Figure 26A) or absence (Figure 26B) of thrombin (0.01 U/mL).

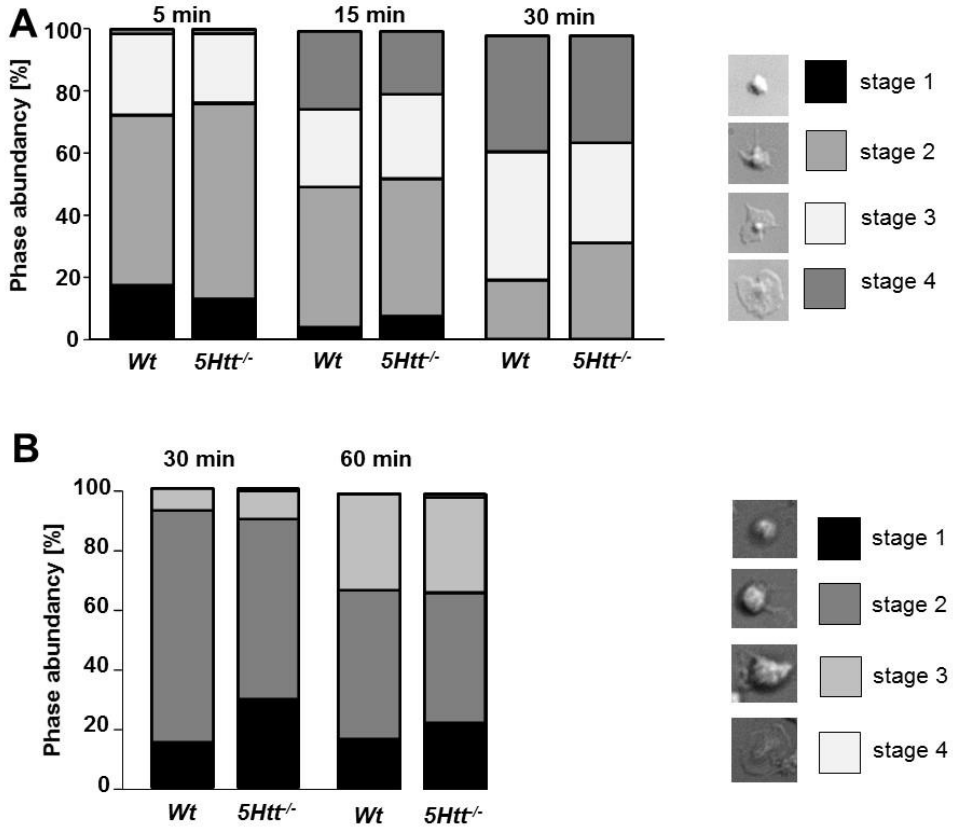

Figure 26: Unaltered spreading of *5Htt*$^{-/-}$ platelets. Washed platelets were allowed to spread on fibrinogen coated cover slips (A) in the presence of 0.01 U/mL thrombin or (B) absence of thrombin. The different stages of spread platelets at the indicated time points were scored according to the appearance of distinct structural features as depicted in the panels on the right (stage 1: roundish; stage 2: filopodia only; stage 3: filopodia and lamellipodia; stage 4: fully spread). (Wolf *et al.*, PlosOne, 2016)[143]

In contrast to the results seen in clot retraction, *5Htt*$^{-/-}$ platelets formed filopodia and lamellipodia with similar kinetics to *Wt* platelets. After 30 min approximately 40 % of *Wt* and *5Htt*$^{-/-}$ platelets were fully spread (Figure 26)

.

4.1.13. Mild reduction of coagulation factors II, VII and X in the *5Htt*$^{-/-}$ plasma of mice

Activated platelets together with the activation of the coagulation system induce the cleavage of platelet released and plasma born fibrinogen to form fibrin- and platelet-rich clots. This mechanism of clot formation through the extrinsic pathway is based on the exposure of TF and its binding of coagulation factor FVII to the endothelium, leading to the activation of the coagulation factors FIX and FX and thus thrombin generation.[156-158] To test whether the lack of 5Htt or platelet stored 5-HT, or indeed the unanticipated reduction in plasma 5-HT levels in *5Htt*$^{-/-}$ mice has an effect on the activation of the coagulation system, plasma samples from *Wt* and 5*Htt*$^{-/-}$ mice were analyzed. The plasma was obtained by centrifugation to measure several coagulation factors and tests (quick, antithrombin, FII, FV, FVII, FX and FXIII). Interestingly, the only alteration observed was a slight reduction in the levels of the coagulation factors II, VII and X in *5Htt*$^{-/-}$ plasma (Table 17).

Table 17: Coagulation factors measured in *Wt* and *5Htt*$^{-/-}$ plasma samples. Non-heparinized blood samples from *Wt* and *5Htt*$^{-/-}$ were collected into sodium citrate. The samples were centrifuged to obtain PPP which was analyzed at the central laboratory at the University Hospital of Würzburg. Partial thromboplastin time (PTT), * p<0.05, ** p<0.01.

	Wt	*5Htt*$^{-/-}$	significance
PTT [s]	26.3±1.4	27.2±1.2	n.s.
Quick [%]	21±0	21±0	n.s.
Antithrombin [%]	134±13	125±19	n.s.
Fibrinogen [g/L]	0.98±0.28	0.78±0.20	n.s.
FII [%]	88±5	72±15	*
FV [%]	642±0	571±52	n.s.
FVII [%]	347±61	259±55	**
FVIII [%]	96±20	80±11	n.s.
FIX [%]	127±11	108±17	n.s.
FX [%]	347±43	281±72	*
FXI [%]	108±24	84±9	n.s.
FXII [%]	141±2	129±9	n.s.
FXIII [%]	344±35	308±19	n.s.

The mRNA expression levels of factor VII and X in liver samples were not altered in *5Htt*$^{-/-}$ mice (Figure 27). This indicated that the observed reduction in the levels of these

proteins was more likely due to a reduced life time in the circulation and/or their faster metabolism than altered protein production.

As there was a minor reduction in coagulation factors II, VII and X detected in plasma samples of *5Htt*$^{-/-}$ mice, thrombin generation was analyzed.

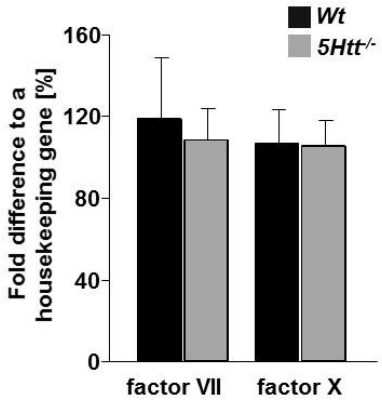

Figure 27: Expression levels of FVII and X in liver samples. Livers of *Wt* and *5Htt*$^{-/-}$ mice were dissected, homogenized and processed for qPCR. The samples were analyzed in collaboration with the Department of Hepatology of the University Hospital of Würzburg.

The lack of the 5-HT transporter, resulting in lower amount of 5-HT in the plasma had no effect on the overall amount (Figure 28A) or the maximal amount (Figure 28B) of newly generated thrombin. The time to peak (Figure 28C), as well as the lagtime of thrombin generation (Figure 28D) was unaltered in *5Htt*$^{-/-}$ plasma compared to the *Wt* samples.

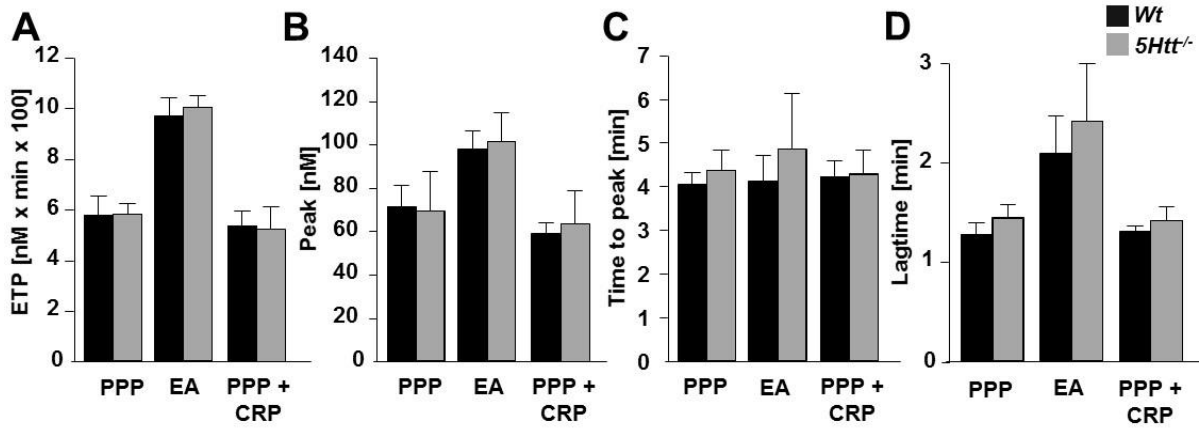

Figure 28: Thrombin generation was unaltered in *5Htt*$^{-/-}$ platelets compared to *Wt* controls. Thrombin generation was measured in unstimulated or CRP-stimulated PPP using the Thrombinoscope. Thrombin generation was triggered by TF and phospholipids or ellagic acid (EA). (A) Endogenous Thrombin Potential (ETP), (B) peak, (C) time to peak and (D) lagtime were unaltered in *5Htt*$^{-/-}$ plasma compared to *Wt* controls. Results are mean ± SD. Analyses were performed by Sarah Beck and Tano Marth in our laboratory.

4.1.14. *5Htt*$^{-/-}$ mice show abnormal platelet adhesion and procoagulant activity under flow

To further investigate the importance of secreted platelet 5-HT for aggregation under shear flow conditions, heparinized blood of *Wt* or *5Htt*$^{-/-}$ mice was perfused over a collagen coated surface at a shear rate of 1000 s^{-1} in the presence of a DyLight488 conjugated anti-GPIX Ig derivative that labels platelets. *Wt* platelets initially adhered to the collagen surface and then recruited additional platelets resulting in the formation of stable, three-dimensional thrombi that finally covered about 40 % of the total surface area. In sharp contrast, in *5Htt*$^{-/-}$ blood samples this process of aggregate formation was strongly reduced by almost three-fold (~15 % surface coverage) (*5Htt*$^{-/-}$: 15.79 ± 14.60 % vs. *Wt*: 43.18 ± 13.79 %, Figure 29B). In line with the reduced surface coverage, the relative thrombus volume was also reduced (*5Htt*$^{-/-}$: 0.45 ± 0.49 vs. *Wt*: 1.32 ± 0.52; Figure 29C).

Ca^{2+} measurements had shown reduced Ca^{2+} influx in *5Htt*$^{-/-}$ platelets. As Ca^{2+} influx is important for the generation of procoagulant platelets the possible effect of 5Htt in the regulation of the procoagulant activity of platelets was assessed,[28,159] heparinized whole blood from *Wt* and *5Htt*$^{-/-}$ mice was perfused over immobilized collagen at a shear rate of 1,000 s^{-1}. Platelets were stained with Annexin-A5-DyLight488 to detect PS exposure. In addition to the surface coverage and relative thrombus volume, the number of platelet exposing PS was dramatically reduced in the aggregates of the mutant animals resulting in a significantly reduced procoagulant index (Figure 29D-F).

4.1.15. Absence of released 5-HT leads to prolonged bleeding times, but unaltered thrombus formation in mesenteric arterioles

The *in vitro* functional analyses of *5Htt*$^{-/-}$ platelets revealed a role for platelet stored 5-HT release and its subsequent signaling in potentiation of Ca^{2+} entry initiated by (hem)ITAM signaling. To address the importance of this 5-HT mediated feed-forward pathway in the more complex processes of thrombosis and hemostasis, *5Htt*$^{-/-}$ mice were subjected to bleeding time analyses and a model of *in vivo* thrombus formation. Prolonged bleeding times were observed in *5Htt*$^{-/-}$ mice (Figure 30A) (*Wt*: 291 ± 194 s vs. *5Htt*$^{-/-}$: 482 ± 279 s) reflecting the increased bleeding risk described to occur upon SSRI treatment.

To test thrombus formation *in vivo*, we subjected the *5Htt*$^{-/-}$ mice to the model of $FeCl_3$-induced mesenteric arteriole injury. Two time points, the time to appearance of first thrombi and the time to full occlusion of the vessel were documented. Interestingly, despite the clear prolongation of bleeding seen in these mice the mean time to appearance of first thrombi larger than 10 µm was similar for *5Htt*$^{-/-}$ mice and *Wt* mice (*5Htt*$^{-/-}$: 8.03 ± 1.41 min; *Wt*: 8.48 ± 1.68 min; Figure 30C). The same is true for the mean time to vessel occlusion of *Wt* 16.15 ± 3.41 min compared to the *5Htt*$^{-/-}$ mice with 16.88 ± 5.29 min (Figure 30D). Representative images of $FeCl_3$-injured vessel of *Wt* and *5Htt*$^{-/-}$ mice are shown in Figure 30B.

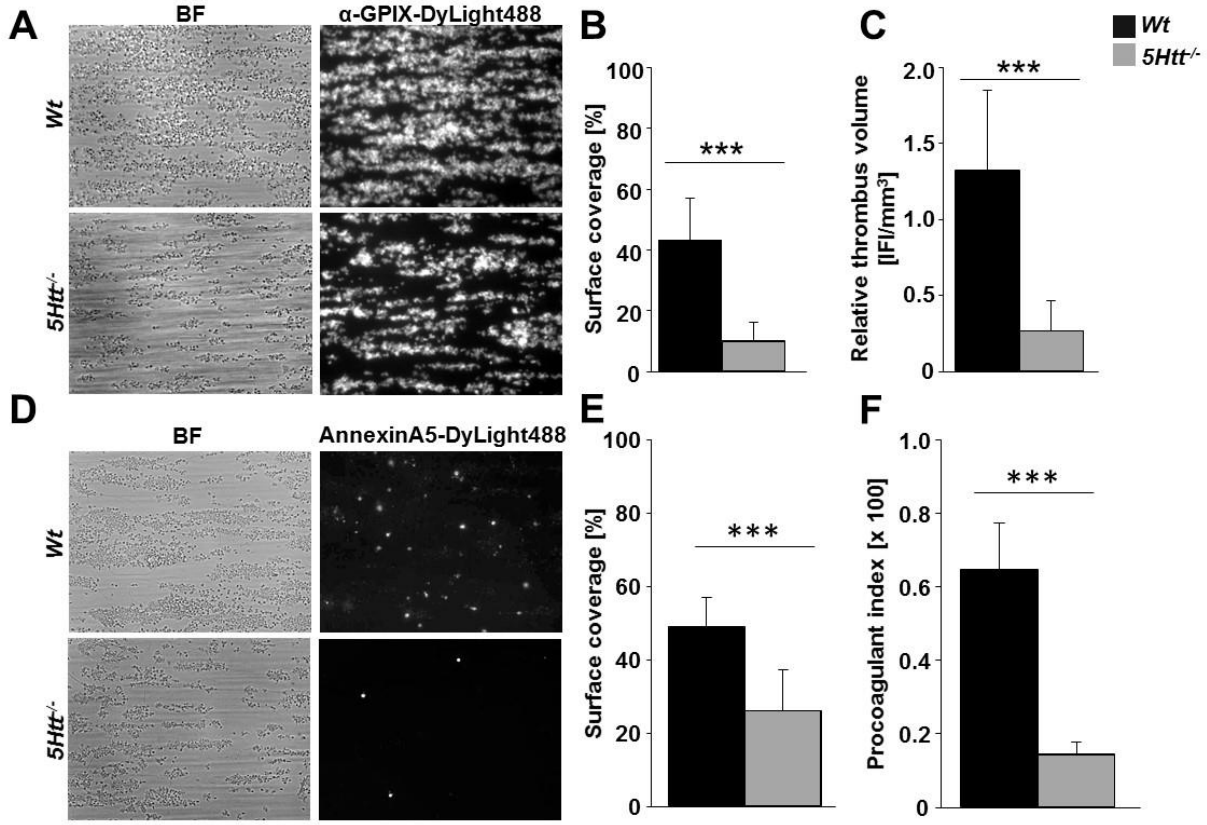

Figure 29: Reduced surface coverage, thrombus formation and procoagulant activity in 5*Htt*$^{-/-}$ mice. Whole blood of *Wt* and *5Htt*$^{-/-}$ mice was perfused over a collagen coated surface with a shear rate of 1000 s^{-1}. Phase contrast videos were recorded and platelet surface coverage, relative thrombus volume and procoagulant index were analyzed. (A) Representative images of surface coverage (left) and relative thrombus volume (right) are shown. Platelets were labeled with an anti-GPIX-DyLight488 derivate to obtain fluorescence images. Statistical evaluation of (B) surface coverage and (C) relative thrombus volume. (D-F) Heparinized whole blood of *Wt* and *5Htt*$^{-/-}$ mice was perfused over a collagen-coated surface with a shear rate of 1,000 s^{-1}. Phase contrast videos were recorded and the chamber was rinsed with Tyrode's-HEPES buffer containing Ca^{2+} and Annexin-A5-DyLight488. Platelet surface coverage and procoagulation index were analyzed. (D) Representative images of surface coverage (left) and procoagulant index (right) are shown. Statistical evaluation of (E) surface coverage and (F) procoagulation index. Results are mean ± SD. Bright field (BF). *** p<0.001. (Wolf *et al.*, PlosOne, 2016)[143]

4.1.16. The lack of secreted 5-HT protects mice from thrombosis

Mechanical injury of the abdominal aorta induces exposure of collagen embedded in the ECM. Therefore this model of experimental arterial thrombosis is understood to be reliant on GPVI expression and signaling.[96] The blood flow in the vessel is monitored with an ultrasonic flow probe for 30 min or until full occlusion occurs. Strikingly, in comparison to the relatively mild hemostatic defect and the unaltered time until vessel occlusion of mesenteric arterioles 80 % of *5Htt*$^{-/-}$ mice were not able to form occlusive thrombi in response to mechanical injury of the abdominal aorta within the observed time period (Figure 31A), whereas 100 % of the *Wt* control mice did. A representative blood flow of *Wt* and *5Htt*$^{-/-}$ mice is shown in Figure 31B.

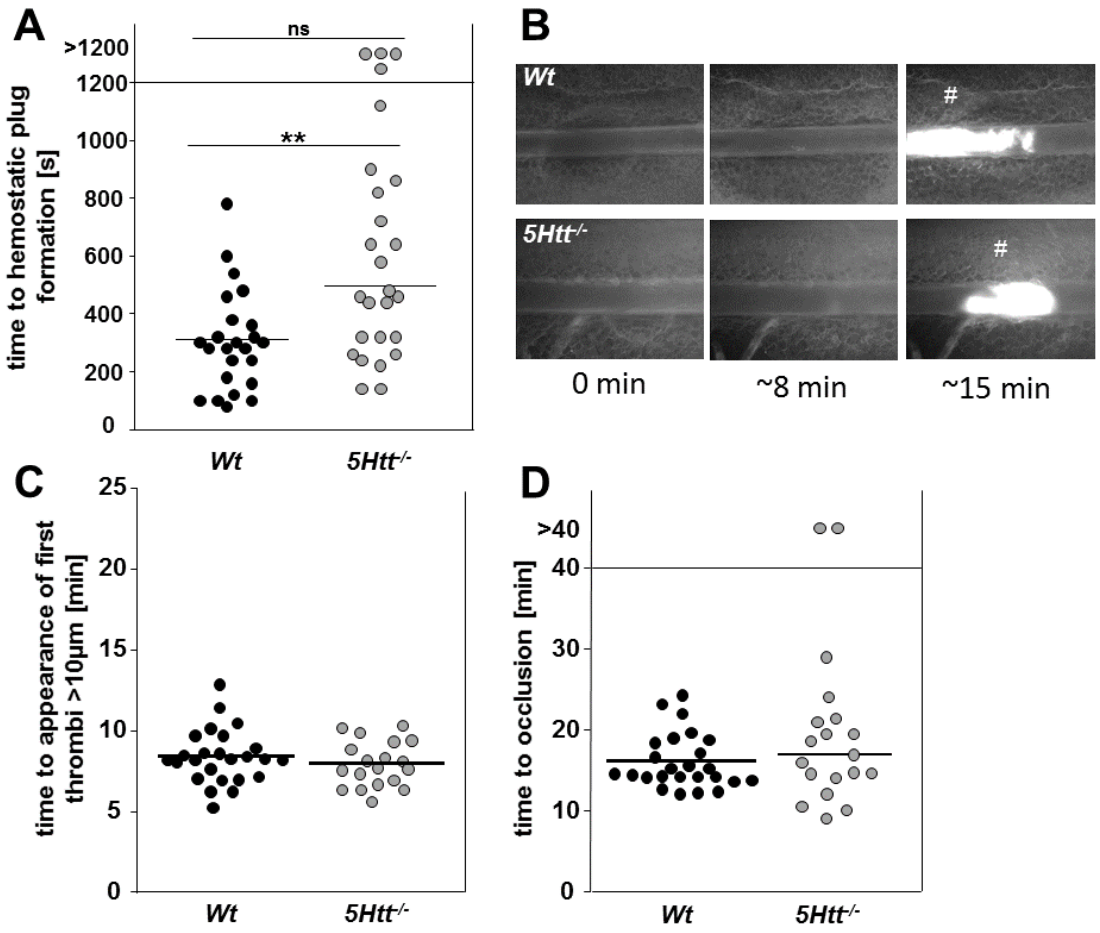

Figure 30: Prolonged bleeding times in 5*Htt*$^{-/-}$ mice, but unaltered thrombus formation upon chemical injury of the mesenteric arterioles in 5*Htt*$^{-/-}$. Altered hemostasis in *5Htt*$^{-/-}$ mice. (A) Time to hemostatic plug formation of *Wt* and *5Htt*$^{-/-}$ mice in the tail bleeding assay. Every symbol represents one animal. (B) Representative images of *Wt* and *5Htt*$^{-/-}$ mice upon chemical injury of mesenteric arteries. (C) Time to appearance of first thrombi >10 µm and (D) time to occlusion of the vessels. Every symbol represents one artery. Horizontal lines represent mean values. Hash indicates stable vessel occlusion. n.s.: not significant, ** p<0.01. (Wolf *et al.*, PlosOne, 2016)[143]

Subsequently *in vivo* thrombus formation was also analyzed in the chemically ($FeCl_3$)-injured carotid artery. Thrombus formation in this medium sized vessel occurs through a collagen- and thrombin-driven mechanism.[160] In the control group, all mice formed occlusive thrombi in 416 ± 102 s, whereas in *5Htt*$^{-/-}$ mice, the time was prolonged to 678 ± 393 s or stable thrombi were not formed at all (Figure 31C).

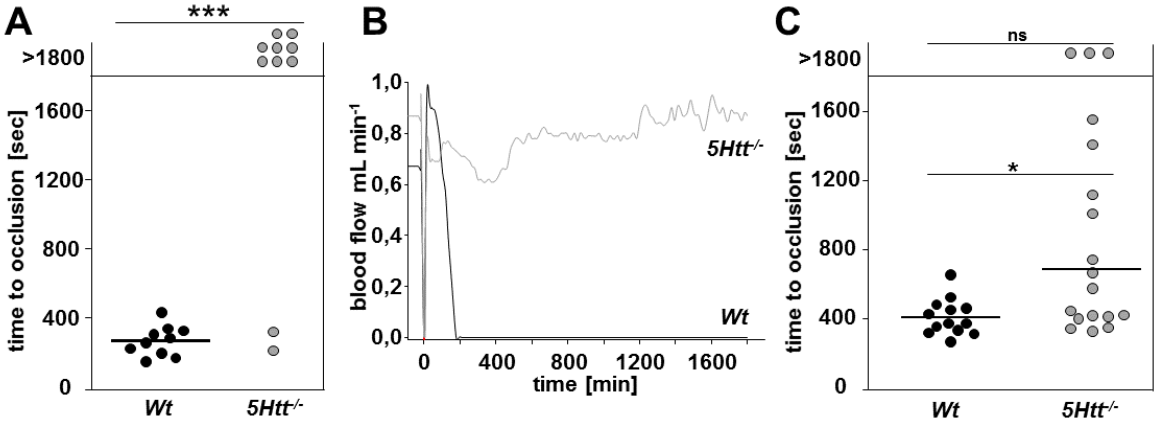

Figure 31: Altered thrombus formation in *5Htt*$^{-/-}$ mice. (A) Time to occlusion with a stable thrombus in the mechanically injured abdominal aorta of *Wt* and *5Htt*$^{-/-}$ mice. (B) Blood flow chart of a representative mechanical injured abdominal aorta of *Wt* and *5Htt*$^{-/-}$ mice. (C) Time to occlusion of the chemical injured carotid artery (10 % $FeCl_3$). Every symbol represents one mouse. Horizontal lines indicate mean time values. n.s.: not significant, * p<0.5, *** p<0.001. (Wolf *et al.*, PlosOne, 2016)[143]

4.1.17. Loss of 5HTT in mice does not alter brain infarct progression after ischemic stroke

Platelets play a unique role in the initiation of brain infarct growth after transient ischemia. This process, as it is currently understood, involves a complex interplay between platelets and immune cells but is not dependent on platelet aggregation. Interestingly, SSRI treatment of stroke patients is described to enhance brain function recovery, indicating a therapeutic benefit of the direct blockade of 5HTT function.[161-163] Given the distinct mechanisms thought to be involved in thrombo-inflammation and the described benefit of SSRI treatment of stroke patients, *5Htt*$^{-/-}$ mice were subjected to the tMCAO model of acute ischemic stroke to further investigate the direct role of 5HTT and platelet stored 5-HT under ischemic conditions.

Although *5Htt*$^{-/-}$ mice were moderately protected in the carotid artery injury model of thrombosis (Figure 31C), unexpectedly, these mice developed large brain infarcts following tMCAO (Figure 32A) with neurological outcomes indistinguishable to those in *Wt* mice as assessed by the Bederson score (Figure 32C) and grip test (Figure 32D). Of note, leukocyte infiltration into the infarct area was not elevated in *5Htt*$^{-/-}$ brain tissue

(Figure 33), and no significant difference between *Wt* and *5Htt*$^{-/-}$ mice were detected in the tMCAO model after 30 min ischemia (Figure 32E-H).

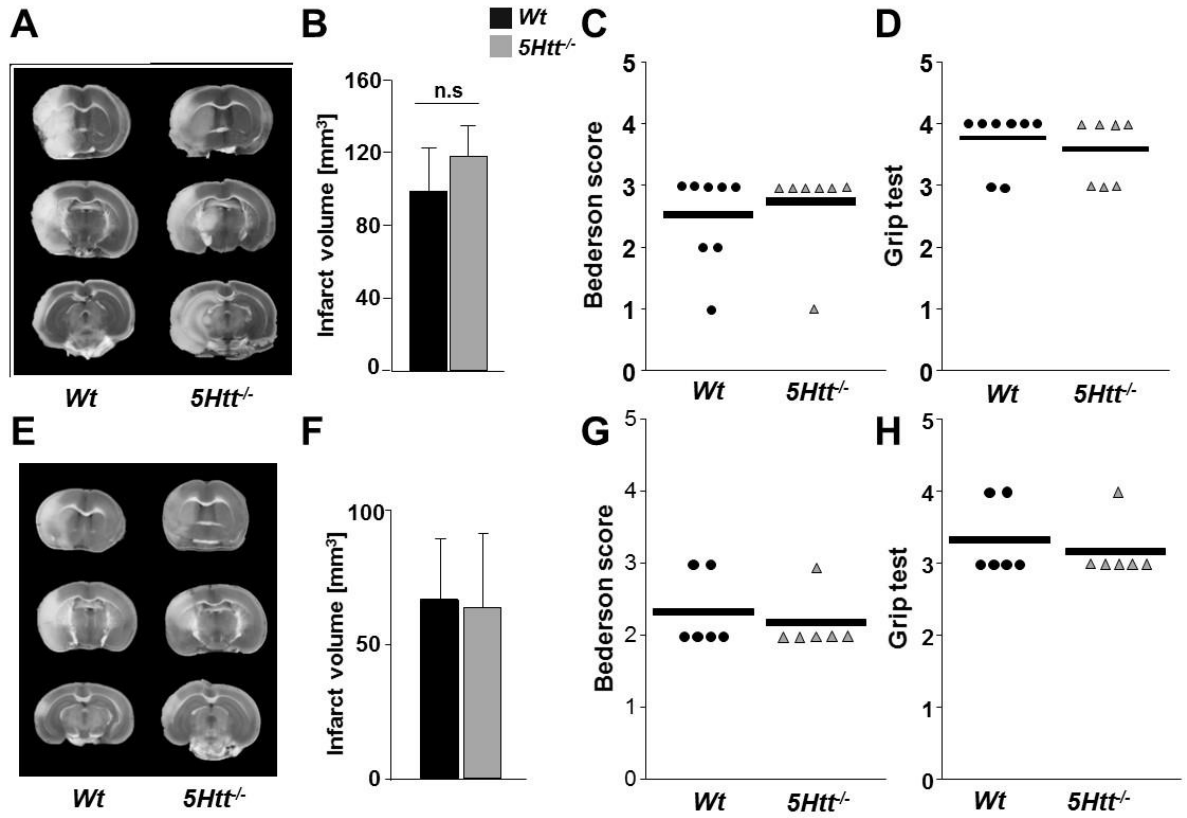

Figure 32: Similar brain infarct volume in 5*Htt*$^{-/-}$ and *Wt* mice in reperfusion injury of 60 and 30 min. (A) Representative images of 3 coronal brain sections stained with TTC 24 h after the 1 h tMCAO. (B) Infarct volume was analyzed by planimetry of *Wt* and 5*Htt*$^{-/-}$ mice 24 h after focal cerebral ischemia in *Wt* and 5*Htt*$^{-/-}$ mice. (C) Bederson score and (D) grip test were determined 24 h after tMCAO. (E) Representative images of 3 coronal brain sections stained with TTC after 24 h following the 30 min tMCAO model. (F) Infarct volume was analyzed by planimetry of *Wt* and *5Htt*$^{-/-}$ mice 24 h after focal cerebral ischemia in *Wt* and 5*Htt*$^{-/-}$ mice. (G) Bederson score and (H) grip test were determined 24 h after tMCAO. Each symbol represents one animal. n.s.: not significant. The experiment was performed in collaboration with Dr. Peter Kraft and Dr. Michael Schuhmann in the Department of Neurology at the University Hospital of Würzburg, Germany. (Wolf *et al.*, PlosOne, 2016)[143]

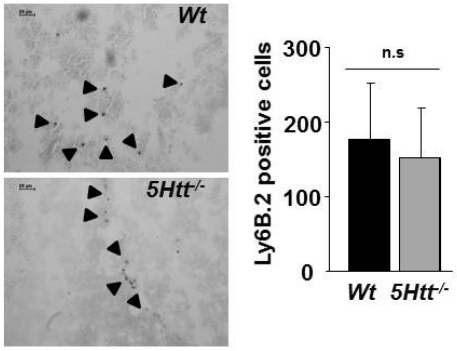

Figure 33: Leukocyte infiltration in ischemic stroke brains of *Wt* and *5Htt*$^{-/-}$ mice. Number of infiltrated leukocytes in the ischemic brain of *Wt* and *5Htt*$^{-/-}$ mice. Representative pictures of Ly6B.2 immunostaining shows similar numbers of leukocytes in ischemic brains of *Wt* and *5Htt*$^{-/-}$ mice. Arrows indicate leucocytes. Results are mean ± SD. (Wolf *et al.*, PlosOne, 2016)[143]

4.2. Addition of extracellular 5-HT rescues the phenotype of *5Htt*$^{-/-}$ mice

4.2.1. The integrin activation and degranulation defect of *5Htt*$^{-/-}$ platelets is rescued by the addition of 5-HT

Integrin activation and degranulation in *5Htt*$^{-/-}$ platelets was reduced upon stimulation with GPVI or CLEC-2 agonists (Figure 17). It is known that 5-HT infused mice show higher integrin activation and degranulation in comparison to saline infused mice, indicating that 5-HT can promote platelet activation.[53] To test whether the addition of 5-HT can revert the phenotype, integrin activation and P-selectin exposure in the presence of 5-HT were measured by flow cytometry. Integrin activation (Figure 34A) and degranulation (Figure 34B) upon stimulation with GPCR agonists were unaltered in *5Htt*$^{-/-}$ mice, whereas it was impaired in response to GPVI and CLEC-2 agonists.

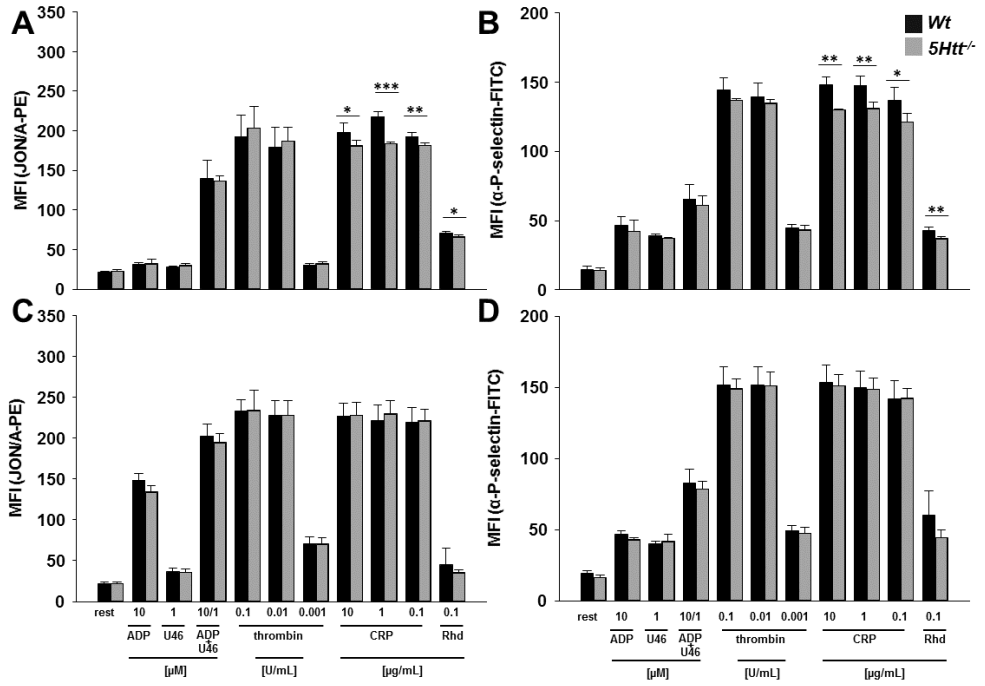

Figure 34: Integrin activation and degranulation can be rescued by the addition of 10 µM 5-HT. Flow cytometric analyses of (A, C) integrin activation and (B, D) degranulation, shown by P-selectin exposure on platelets. Washed blood was incubated for 15 min at RT with the indicated agonists and measured with a FACSCalibur. Flow cytometry analyses of (C) integrin activation and (D) degranulation rescued by the addition of 5-HT. Washed blood was incubated for 15 min at RT with indicated agonists in the presence of 10 µM 5-HT and measured with a FACSCalibur. Results are MFI ± SD (n = 5 vs 5 mice, 3 independent experiments). Resting (rest), adenosine diphosphate (ADP), U46619 (stable TxA_2 analog, U46), collagen-related peptide (CRP), rhodocytin (Rhd). * p<0.05, ** p<0.01, *** p<0.001. (Wolf *et al.*, PlosOne, 2016)[143]

This defect upon activation with GPVI and CLEC-2 agonists was rescued by the *in vitro* addition of 10 µM 5-HT to the washed platelets. Integrin activation (Figure 34C) and P-selectin exposure (Figure 34D) were normalized to *Wt* values. These results indicate that not the lack of 5HTT, but the resulting lack of 5-HT in the platelets is responsible for the defects in integrin activation and degranulation. To be more specific, the second feedback loop of 5-HT triggered by the receptor 5-HT_{2A} on the platelet surface appears to potentiate the signaling downstream of (hem)ITAM receptors.

4.2.2. Aggregation responses of *5Htt*$^{-/-}$ platelets are normalized to *Wt* platelets in the presence of 5-HT

Aggregation responses were reduced upon stimulation with different agonists in *5Htt*$^{-/-}$ platelets (Figure 21). As addition of 10 µM 5-HT rescued integrin activation and degranulation responses in *5Htt*$^{-/-}$ platelets, it prompted us to test if defective aggregation could also be rescued in this way. To test this platelet aggregation experiments were performed with a Fibrintimer 4-channel aggregometer and platelet activation was recorded upon stimulation with indicated agonists in the presence of 10 µM 5-HT. Consistent with the results obtained in flow cytometry, platelet aggregation was rescued by the addition of 10 µM 5-HT (Figure 35).

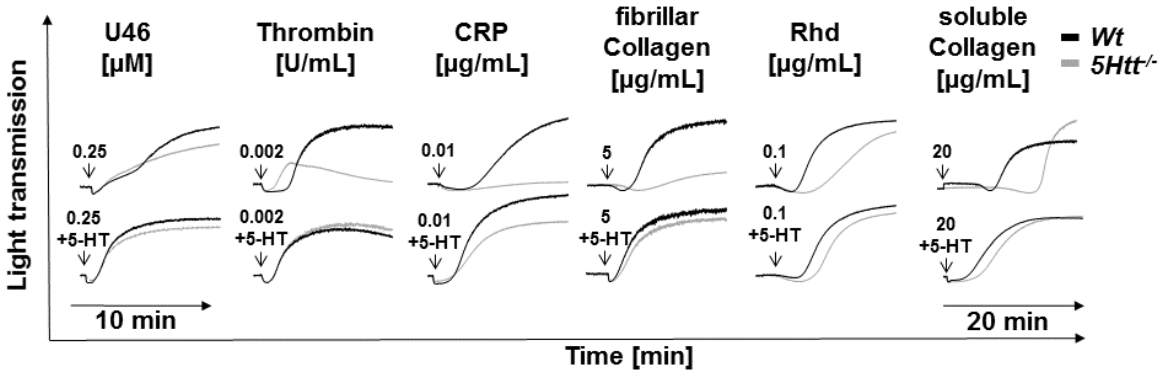

Figure 35: The addition of 10 µM 5-HT can rescue aggregation responses in *5Htt*$^{-/-}$ platelets. Washed platelets were activated with the indicated agonists and 5-HT was added. Light transmission was recorded with a Fibrintimer 4-channel aggregometer. Addition of the agonists is indicated with an arrow. ADP measurements were performed in PRP, whereas all others were done with washed platelets. (Wolf *et al.*, PlosOne, 2016)[143]

4.2.3. Ca^{2+}-mobilization in *5Htt*$^{-/-}$ platelets downstream of (hem)ITAM signaling is rescued by co-stimulation with 5-HT

In line with the previous results, Ca^{2+}-response in *5Htt*$^{-/-}$ platelets upon stimulation with different agonists in the presence of extracellular Ca^{2+} was also rescued by the addition

of 10 µM 5-HT (Figure 36B). This result is a reflection of the well-known potentiation effect of 5-HT on platelet activation mediated by the $G_{q/11}$ signaling of its receptor 5-HT_{2A}.

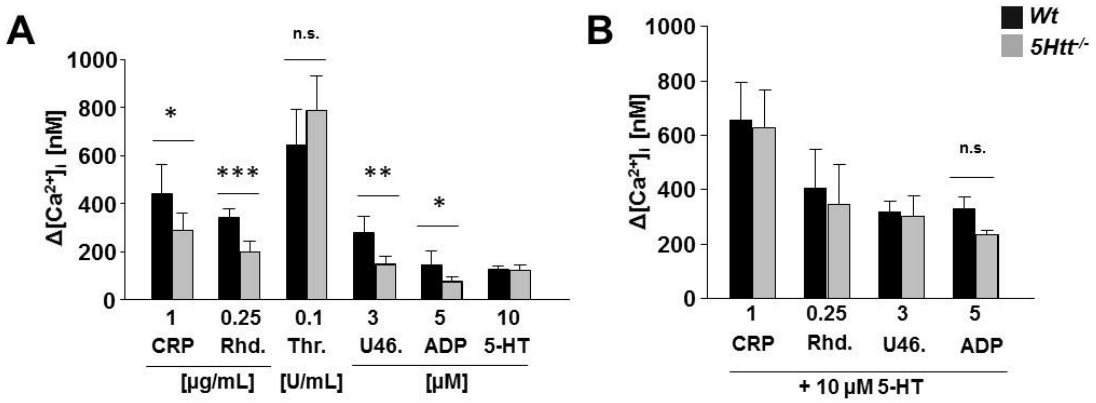

Figure 36: SOCE mediated Ca^{2+} mobilization with and without extracellular 5-HT. Washed platelets were labeled with fura-2AM in the presence of pluronic F-127 for 20 min at 37°C. Excess dye was removed by centrifugation and the platelet pellet was resuspended in Tyrode's-HEPES buffer containing Ca^{2+}. Platelets were activated with the indicated agonists in the absence (A) or presence (B) of 10 µM 5-HT under stirring conditions and fluorescence was measured with a LS 55 fluorimeter. n.s.: not significant, * p<0.05, ** p<0.01, *** p<0.001. (Wolf *et al.*, PlosOne, 2016)[143]

4.2.4. Adhesion defect of *5Htt*$^{-/-}$ platelets under flow is rescued by coinfusion of 5-HT

In vitro analyses of *5Htt*$^{-/-}$ platelets activated with different agonists in the presence of 5-HT showed a rescue of their phenotype, indicating that *ex vivo* responses of aggregation and thrombus formation may also be reverted by the addition of 5-HT.

To test the effect of extracellular 5-HT on the ability of *5Htt*$^{-/-}$ platelets to form thrombi under shear conditions, heparinized whole blood coinfused with 5-HT was perfused over a collagen coated surface at a shear rate of 1,000 s^{-1}. Under these conditions the surface coverage (*5Htt*$^{-/-}$: 58.57 ± 6.01 % vs. *Wt*: 64.4 ± 4.79 %; Figure 37B) and relative thrombus formation (*5Htt*$^{-/-}$: 1.86 ± 0.50 unit vs. *Wt*: 2.29 ± 0.69 unit; Figure 37C) in *Wt* and *5Htt*$^{-/-}$ samples were not significantly different.

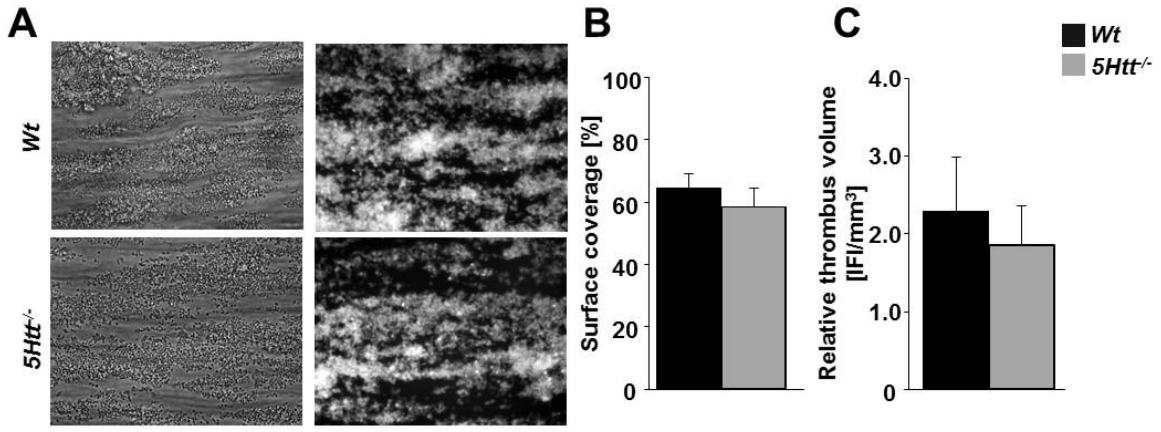

Figure 37: Surface coverage and thrombus volume in the flow chamber assay is similar between *Wt* and *5Htt*$^{-/-}$ mice coinfused with 5-HT. Whole blood was perfused over a collagen coated surface. (A) 5-HT was coinfused at 1,000 s^{-1}. Afterwards surface coverage (B) and relative thrombus volume (C) was analyzed. Fluorescence pictures were obtained by staining of platelets with anti-GPIX-DyLight488. Results are mean ± SD. (Wolf *et al.*, PlosOne, 2016)[143]

4.3. *In vivo* studies of genetically modified mice in different arterial thrombosis models

4.3.1. *Tph1*$^{-/-}$ mice show slightly reduced thrombus formation upon chemical or mechanical injury of the vessel wall

The observed *in vitro* defects translated into defective *in vivo* thrombus formation in *5Htt*$^{-/-}$ mice. To investigate the role of plasma 5-HT in thrombus formation, a mouse strain (*Tph1*$^{-/-}$) lacking the enzyme responsible for the production of 5-HT in the periphery, leading to the absence of 5-HT in the whole circulation, but not in the brain, was analyzed *in vivo*. The platelets of *Tph1*$^{-/-}$ mice showed normal aggregation curves upon stimulation with U46619, thrombin and collagen, whereas bleeding times were prolonged in the *Tph1*$^{-/-}$ mice. The defective hemostasis in *Tph1*$^{-/-}$ mice was reflected in the defective *in vivo* thrombus formation seen in the thrombosis injury model of mesenteric arteries.[49]

Time to appearance of first thrombi upon chemical injury of mesenteric arterioles was similar between *Wt* and *Tph1*$^{-/-}$ mice (*Wt*: 7.31 ± 1.27 min and *Tph1*$^{-/-}$: 8.88 ± 3.65 min; Figure 38B). In line data reported by Walther *et al.*,[49] these mice displayed a defect in thrombus formation upon chemical injury of the mesenteric arterioles with a slightly prolonged time to vessel occlusion (*Wt* 13 ± 4.94 min, *Tph1*$^{-/-}$ 20.05 ± 6.41 min, Figure 38C). Similarly, the time to occlusion by mechanical or chemical injury of the abdominal aorta or carotid artery was also prolonged in this mouse line (Aorta: *Wt*: 246 ± 72 s;

Tph1$^{-/-}$: 429 ± 188 s; Figure 38D; Carotis: *Wt:* 224 ± 30 s; *Tph1*$^{-/-}$: 452 ± 177 s; Figure 38E).

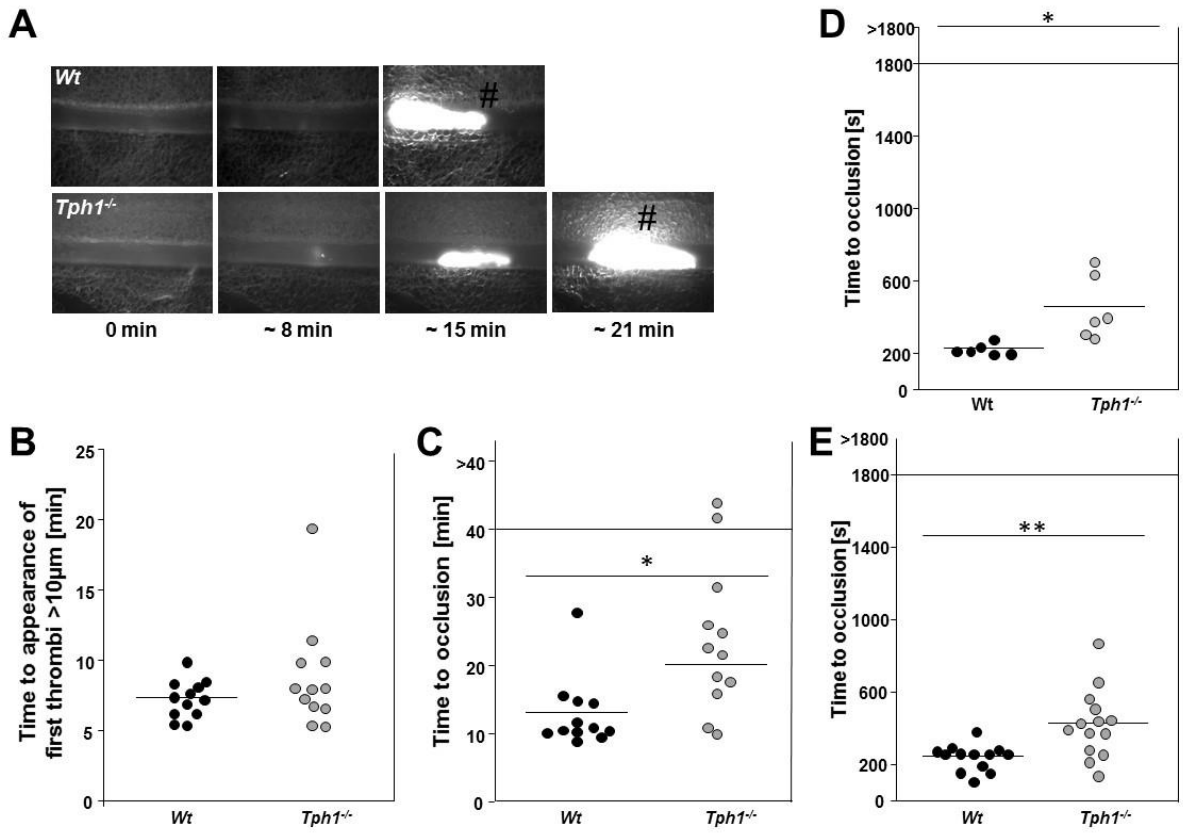

Figure 38: Defective thrombus formation in *Tph1*$^{-/-}$ mice. (A) Representative images of thrombus formation in *Wt* and *Tph1*$^{-/-}$ mice. (B) Time to appearance of first thrombi (C) and time to occlusion in $FeCl_3$-injured mesenteric arteries. Each symbol represents one artery. (D) Occlusive thrombus formation in the mechanically injured abdominal aorta in *Tph1*$^{-/-}$ mice.(E) Occlusive thrombus formation in the thrombosis model of chemically injured carotid artery in *Tph1*$^{-/-}$ mice. Each symbol represents one mouse. The horizontal lines indicate the mean time to appearance of first thrombi or vessel occlusion. Hash indicates stable occlusion of the vessel. * = p<0.05, *** = p<0.001.

4.3.2. *Unc13d*$^{-/-}$*/Nbeal2*$^{-/-}$ mice have a severe defect in thrombosis

Under physiological conditions, 5-HT is stored in dense granules of resting platelets and released upon stimulation. The defective occlusive thrombus formation in *5Htt*$^{-/-}$ mice indicated a major role of granules and their contents in thrombus formation and stability. Mice lacking α-granules and dense granule release (*Unc13d*$^{-/-}$*/Nbeal2*$^{-/-}$) were analyzed to investigate the role of granules and their content in the process of thrombus formation *in vivo*.

Stegner *et al.*[107] and Deppermann *et al.*,[108] from our group showed a protection of the Munc13d and Nbeal2 single *Ko* mice, in different thrombosis models, indicating that the fusion of granules with the PM and the release of their contents plays a major role

in platelet activation, thrombus growth and stability. In line with these results, we could show a strong defect in thrombus formation and stability upon mechanical injury of the abdominal aorta of the double deficient mice. The mice had only small aggregates forming at the site of the injury, but there were no larger thrombi detected in this mouse line upon mechanical injury of the abdominal aorta. No occlusive thrombi were detected in the arteries of the *Ko* mice, whereas all arteries of the *Wt* mice displayed occlusive thrombi within the normal time frame (time to occlusion *Wt:* 270 ± 74 s; Figure 41C).

These results indicated a major role of granule contents in the process of thrombus formation and stability. Various mediators (like 5-HT, ADP, TxA_2 and TGF-β), coagulation factors (like FV, FXI and FXIII) and several other molecules are stored in the granules and are thus important in platelet activation, hemostasis and thrombosis.[164]

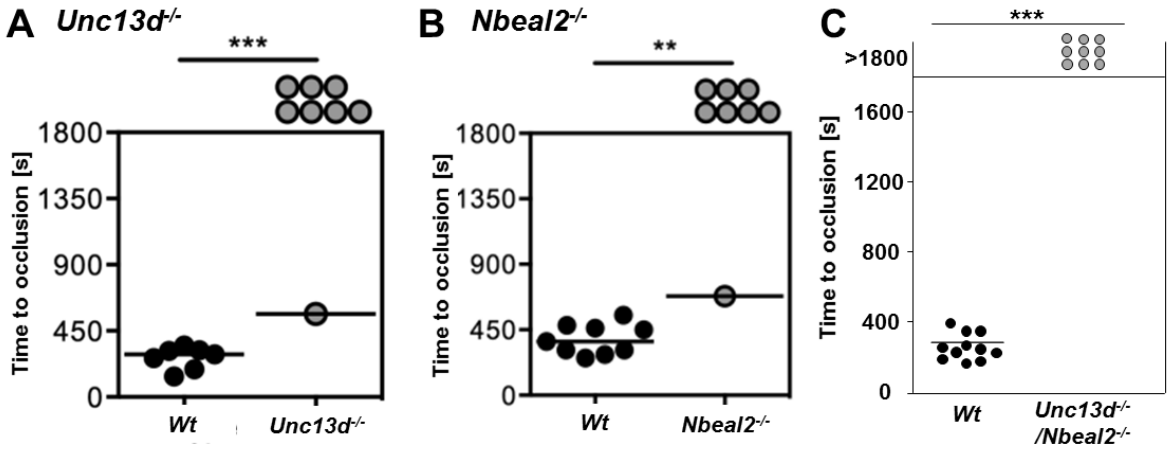

Figure 39: The lack of granules and degranulation protected mice from occlusive thrombi upon mechanical injury of the abdominal aorta. (A) Time to occlusion of *Unc13d*$^{-/-}$ mice, (B) *Nbeal2*$^{-/-}$ mice and (C) *Unc13d*$^{-/-}$/*Nbeal2*$^{-/-}$ mice in the mechanical injury of the abdominal aorta. Each symbol represents one mouse. The horizontal lines indicate the mean time to vessel occlusion. ** = p<0.01, *** = p<0.001. (Figures taken from (A) Stegner *et al.*; JTH 2013 and (B) Deppermann *et al*.; J Clin Invest 2013)[107,108]

4.3.3. TRPM7 channel is dispensable for thrombosis

The uptake of 5-HT via its transporter is important to clear the external milieu from 5HT and to store it for later use in potentiating platelet activation and thrombus stability. Several other molecules or cations are also taken up and stored by platelets. To investigate the role of Ca^{2+}/Mg^{2+} and its transporters in thrombus formation, three different mouse lines, *MagT1*$^{y/-}$ (lacking the specific Mg^{2+} transporter), *Trpm7*$^{fl/fl\text{-}Pf4Cre}$ (lacking

the non-specific Mg^{2+} channel) or *Trpm7^{KI}* (point mutation in the kinase domain of Trpm7 channel, lacking kinase activity) were analyzed in *in vivo* models of thrombosis.

To test the role of the Trpm7 channel activity in platelet activation, thrombus growth and stability was assessed *in vivo*. Upon chemical injury of the mesenteric arterioles, the time to appearance of first thrombi (8.60 ± 1.77 min; 9.16 ± 2.08 min; Figure 40B), as well as the time to occlusion (*Wt* 17.11 ± 4.70 min, *Trpm7$^{fl/fl\text{-}Pf4Cre}$* 17.23 ±6.71 min, Figure 40C) was not significantly different between *Wt* and *Trpm7$^{fl/fl\text{-}Pf4Cre}$* mice.

Representative images are shown in Figure 40A. The same was also true for the mechanical injury of the abdominal aorta, where no difference between *Wt* and *Trpm7$^{fl/fl\text{-}Pf4Cre}$* mice were detectable (302.64 ±116.06 s; 299.22 ±173.37 s, Figure 40D). In line with the previous experiments, time to occlusion upon chemical injury of the carotid artery was similar in *Wt* and *Trpm7$^{fl/fl\text{-}Pf4Cre}$* mice (*Wt*: 361.54 ± 80.50 s, *Trpm7$^{fl/fl\text{-}Pf4Cre}$*: 504.77 ± 143.14 s, Figure 40E).

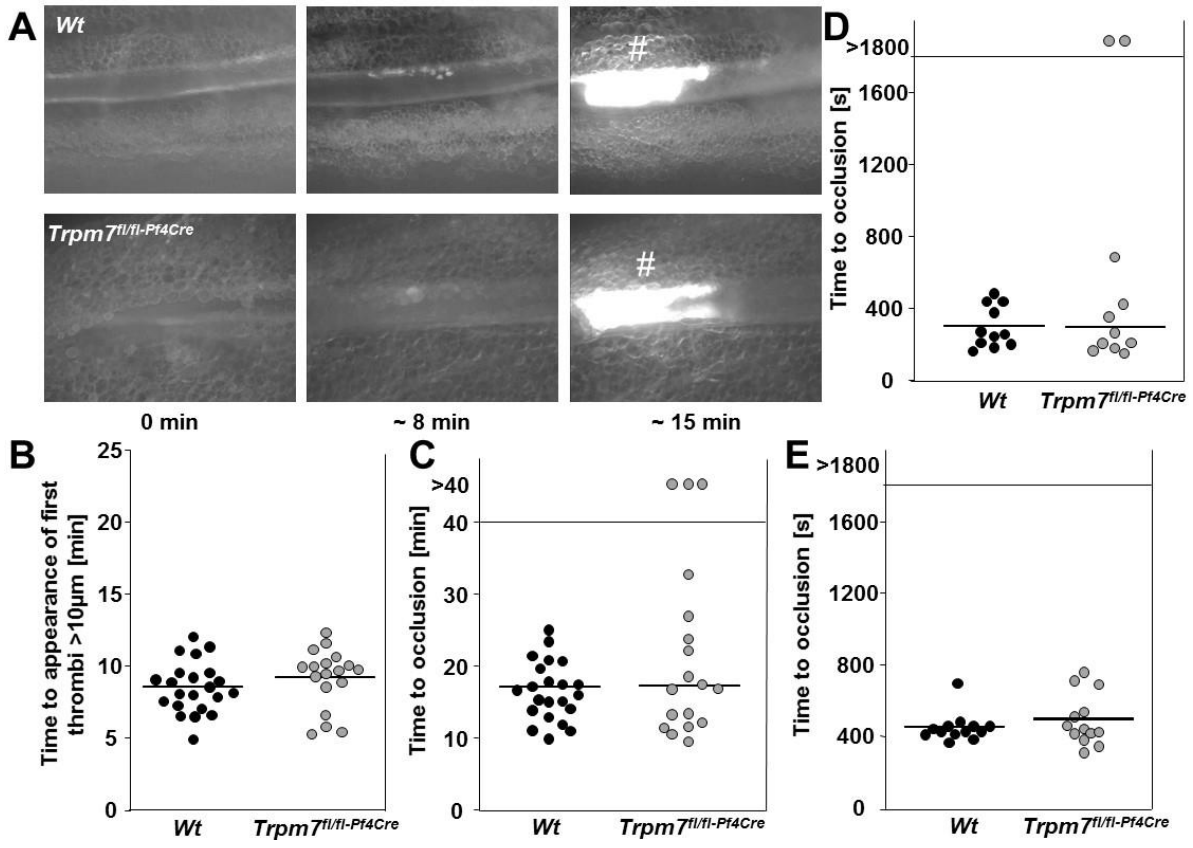

Figure 40: *Trpm7$^{fl/fl\text{-}Pf4Cre}$* mice show no alteration in the different thrombosis models. (A) Representative images of $FeCl_3$-injured mesenteric arterioles of *Wt* and *Trpm7$^{fl/fl\text{-}Pf4Cre}$* mice. (B) Time to appearance of first thrombi and (C) time to occlusion after chemical injury of the mesenteric arteries. Each symbol represents one arteriole. (D) Occlusive thrombus formation upon mechanical injury of the abdominal aorta. One symbol represents one artery. (E) Occlusive thrombus formation in the $FeCl_3$-injured carotid model. Each symbol represents one mouse. The horizontal lines indicate the mean value to appearance of first thrombi or vessel occlusion. Hash indicates stable vessel occlusion.

4.3.4. *Trpm7^{KI}* mice show impaired thrombus formation upon injury

The non-selective Mg^{2+} channel TRPM7 is an unusual ion channel as it also contains an intracellular kinase domain in its C terminal tail. To determine the contribution of this serine/threonine alpha kinase to the function of the channel, and indeed to platelet function, mice were generated with a point mutation (K1646R) in the Mg^{2+}/ATP binding pocket of the kinase domain resulting in abolished kinase activation. Initial *in vitro* studies with heparinized whole blood from *Trpm7^{KI}* mice perfused over collagen showed reduced platelet adhesion and thrombus formation.

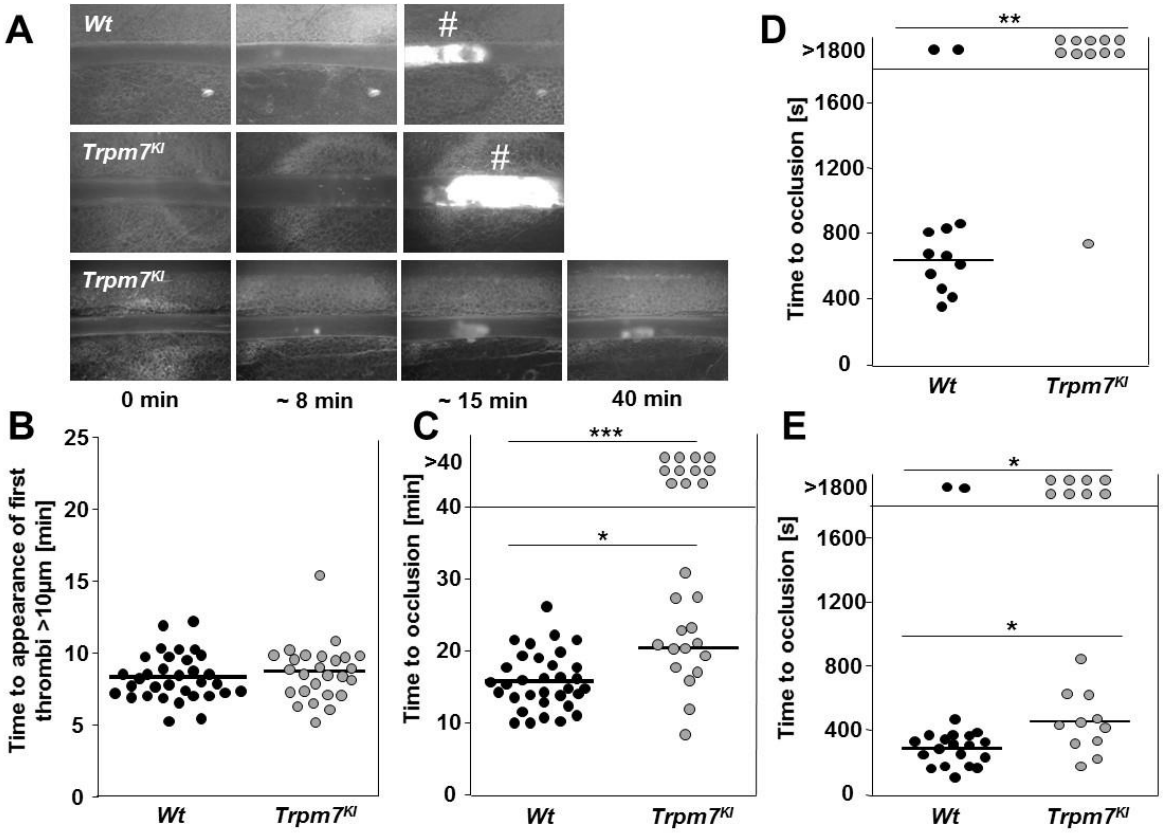

Figure 41: *Trpm7^{KI}* mice show impaired thrombus formation upon injury. (A) Representative images of $FeCl_3$-injured mesenteric arteries of *Wt* and *Trpm7^{KI}* mice. (B) Time to appearance of first thrombi and (C) time to occlusion in the chemical injury of the mesenteric arterioles is shown. Each symbol represents one artery. (D) Occlusive thrombus formation in the $FeCl_3$-injured carotid model. Each symbol represents one mouse. (E) Occlusive thrombus formation upon mechanical injury of the abdominal aorta. Each symbol represents one vessel. The horizontal lines indicate the mean time to appearance of first thrombi or vessel occlusion. Hash indicates stable occlusion in the vessel. * = $p<0.05$, ** = $p<0.01$, *** = $p<0.001$. Graphs B,C and E are combined work by Dr. Martina Morowski and Karen Wolf.

Therefore we performed *in vivo* thrombosis analyses of this mouse line and compared to the results obtained from mice lacking the whole TRPM7 protein. Upon chemical

injury of the mesenteric arteries we could show that the time of appearance of first thrombi was not significantly different between *Wt* and *Trpm7^{KI}* mice (8.43 ± 1.59 min; 8.80 ± 1.96 min; Figure 41B). However when time to occlusion was analyzed, we could observe two populations. 42 % of the mice showed a prolonged time until vessel occlusion and the remaining mice were protected from occlusive thrombus formation in the observed time period. In *Wt* mice all arteries occluded with a mean time to occlusion of 16.10 ± 3.91 min, in *Wt* compared to 20.60 ± 5.66 min in *Trpm7^{KI}* mice (Figure 41C).

Similar to the injury of the mesenteric arterioles, we could observe these two populations in the thrombosis model of mechanical injury of the abdominal aorta, a largely ITAM-signaling-driven thrombosis model.[96] In *Wt* mice 92 % of the arteries were occluded, whereas in the *Trpm7^{KI}* mice 42 % of the arteries showed no occlusion. Time to occlusion in the *Trpm7^{KI}* mice was significantly prolonged in comparison to the *Wt* mice (454 ± 189 s; 297 ± 89 s; Figure 41E).

As we could see these two populations in the two different models, we subjected these mice to a third thrombosis model, the chemical injury of the carotid artery. Upon chemical injury of the carotis, we could observe a protection from occlusive thrombus in the *Trpm7^{KI}* mice. Only one out of 11 arteries showed an occlusive thrombi in the *Trpm7^{KI}* mice, whereas in 83 % of the *Wt* arteries an occlusive thrombi was detected upon injury (Figure 41D).

4.3.5. *MagT1$^{y/-}$* mice display a pro-thrombotic phenotype *in vivo*

MagT1$^{y/-}$ mice showed a pro-thrombotic phenotype in different *in vitro* assays of platelet activation. To test if the *in vitro* defects translated into a pro-thrombotic phenotype *in vivo*, *MagT1$^{y/-}$* mice were subjected to different thrombosis models. The concentration of $FeCl_3$ for chemical injury of mesenteric arteries was reduced from 20 % to 13 % to allow the observation of potential pro-thrombotic phenotype. Under these conditions, *Wt* mice should exhibit delayed occlusive thrombus formation due to the reduced concentration of $FeCl_3$ and the resulting milder injury.[165]

The mean time to appearance of first thrombi upon chemical injury of the mesenteric arteries was significantly reduced in *MagT1$^{y/-}$* mice (*Wt*: 9.28 ± 3.60 min, *MagT1$^{y/-}$*: 6.96 ± 1.21 min; Figure 42B). The time to occlusion in *Wt* mice was prolonged or they were not able to form stable thrombi (47 % of the vessels showed no occlusion),

whereas all vessels of the *MagT1*$^{y/-}$ mice occluded. Mean time to occlusion in *Wt* mice was 17.47 ± 6.29 min and reduced to 11.34 ± 3.38 min in *MagT1*$^{y/-}$ mice (Figure 42C). The mice were in addition subjected to the $FeCl_3$-injured carotid model of thrombosis, the time to occlusion was reduced in *MagT1*$^{y/-}$ mice in comparison to *Wt* mice (time to occlusion: 370 ± 112 s vs. 699 ± 133 s, Figure 42D).

MagT1 is expressed in many different tissues and cells throughout the body.[166] As the *MagT1*$^{y/-}$ mouse was a constitutive knock-out model and not specific to platelets the results from the *in vivo* thrombosis model experiments were not definitive enough to allow the conclusion that the pro-thrombotic phenotype in these mice was solely due to platelet hyperreactivity.

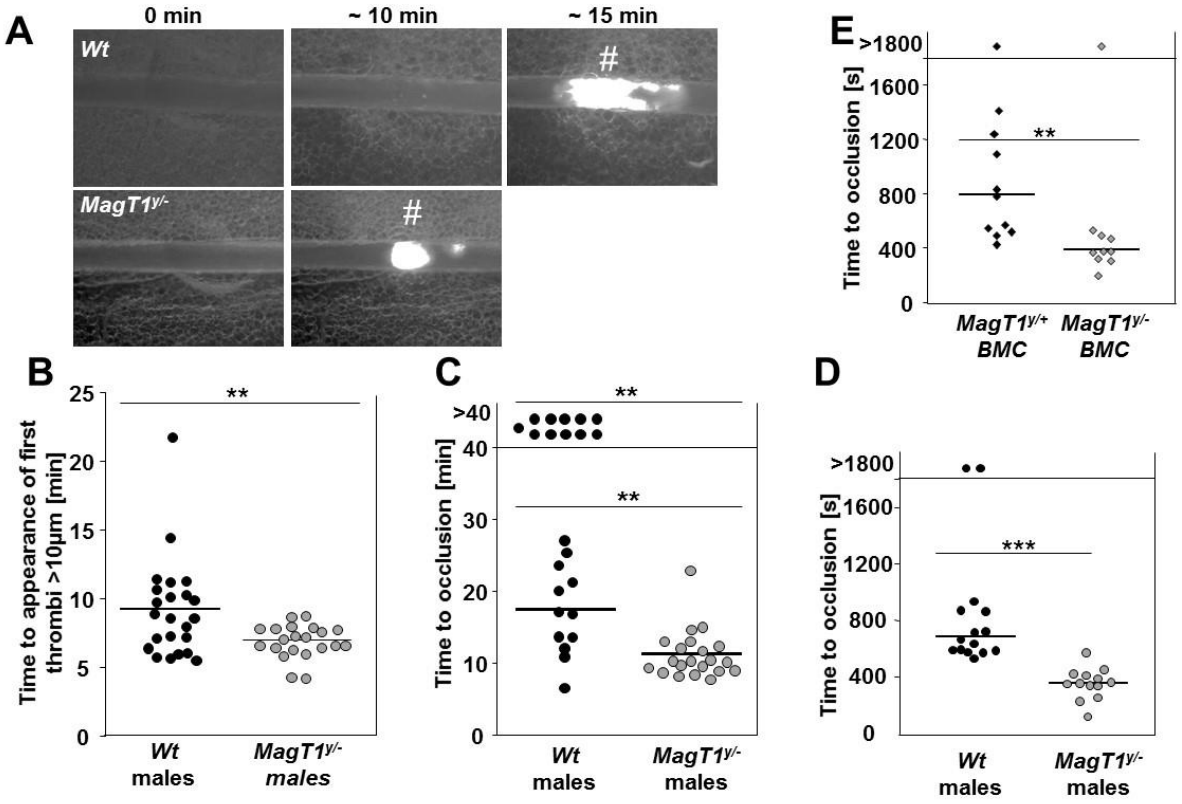

Figure 42: *MagT1*$^{y/-}$ mice show a pro-thrombotic phenotype in the chemically-induced injury of mesenteric arterioles and the carotis. (A) Representative images of the injury of the mesenteric arteries in *MagT1*$^{+/+}$ and *MagT1*$^{y/-}$ mice. (B) Time to appearance of first thrombi and (C) time to occlusion of *MagT1*$^{+/+}$ and *MagT1*$^{y/-}$ mice in the $FeCl_3$-induced (13 %) injury model of mesenteric arterioles, each symbol represents one artery. (D) Occlusive thrombus formation in the $FeCl_3$-injured (6 %) carotid model of *MagT1*$^{+/+}$ and *MagT1*$^{y/-}$ mice. Each symbol represents one vessel.(E) $FeCl_3$-injured (6 %) carotis model in irradiated *Wt* mice transfused with *MagT1*$^{+/+}$ and *MagT1*$^{y/-}$ BMCs. Each symbol represents one artery. Hash indicates stable occlusion in the vessel and the horizontal lines indicate the mean value to appearance of first thrombi or vessel occlusion. ** = p<0.01, *** = p<0.001.

To test whether the enhanced platelet activation seen *in vitro* was responsible for the pro-thrombotic phenotype of *MagT1*$^{y/-}$ mice, we analyzed irradiated *Wt* mice that had

been transplanted with bone marrow cells (BMC) of *Wt* or *MagT1*$^{y/-}$ mice. Similar to the results of the non-chimeric mice, *Wt* mice transplanted with *MagT1*$^{y/-}$ BMCs showed enhanced thrombus formation and the *Wt* mice transplanted with *Wt* BMCs showed a prolonged time until an occlusion of the vessel appeared upon chemical injury of the mesenteric arterioles. The mean time to occlusion of *Wt* mice transplanted with *Wt* BMCs was 795 ± 349 s, whereas in *Wt* mice transplanted with *MagT1*$^{y/-}$ BMCs, the mean time was 383 ± 104 s. (Figure 42E).

4.3.6. *RIAM*$^{-/-}$ mice show normal thrombosis

"Inside-out" integrin activation is an important step in platelet activation. RIAM has been proposed as an important linker between RAP1-GTP and talin1 in αIIbβ3 integrin activation, leading to the high-affinity state of the αIIbβ3 integrin. In contrast to these recent publications,[125,126,167,168] we could not observe any platelet defect *in vitro* in the mutant mice. *RIAM*$^{-/-}$ mice were analyzed in the thrombosis model of chemical injury of the mesentery arterioles, to assess thrombus formation by *RIAM*$^{-/-}$ platelets. Time to stable thrombus formation in this model was similar in *RIAM*$^{-/-}$ mice compared to *Wt* controls (time to occlusion: 982 ± 230 s; 915 ± 293 s; Figure 43B).

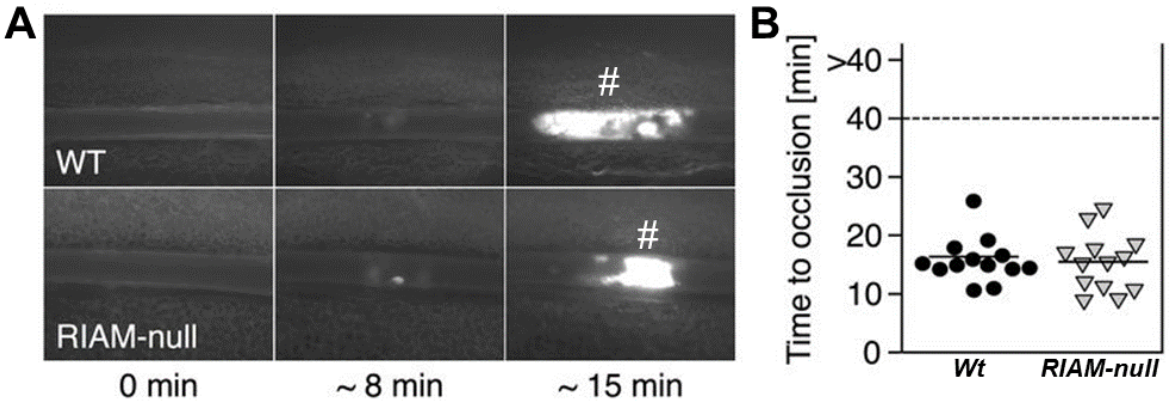

Figure 43: RIAM is dispensable for thrombus formation *in vivo*. (A) Representative images of $FeCl_3$-injured mesenteric arterioles in *Wt* and *RIAM*$^{-/-}$ mice. (B) Time to occlusion in $FeCl_3$-injured mesenteric arterioles. Each symbol represents one artery. Hash indicates stable occlusion of the vessel by thrombi. (Figures taken from Stritt *et al.*; Blood; 2014)[124]

5. Discussion

The major causes of death in the western world are diseases associated with thrombotic events such as myocardial infarction and stroke.[89] Under normal conditions platelet activation and aggregation are essential in the process of hemostatic plug formation, preventing blood loss and sealing wounds after vascular injury. However, uncontrolled platelet activation leading to pathological thrombus formation can result in acute cardiovascular disease states, like thrombosis and ischemic infarction. To combat thrombosis-related disease, research has focused on anti-thrombotic drugs targeting both coagulation and platelets. These include heparin, clopidogrel, aspirin and platelet integrin antagonists.[169,170] The limitations of these drugs lie in their bleeding risks, an issue most acutely relevant for surgical interventions and patients who have suffered stroke. Therefore, despite the success of cheap but effective drugs such as aspirin there remains a requirement for a more targeted and balanced approach to anti-platelet therapy ideally targeting new platelet pathways that play a role in thrombosis but are more or less dispensable for hemostasis. To achieve this aim a detailed understanding of platelet function in health and disease is necessary for the selection of new drug targets and the subsequent design of new anti-thrombotics.

The major focus of this work was to identify the role of platelet stored 5-HT in platelet activation, thrombosis and hemostasis. It is known that elevated levels of circulating 5-HT can lead to hyperreactive platelets,[53,171] resulting in increased thrombotic events. Furthermore, humans suffering from psychiatric disorders, such as depression and anxiety disorders are treated with SSRIs with an interesting side effect being a reduced risk for thrombotic events.[161-163,172] SSRIs specifically block the uptake of 5-HT into cells by the 5-HT transporter 5HTT. In the presynaptic neuron (where the action of this drug is intended), the inhibition of 5HTT leads to a high concentration of 5-HT in the synaptic cleft enhancing its signaling capacity in downstream neurons. Due to the fact that 5HTT is expressed ubiquitously, SSRIs also inhibit the uptake of 5-HT in the periphery. Long-term treatment with an SSRI can lead to reduced levels of 5-HT in cells throughout the body, especially in cells incapable of synthetizing 5-HT. One such cell type is platelets, which uptake 5-HT from the circulation and store it in their dense granules at concentrations up to 65 mM for later release.[49] The release of this platelet stored 5-HT during platelet activation is known to constitute one of several so termed “second wave” feedback loops which promote thrombus growth and stability. To understand in more detail the importance of platelet released 5-HT and its uptake system

in platelets, a constitutive *5Htt*$^{-/-}$ mouse line was generated and analyzed in several *in vitro* and *in vivo* studies focused on platelet activation and function in hemostasis, thrombosis and thrombo-inflammation.

5.1. Platelet 5-HT is important for hemostasis, thrombosis and stroke

In human platelets, several 5-HT transporters have been detected at the mRNA level, including 5Htt (*Slc6a4*) and DAT (*Slc6a3*).[173] In line with a previous observation,[53] genetic ablation of *5Htt* in mice completely blocks 5-HT uptake by platelets (Figure 16A). Therefore, we conclude that other pathways cannot compensate for the lack of 5HTT function in these cells. As platelets are the major store of 5-HT in the blood, we hypothesized that blocking the platelet 5-HT uptake mechanism would increase 5-HT levels in the blood, as previously observed in *5Htt*$^{-/-}$ brain.[174] Surprisingly, however, we found strongly reduced 5-HT levels in the blood plasma of *5Htt*$^{-/-}$ mice (Figure 16B). We speculate that the expected increased free 5-HT in the circulation is metabolized by exo-enzymes such as MAO A/B, or alternatively, removed by other cells expressing DAT, NET and OCT1/3 on their surface. It has been described that in the periphery, such as in the in vena cava, 5-HT uptake cannot be blocked with SSRI, indicating that 5-HT is taken up via different transporters expressed in the vasculature.[56]

In β3 integrin knock-out platelets 5-HT uptake was strongly reduced indicating a functional crosstalk between 5HTT and β3 integrins.[145] Our finding that the αIIbβ3 activation defect in response to GPVI or CLEC-2 stimulation in *5Htt*$^{-/-}$ platelets (Figure 17) was fully rescued in the presence of extracellular 5-HT (Figure 34) clearly demonstrates that the crosstalk between 5HTT and β3 is not essential for integrin activation. To further support this, fibrinogen binding to integrins and outside-in signaling of αIIbβ3 integrin were normal during spreading of *5Htt*$^{-/-}$ platelets (Figure 20A and Figure 26). Therefore we assume that the observed activation defect is due the lack of the secreted platelet 5-HT which potentiates (hem)ITAM signaling and thereby “inside-out” activation of integrins through Ca^{2+} dependent (CalDAGGEF) and independent pathways (PKC), induced by 5-HT_{2A}-Gq-PLCβ signaling.

Although 5-HT significantly amplifies platelet reactivity through 5-HT_{2A} signaling and induces platelet shape change, it has been proposed to play a minor role in aggregate formation, since 5-HT alone cannot induce aggregation responses. We found that aggregation responses to collagen or rhodocytin were strongly reduced in *5Htt*$^{-/-}$ platelets (Figure 21) indicating an important role for 5-HT in these signaling pathways. Indeed,

the blockade of 5HTT with the SSRI citalopram reduces the aggregation response to collagen in human platelets,[175] due to reduced Syk phosphorylation in the GPVI signalosome. Additionally, Syk can bind and phosphorylate 5HTT.[176] These results supported the hypothesis that an interaction between 5HTT and Syk might contribute to (hem)ITAM signaling. To test this concept, we activated *5Htt*$^{-/-}$ platelets in different experimental conditions to dissect the possible role of 5HTT in (hem)ITAM signaling. Surprisingly, we could not find any abnormalities in the initial phase of tyrosine phosphorylation cascade of the GPVI or CLEC-2 signalosomes (Figure 22). Demonstrating the indirect role of 5HTT in platelet signaling, we could completely rescue GPVI or CLEC-2 mediated Ca^{2+} influx (Figure 24), integrin activation, degranulation (Figure 17A+B) and aggregation defects (Figure 21) in *5Htt*$^{-/-}$ platelets by the addition of extracellular 5-HT. Furthermore, the significantly reduced platelet covered surface area and aggregate volume observed under flow conditions on a collagen coated surface in *5Htt*$^{-/-}$ blood (Figure 29) was completely rescued by a 5-HT co-infusion (Figure 37). Taking these results together, we conclude that the published interaction between Syk and 5HTT is dispensable for GPVI and CLEC-2 mediated platelet activation.[177]

During platelet activation both integrin activation and degranulation requires the increase in $[Ca^{2+}]_i$ levels mainly mediated by SOCE.[74] Orai1 mediated SOCE is triggered through the release of Ca^{2+} from intracellular stores and is tightly regulated by functional coupling of activated STIM1 to the Orai1 complex.[178] Interestingly, we found a strongly reduced SOCE in *5Htt*$^{-/-}$ platelets in response to stimulation with not only (hem)ITAM agonists. In agreement with previously published results,[74,178] 5-HT enhanced SOCE through binding to 5-HT_{2A} which activates Gq-PLCβ mediated Ca^{2+} store release, thus contributing to sustained $[Ca^{2+}]_i$ signaling. This was demonstrated by the normalization of SOCE responses after the addition of extracellular 5-HT.[179]

Interestingly, release of Ca^{2+} from the platelet store (triggered by the Ca^{2+}-ATPase inhibitor thapsigargin) was also reduced in *5Htt*$^{-/-}$ platelets. To distinguish the role of intracellular and extracellular 5-HT in SOCE activation, *Unc13d*$^{-/-}$ platelets were used in which dense granule release (responsible for the secretion of many “second wave” mediators, including 5-HT) is abrogated.[180] Similarly to *5Htt*$^{-/-}$ platelets, TG induced SOCE was reduced in *Unc13d*$^{-/-}$ platelets indicating a dispensable role of intracellular 5-HT in SOCE activation (Figure 44) and underscoring the role of secreted platelet 5-HT in the second phase of Orai1 activation. Additionally, it has been shown that TG induced SOCE strongly inhibits 5-HT uptake in human platelets.[83,84]

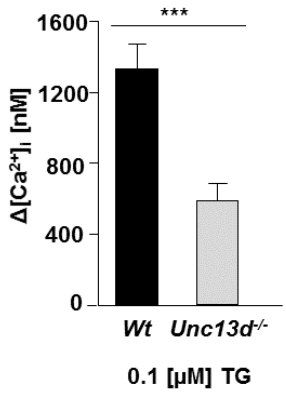

Figure 44: Reduced store release after TG stimulation in *Unc13d*$^{-/-}$ platelets indicating a dispensable role of intracellular 5-HT. Fura2-labeled platelets were incubated with the indicated concentrations of thapsigargin to analyze TG-induced SOCE. Fluorescence was measured with a LS 55 fluorimeter, the excitation was at 340 and 380 nm and the emission at 509 nm.

This could be an important step to keep 5-HT outside of platelets to maximize 5-HT$_{2A}$ activation on the platelet surface.

At sites of vascular injury, 5-HT release by activated platelets contributes to acute thrombotic events[181,182] by promoting vasoconstriction and activation of platelets. The long term use of SSRI has been shown to decrease the 5-HT concentration in human platelets and thereby exert a significant anti-thrombotic effect.[183,184]

In the carotid artery of rats, a 15-fold increase in 5-HT levels was detected upon injury suggesting that 5-HT release from platelets leads to high local availability of this important “second wave” mediator.[185] In agreement with this result, complete block of 5-HT synthesis in the periphery protects mice from occlusive thrombi in the thrombosis model of chemical-injured mesenteric arteries.[49] Furthermore, a direct effect of 5-HT on vascular smooth muscle was found to stimulate vessel wall contraction.[182,186] Based on published data[181,182] and our results showing defective arterial thrombus formation in *5Htt*$^{-/-}$ mice (Figure 30 and Figure 31) we demonstrate that platelet secreted 5-HT may have a paracrine effect on neighboring platelets and other cells at the site of vessel wall injury acting to promote thrombus stability. Furthermore, our results clearly show an additional autocrine effect through 5-HT$_{2A}$ activation which strongly potentiates SOCE activity. The lack of both paracrine and autocrine effects of 5-HT may explain the observed thrombus instability in *5Htt*$^{-/-}$ mice.

Several studies suggest that long term inhibition of 5-HT uptake systems with SSRI increases the risk of bleeding complication in humans.[65,66,187] Prolonged bleeding times were observed in *Tph1*$^{-/-}$ [49] and *5Htt*$^{-/-}$ mice (Figure 30) and this alteration was rescued by addition of extracellular 5-HT into the blood of *Tph1*$^{-/-}$ mice.[49] In line with this, Ziu *et al.*[171] showed that 5-HT infusion with mini-pumps generated hyperreactive platelets in *Wt* mice with reduced bleeding times and occlusion times of the carotid arteries.[188]

Interestingly, 5-HT has been proposed to be involved not only in the potentiation of platelet activation but also in the generation of a particular subtype of activated platelets thought to be important for their pro-coagulant activity. COAT platelets are identified by their coating of adhesive and procoagulant proteins on their surface after activation. It has been demonstrated that 5-HT specifically contributes to this surface network of fibrinogen and factor V through serotonylation.[149] SSRI treatment has been shown to decrease the generation of COAT platelets in humans.[147,149] In contrast to this hypothesis, however, COAT platelet and MP production were normal in *5Htt*$^{-/-}$ mice (Figure 19 and Figure 20) which precludes a fundamental role of secreted or stored platelet 5-HT in these processes.

Stroke patients often suffer from post-stroke depression.[189] During SSRI treatment for the depression, enhanced motor functional recovery is observed in some of these patients.[161-163] Neuroblast proliferation and cell migration in the brain have been shown to be enhanced and associated with increased microvessel density during SSRI treatment, suggesting a possible role for the 5-HT uptake system in tissue repair after ischemic insults.[161] However, using a permanent occlusion model of branches of the middle cerebral artery, SSRI treatment did not reduce infarct size or cerebral edema in mice[161] suggesting that SSRI treatment cannot protect neurons or other cells in the brain during ischemic insults. Therefore, we conclude that SSRI treatment may have a long-term effect in the neurons of ischemic brain which positively influences post-stroke recovery. Using our tMCAO model of ischemic stroke with different time periods of the middle cerebral artery blockage (30min and 1 h) we could not observe major differences between *Wt* and *5Htt*$^{-/-}$ mice (Figure 32). It is important to note that in the brains of *5Htt*$^{-/-}$ mice elevated extracellular 5-HT levels were detected. Given the disruption of the blood brain barrier in the acute and subacute phase after ischemic stroke, elevated level of 5-HT in the brain may induce infiltration of detrimental inflammatory cells from the blood into the brain parenchyma. However, we could not observe increased number of leukocytes in the ischemic infarct area of *5Htt*$^{-/-}$ mice (Figure 33). Further characterization of *5Htt*$^{-/-}$ mice is necessary to understand the role of 5HT in the context of thrombo-inflammation during stroke and infarct progression.

In summary, our results identify 5HTT as the major route of 5-HT uptake in platelets and show that platelet stored 5-HT is critical for hemostasis and thrombosis, but not for cerebral infarct progression in a model of experimental stroke.

5.2. Analyses of genetically modified mice in arterial thrombosis models

The chemical injury of vessels in the mouse with $FeCl_3$ is a well-accepted and widely used method to induce thrombosis. The advantage of this model is the possibility to induce different injury strengths depending on the concentration, amount and exposure time of applied $FeCl_3$. Furthermore, the composition of thrombi formed after $FeCl_3$ injury is similar to those seen in human arterial thrombosis which is important when investigating potential therapeutic targets and treatments.[91] GPVI is the major platelet collagen receptor and has been extensively studied due to hat nature as an attractive anti-thrombotic target. The success of targeting the interaction of GPVI and hat ligands, (with current research in phase II clinical trials[190]) has reinforced the relevance and importance of continuing the focus on platelets in the search for novel anti-thrombotics. There are several other receptors, transporters and indeed intracellular proteins that critically contribute to thrombosis but which have not yet been systematically assessed for anti-thrombotic potential. In the following, I will discuss results from arterial thrombosis analysis of several mouse models which highlight the potential of some of these novel anti-thrombotic targets. In addition, the analysis of two mouse strains that complement the *5Htt*$^{-/-}$ mouse model are also discussed, providing further evidence to support the notion that platelet released 5-HT is a critical contributor to arterial thrombosis.

5.2.1. The lack of TPH1 leads to reduced thrombosis

The contribution of platelet released 5-HT to the stabilization of formed thrombi was confirmed by the studies of the *5Htt*$^{-/-}$ mice. However, as these mice also had (albeit reduced) circulating 5-HT in the plasma the specific role of plasma 5-HT versus platelet released 5-HT in the process of thrombus formation and stabilization remained to be fully clarified. To address this question and to compare the effects of stored and circulating 5-HT in thrombosis, we compared the results of different thrombosis models in *5Htt*$^{-/-}$ mice (lacking platelet 5-HT) and *Tph1*$^{-/-}$ mice (lacking the enzyme responsible for 5-HT synthesis in the periphery), leading to the absence of 5-HT in the circulation and in platelets. It is published that *Tph1*$^{-/-}$ mice have normal platelet counts with a normal platelet morphology in comparison to *Wt* controls providing additional evidence that 5-HT is not required for platelet production.[49] However, the lack of 5-HT in the periphery leads to prolonged bleeding times,[49] similar to those seen in *5Htt*$^{-/-}$mice (*5Htt*$^{-/-}$: 490 ± 267 s vs. *Wt:* 304 ± 173 s), which could be normalized by the injection of

5-HT. In line with published data,[49] we could show that thrombus formation upon chemical injury of the mesenteric arterioles was reduced in the *Tph1*$^{-/-}$ mice in contrast to *Wt* controls (Figure 38). Interestingly, thrombus formation in the *5Htt*$^{-/-}$ mice (Figure 30D) was normal in this thrombosis model. Surprisingly, the converse was true for the mechanical injury of the aorta in which *5Htt*$^{-/-}$ mice were strongly protected from thrombosis (Figure 31A; 81 % of the mice did not show an vessel occlusion with a formed thrombi) and *Tph1*$^{-/-}$ mice showed only a mild prolongation in occlusion times (Figure 38D; *Tph1*$^{-/-}$*:* 429 ± 188 s vs. *Wt:* 245 ± 72 s). Similarly, after $FeCl_3$ injury of the carotid artery *5Htt*$^{-/-}$ mice clearly had destabilized thrombus formation (Figure 31C; 678 ± 393 s) and *Tph1*$^{-/-}$ mice show only a slight delay in time to occlusion (Figure 38E 452 ± 177 s).

The $FeCl_3$ injury of the mesenteric arteries is known to be primarily driven by thrombin generation.[94] As *5Htt*$^{-/-}$ platelets had normal responses to thrombin and other platelet GPCR agonists the result that these mice had no protection from thrombosis in this model was not surprising. A similar explanation, evidenced by the presented *in vitro* studies also explains the protection of *5Htt*$^{-/-}$ mice in the mechanical injury model of the aorta. The platelet activation, SOCE and *in vitro* aggregate formation under flow demonstrated that the release of platelet stored 5-HT and the subsequent Gq-coupled signaling of the 5-HT_{2A} receptor is required for maximal platelet activation and aggregate formation after initiation of the (hem)ITAM signaling cascade.[143] As thrombosis in the injury model of the aorta is known to be driven by GPVI and ITAM signaling[96] the activation defects in *5Htt*$^{-/-}$ platelets can clearly explain the protection seen in this model.

In contrast, it is difficult to explain why, despite having the same defects as *5Htt*$^{-/-}$ platelets (due to the lack of 5-HT in their secretome), the *Tph1*$^{-/-}$ mice had opposite results to the *5Htt*$^{-/-}$ mice in both thrombosis models. This suggests that plasma borne 5-HT also has a strong influence in the vascular system and, perhaps therefore indirectly, on thrombosis and hemostasis. It is well known that 5-HT and its signaling in various endothelial and smooth muscle cell types contributes to the regulation of vessel resistance and blood pressure.[182,191] Furthermore it is well described that depending on the 5-HT receptors expressed and the integrity of the vessel endothelium, 5-HT can induce vasoconstriction or vasodilation.[192] In arterial blood vessels, such as the arteries in the GI tract, 5-HT triggers relaxation of the smooth muscle cells by the activation of 5-HT_1 signaling or through an inhibitory effect on 5-HT_2 in the vessel endothelium.[193]

The binding of 5-HT to 5-HT$_1$, the vessel wall can trigger the release of endothelium-derived relaxing factors (EDRFs), such as nitric oxide and thus initiate vessel dilation.[193] This is caused by the activation of soluble guanylate cyclase, and the subsequent accumulation of cyclic GMP which regulate the relaxation of smooth muscle cells.[193] In contrast high concentrations of 5-HT can induce vasoconstriction of the vessel by activating the serotonergic receptors both on the endothelial cells and directly on smooth muscle cells and after vessel wall injury.[193] The regulation of the balance between vasoconstriction and relaxation is highly complex and incompletely understood with the site, time and context dependent effects of the signaling of 5-HT and its various receptors.[182,192,194-196] Alterations in this process in the *Tph1*$^{-/-}$ mice due to chronic loss of 5-HT in the vascular system is one hypothesis to explain both reduced thrombus stability in comparison to *5Htt*$^{-/-}$ mice in the mesentery and the reversal of protection in the aorta, with increased vasodilation in the smaller mesenteric arterioles and increased vasoconstriction in the aorta.

Regarding the contribution of platelet released 5-HT to this process recent evidence suggests that whilst the amount of platelet released 5-HT is much greater than that in the plasma it is unlikely that much of it would be available to bind the endothelium or the underlying smooth muscle cells. Recent modeling publications have indicated that formed thrombi are composed of different areas with different densities and packing, creating varying conditions within a forming thrombus. Based on these differences a thrombus can be divided between a dense core and a loosely packed shell.[197] In the shell the concentration of small released molecules, such as 5-HT are much reduced in contrast to the core of the thrombus and, relevant to 5-HT, it was found that this concentration of platelet releasate in the core was because of limited diffusion in this part of the thrombus.[197] Therefore, it is most likely that platelet released 5-HT mainly acts in a para- and autocrine fashion on platelets rather than on the underlying damaged vessel wall, thus contributing to thrombus stability as reflected in the data from the analysis of *5Htt*$^{-/-}$ mice.

The comparison of thrombosis models in *Tph1*$^{-/-}$ and *5Htt*$^{-/-}$ mice confirms that in larger blood vessels and in (hem)ITAM driven thrombosis platelet released 5-HT is critical for thrombus stability. However, it does appear that plasma borne 5-HT has an important role to play in thrombosis. Given that the sole mediator of 5-HT uptake in platelets is 5HTT there is clear potential role for SSRIs in acute and secondary treatment for vas-

cular events.[198,199] Furthermore, as both 5-HT and platelets have roles in many processes beyond thrombosis and hemostasis their interplay and its modulation by SSRIs requires further research in fields as diverse as cancer,[200] inflammation,[201] deep vein thrombosis and fibrosis.[202]

5.2.2. *Unc13d*$^{-/-}$*/Nbeal2*$^{-/-}$ mice

As 5-HT is stored in platelet granules, along with many other proteins of the platelet secretome, we wanted to assess the extent of the contribution of platelet granules, both alpha and dense, to thrombus stability and formation. Besides 5-HT, several mediators for thrombus stability are stored in platelet granules, such as adhesion molecules, coagulation factors and other important secondary mediators, in particular ATP/ADP. To investigate the role of platelet granule contents at the site of vascular injury, a mouse line deficient of α-granules and defective in the secretion of dense granules was generated and analyzed *in vivo*. These mice showed a reduction in P-selectin exposure,[203] due to the lack of the secretion of platelet granules and their contents. Furthermore the platelets displayed reduced aggregation responses upon stimulation with CRP or collagen,[203] highlighting the role of secondary mediators stored in platelet granules in potentiating (hem)ITAM signaling.[204] In line with this, these mice showed reduced aggregation and thrombus formation under flow on collagen coated surface.[203] Due to the defects downstream of GPVI, this mouse line was analyzed in the thrombosis model of mechanical injury of the abdominal aorta. The analyses of the single knock-out mouse lines (*Unc13d*$^{-/-}$ and *Nbeal2*$^{-/-}$) showed a protection in thrombus formation upon injury of the abdominal aorta (Figure 39).[203] In line with this, the double-deficient mice were also fully protected in this thrombosis model (Figure 39), indicating an important role of platelet granule contents in thrombus formation and stability.

5.2.3. TRPM7

We could show that platelet granule contents are essential for thrombus formation and stability, but also cations play a major role in this process. It is well known that Ca^{2+} mobilization in platelets is the central mediator of platelet activation and thus for thrombus formation,[74] but other much less studied cations, such as Mg^{2+}, seems to also play a key role in thrombosis and hemostasis.[205]

Mg^{2+} supplementation is proposed as a treatment for many diverse diseases and syndromes including restless legs syndrome (RLS),[206,207] periodic limb movements during

sleep (PLMS),[206] muscle cramps,[208] diabetes,[209] cystic fibrosis,[210] preeclampsia,[211] migraine[212] and also more importantly for the following studies, for reducing cerebral ischemic events[213] and arrhythmia suppression after MI.[214] Interestingly, in many cases the mechanisms governing the effects of Mg^{2+} supplementation are unknown and in many tissues of the body the role of Mg^{2+} is largely still a mystery. One massively understudied area is Mg^{2+} and platelets and platelet signaling, thus the contribution of Mg^{2+} to thrombosis is unknown. Given the promising responses of cardiovascular patients to Mg^{2+} supplementation we aimed to investigate the role of Mg^{2+} in thrombosis and hemostasis and its regulation in platelets. To this end, mouse models of the only two Mg^{2+} uptake proteins in platelets, the transporter MagT1 and the channel TRPM7, were assessed in thrombosis models.

5.2.3.1. *Trpm7$^{fl/fl\text{-}Pf4Cre}$* mice displayed normal thrombus formation

The loss of TRPM7 in the platelet specific conditional knock-out mouse *Trpm7$^{fl/fl\text{-}Pf4Cre}$* resulted in a reduced Mg^{2+} concentrations in platelets. It has been published that low Mg^{2+} levels were detected in patients with coronary artery disease, indicating that reduced levels of Mg^{2+} maybe contribute to thrombus formation and stability. However, we could not observe any effect on thrombus formation in the different *in vivo* thrombosis models tested. Time to vessel occlusion was not altered in chemical injury of the mesenteric arterioles or carotid arteries nor in the mechanical injury of the abdominal aorta (Figure 40). It is published that the genetic deletion of the Mg^{2+} channel in DT40 B-cells is associated with Mg^{2+} deficiency in the cells, but with an upregulation of the gene expression of MagT1, the selective transporter for Mg^{2+}.[215] An upregulation of the MagT1 could be a possible explanation for the normal thrombosis upon injury although this remains to be assessed in the *Trpm7$^{fl/fl\text{-}Pf4Cre}$* platelets.[215]

5.2.3.2. *Trpm7^{KI}* mice show defective thrombus formation *in vivo*

The C-terminus of TRPM7 channel contains a kinase domain the role of which, and indeed the channel itself, in Mg^{2+} homeostasis is controversially discussed. It is published that homozygous knock-out mice are embryonic lethal, whereas heterozygous mice displayed impaired channel activity, resulting in a defect in Mg^{2+} absorption in the intestine and therefore decreased Mg^{2+} levels in plasma, erythrocytes and bones.[114] In contrast to this publication another group published that the kinase domain modulates the activity of the channel, but is not essential for its activation.[118] The TRPM7 Ser/Thr kinase domain contains several autophosphorylation sites, important for its activation

and initiation of downstream signaling. One interesting substrate in terms of platelet activation are the phospholipase C enzymes that play a critical role in platelet Ca^{2+} mobilization. The *Trpm*7 kinase domain can bind the C2 domain of PLC isoforms, such as PLCβ, PLCγ and PLCδ.[216-218] This binding leads to the phosphorylation of PLC with unclear effects on further Ca^{2+} mobilization. Our group has previously shown that the lack of the kinase activity leads to severe defects in integrin αIIbβ3 activation, P-selectin exposure and aggregation responses upon GPVI stimuli. In addition dense granule content release of ATP and 5-HT upon stimulation with thrombin and CRP were impaired in *Trpm7*^{KI} platelets. These two mediators are important in the second phase of platelet activation and thrombus stability. In line with this, Ca^{2+} mobilization and IP_3 production were reduced in mice lacking the kinase activity, potentially due to the lack of PLC phosphorylation by the kinase. *Ex vivo* analyses displayed reduced platelet adhesion and thrombus formation on a collagen coated surface and tail bleeding times were prolonged *in vivo*. In line with the *in vitro* and the previously *in vivo* data,[219] *Trpm7*^{KI} mice showed a protection upon chemical injury of the mesenteric arteries and a prolonged time until occlusion of the vessel occurred (Figure 41C). The same was true for the mechanical injury of the abdominal aorta (Figure 41E). In agreement with these results, the chemical injury of the carotid artery showed a dramatic defect in thrombus formation. Only one of 11 *Trpm7*^{KI} mice formed an occlusive thrombus, whereas 10 of 12 *Wt* mice showed occluded vessels (Figure 41D). The prolongation of the time to form occlusive thrombi indicated that the *Trpm*7 kinase is important in thrombosis. Interestingly the lack of the kinase activity seems to be compensated in some circumstances with the appearance of two populations in the different thrombosis models. Furthermore, it appears that the kinase domain makes a major contribution to thrombus formation whereas the total lack of the channel, including the kinase domain, causes no alteration in thrombosis or hemostasis. It is proposed that the lack of the kinase activity inhibits platelet function through the loss of its phosphorylation of PLC isoforms which are known to be especially important in platelet activation downstream of (hem)ITAM signaling. This negative effect is counteracted in the platelets that lack the total protein as Mg^{2+} itself is known to be an inhibitor of platelet activation and its reduced levels in *Trpm7*$^{fl/fl\text{-}Pf4Cre}$ platelets leads to hyperreactivity downstream of GPCRs leading to normal platelet function *in vivo*.[219] Further characterization of the channel and the signalosome of the kinase domain is required to fully understand the

contribution and regulation of this protein in thrombosis and hemostasis, in addition to its position in the Mg^{2+} system in platelets.

5.2.4. *MagT1$^{y/-}$* mice show increased thrombus formation *in vivo*

The lack of the Mg^{2+} channel TRPM7 causes complex alterations in several platelet activation mechanism that ultimately had no net effect on thrombosis and hemostasis, however the lack of the activity of the kinase domain in the TRPM7 channel led to a protection from occlusive thrombi. In line with published data regarding low intracellular levels of Mg^{2+} in platelets promoting thrombosis,[205] these results indicate that the modulation of Mg^{2+} could be a target for anti-thrombotics. Whilst it is known that Mg^{2+} supplementation can lead to reduced platelet aggregation in humans[220] much less is known about the mechanism and signaling associated with hyper- or hypomagnesia in thrombus formation and stability.

To further investigate the role of Mg^{2+} *in vivo*, we analyzed a *MagT1$^{y/-}$* mouse line in different models of thrombosis. In line with the published data,[205] we could show, that a lack of the Mg^{2+} transporter leads to a hyperreactivity of platelets due to reduced Mg^{2+} cell content. This destabilization of Mg^{2+} homeostasis resulted in enhanced thrombus formation upon vessel wall injury (Figure 42). As the MAGT1 transporter is ubiquitously expressed throughout the body and the *MagT1$^{y/-}$* mouse is a constitutive knock-out model,[122,166] BMC mice were generated to assess the contribution of platelets to the prothrombotic phenotype, which showed similar results in thrombus formation like the *MagT1$^{y/-}$*.

These results, in combination with those from investigations into TRPM7 in platelets show that modulation of Mg^{2+} levels in platelets can result in enhanced or suppressed thrombus formation. This adds further evidence to the potential of Mg^{2+} as a therapeutic drug target and also begins to shed some light on the mechanisms for some of the effects seen after treatment of patients with magnesium supplementation.

5.2.5. RIAM is dispensable for thrombus formation

In the thesis we could show that platelet granule contents and cations are important in thrombus formation and stability. The release of platelet granule contents and the mobilization of cations trigger and potentiate signaling pathways which all ultimately lead to “inside-out” activation of integrins. This process is regulated by a complex multistep process that involves many adaptor and scaffold proteins; however it is known that one

central effector is the cytoskeletal protein talin 1. Talin 1 is essential for integrin activation, as demonstrated by the *Talin1*$^{-/-}$ mice,[221] which have severely defective primary hemostasis and are protected from thrombosis. Recently the adaptor molecule RIAM was proposed as an essential molecule for the recruitment of talin 1 to the β-tail of integrins *in vitro* and therefore for integrin activation,[125,126,167,168] placing RIAM as a critical adaptor protein in platelet αIIbβ3 integrin activation and therefore in primary hemostasis. Due to the published data we hypothesized that *RIAM*$^{-/-}$ mice would phenocopy the thrombosis defect seen in *Talin*$^{-/-}$ mice,[221] however *RIAM*$^{-/-}$ mice showed no protection from thrombosis upon injury of the mesenteric arteries with $FeCl_3$. This surprising result was explained by the normal αIIbβ3 integrin activation, normal aggregation responses to different agonists, normal aggregate and thrombus formation *ex vivo* and normal spreading and clot retraction seen in *RIAM*$^{-/-}$ platelets.[124]

These results indicate that in platelets the loss of RIAM is perhaps compensated by another scaffold protein of the MLR family or other Rap1 effectors. It could also be possible that other routes of talin 1 recruitment are sufficient to maintain normal integrin activation in *RIAM*$^{-/-}$ platelets, thus RIAM is dispensable for the recruitment of talin 1 in this cell type. Subsequent to the publication of the presented data on RIAM in thrombosis, it was published that RIAM is important in the activation of β2 integrins, which are only expressed on leucocytes.[222,223] This confirms the presence of another route or molecule which replaces RIAM and recruits talin to the β-tail of the integrin in platelets and most likely other cell types.

5.3. Concluding remarks and future plans

The analyses of the *5Htt*$^{-/-}$ mice and the analyses of the other genetically modified mice presented here in the different *in vivo* thrombosis models, demonstrates the physiological importance and /or relevance of the studied transporters, channels, receptors and proteins in platelet activation and their role in thrombosis and hemostasis. The major findings of this thesis are:

- Confirmation that the feedback-loop of platelet released 5-HT is important in platelet activation, resulting in thrombus formation.
- Platelet secreted 5-HT, and indeed that which circulates in the plasma is required for functional hemostasis and stable thrombus formation.
- The function of platelet released 5-HT in hemostasis and thrombosis does not contribute to infarct progression after ischemic stroke.

- Together the results from the *5Htt*$^{-/-}$ and *Tph1*$^{-/-}$ mice allow a better understanding and insight into the effect of SSRIs and their use as potential anti-thrombotic agents
- RIAM is dispensable for talin-1 recruitment to the β3-integrin tail and thus dispensable for integrin “inside-out” activation in platelets.
- Released platelet granule contents are important in thrombus formation and stability upon injury of the vessel wall (*Unc13d*$^{-/-}$/*Nbeal2*$^{-/-}$).
- The lack of the Mg^{2+} channel TRPM7 results in reduced Mg^{2+} in platelets, but with normal thrombosis upon injury.
- The lack of functional kinase activity in the TRPM7 channel leads to a protection from occlusive thrombus formation.
- The lack of the transporter for Mg^{2+} leads to hyperreactive platelets and thus a prothrombotic phenotype.

The results about the TRPM7 and MagT1 genetically modified mice showed the importance of Mg^{2+} in hemostasis and thrombosis. The supplementation of Mg^{2+} could be a possible medication for patients lacking the MagT1 channel or having mutations in the TRPM7 channel. Mg^{2+} supplementation could be also a treatment to prevent stroke. Serotonin is important in hemostasis, thrombosis and ischemic stroke, confirmed by the experiments in this study and by published data.[49,53,145] But the fact that the 5-HT transporter is widely expressed on different cells throughout the body and is also important in brain, raises the question whether the constitutive knock-out is the right model to use to investigate the role of platelet serotonin, particularly in the tMCAO model. A way to address this issue, would be the analysis of bone marrow chimeric mice, just lacking the transporter in all hematopoietic cells. But in this model also immune cells are devoid of the transporter and not just MK’s and platelets. Another way to address this would be the generation of conditional knock-out mice, using the Cre/loxP system and Pf4-Cre transgenic mice. This system enables the specific deletion of the gene of interest in MK’s and also in platelets. In this mouse line, all other cells express the transporter and can take up 5-HT, also in the brain like in normal conditions.

The proof of principle of the mentioned hypothesis in this thesis about the role of secreted and plasma 5-HT in the process of thrombosis, would be platelet transfer experiments between the 3 different strains, *Wt*, *Tph1*$^{-/-}$ mice and the *5Htt*$^{-/-}$ mice prior treated with platelet-depleting anti-GPIbα antibody.

To prove the role of secreted 5-HT in thrombosis, the transfer of *5Htt*$^{-/-}$ platelets to *Wt* platelet-depleted mice could show the effect of secreted 5-HT in an environment with normal plasma 5-HT concentrations. The transfer of *Wt* platelets to platelet-depleted *Tph1*$^{-/-}$ mice could show the specific role of plasma 5-HT in the process of thrombosis upon injury.

6. References

1. Daly ME. Determinants of platelet count in humans. *Haematologica*. 2011;96(1):10-13.
2. Levin J, Ebbe S. Why are recently published platelet counts in normal mice so low? *Blood*. 1994;83(12):3829-3831.
3. Ault KA, Knowles C. In vivo biotinylation demonstrates that reticulated platelets are the youngest platelets in circulation. *Exp Hematol*. 1995;23(9):996-1001.
4. Grozovsky R, Hoffmeister KM, Falet H. Novel clearance mechanisms of platelets. *Current opinion in hematology*. 2010;17(6):585-589.
5. Italiano JE, Patel-Hett S, Hartwig JH. Mechanics of proplatelet elaboration. *Journal of Thrombosis and Haemostasis*. 2007;5:18-23.
6. Chang Y, Bluteau D, Debili N, Vainchenker W. From hematopoietic stem cells to platelets. *Journal of Thrombosis and Haemostasis*. 2007;5:318-327.
7. Nieswandt B, Stritt S. Megakaryocyte rupture for acute platelet needs. *The Journal of Cell Biology*. 2015;209(3):327-328.
8. Davì G, Patrono C. Platelet Activation and Atherothrombosis. *New England Journal of Medicine*. 2007;357(24):2482-2494.
9. White JG, Clawson CC. The surface-connected canalicular system of blood platelets--a fenestrated membrane system. *The American Journal of Pathology*. 1980;101(2):353-364.
10. Ruggeri ZM. Platelets in atherothrombosis. *nature medicine*. 2002;8:1227-1234.
11. Rendu F, Brohard-Bohn B. The platelet release reaction: granules' constituents, secretion and functions. *Platelets*. 2001;12(5):261-273.
12. Whiteheart SW. Platelet granules: surprise packages. Vol. 118; 2011.
13. Harrison P, Cramer EM. Platelet alpha-granules. *Blood Rev*. 1993;7(1):52-62.
14. Blair P, Flaumenhaft R. Platelet α–granules: Basic biology and clinical correlates. *Blood reviews*. 2009;23(4):177-189.
15. Ciferri S, Emiliani C, Guglielmini G, Orlacchio A, Nenci GG, Gresele P. Platelets release their lysosomal content in vivo in humans upon activation. *Thromb Haemost*. 2000;83(1):157-164.
16. King SM, Reed GL. Development of platelet secretory granules. *Seminars in Cell & Developmental Biology*. 2002;13(4):293-302.
17. Varga-Szabo D, Pleines I, Nieswandt B. Cell Adhesion Mechanisms in Platelets. *Arteriosclerosis, Thrombosis, and Vascular Biology*. 2008;28(3):403-412.
18. Bluestein D, Niu L, Schoephoerster R, Dewanjee M. Fluid mechanics of arterial stenosis: Relationship to the development of mural thrombus. *Annals of Biomedical Engineering*. 1997;25(2):344-356.
19. Mailhac A, Badimon JJ, Fallon JT, et al. Effect of an eccentric severe stenosis on fibrin(ogen) deposition on severely damaged vessel wall in arterial thrombosis. Relative contribution of fibrin(ogen) and platelets. *Circulation*. 1994;90(2):988-996.

20. Papaioannou TG, Stefanadis C. Vascular wall shear stress: basic principles and methods. *Hellenic J Cardiol*. 2005;46(1):9-15.

21. Nesbitt WS, Westein E, Tovar-Lopez FJ, et al. A shear gradient-dependent platelet aggregation mechanism drives thrombus formation. *Nat Med*. 2009;15(6):665-673.

22. Ruggeri ZM, Orje JN, Habermann R, Federici AB, Reininger AJ. Activation-independent platelet adhesion and aggregation under elevated shear stress. *Blood*. 2006;108(6):1903-1910.

23. Savage B, Almus-Jacobs F, Ruggeri ZM. Specific Synergy of Multiple Substrate–Receptor Interactions in Platelet Thrombus Formation under Flow. *Cell*. 1998;94(5):657-666.

24. Stegner D, Nieswandt B. Platelet receptor signaling in thrombus formation. *J Mol Med (Berl)*. 2011;89(2):109-121.

25. Maxwell MJ, Westein E, Nesbitt WS, Giuliano S, Dopheide SM, Jackson SP. Identification of a 2-stage platelet aggregation process mediating shear-dependent thrombus formation. *Blood*. 2007;109(2):566-576.

26. Li N, Wallen NH, Ladjevardi M, Hjemdahl P. Effects of serotonin on platelet activation in whole blood. *Blood Coagul Fibrinolysis*. 1997;8(8):517-523.

27. Nieswandt B, Pleines I, Bender M. Platelet adhesion and activation mechanisms in arterial thrombosis and ischaemic stroke. *Journal of Thrombosis and Haemostasis*. 2011;9:92-104.

28. Dutting S, Bender M, Nieswandt B. Platelet GPVI: a target for antithrombotic therapy?! *Trends Pharmacol Sci*. 2012;33(11):583-590.

29. Bergmeier W, Hynes RO. Extracellular Matrix Proteins in Hemostasis and Thrombosis. *Cold Spring Harbor Perspectives in Biology*. 2012;4(2):a005132.

30. Shattil SJ, Newman PJ. Integrins: dynamic scaffolds for adhesion and signaling in platelets. Vol. 104; 2004.

31. Li Z, Delaney MK, O'Brien KA, Du X. Signaling during platelet adhesion and activation. *Arteriosclerosis, thrombosis, and vascular biology*. 2010;30(12):2341-2349.

32. Carr ME, Jr. Development of platelet contractile force as a research and clinical measure of platelet function. *Cell Biochem Biophys*. 2003;38(1):55-78.

33. Shen B, Delaney MK, Du X. Inside-out, outside-in, and inside-outside-in: G protein signaling in integrin-mediated cell adhesion, spreading, and retraction. *Current opinion in cell biology*. 2012;24(5):600-606.

34. Underhill DM, Goodridge HS. The many faces of ITAMs. *Trends in Immunology*. 2007;28(2):66-73.

35. Offermanns S. Activation of platelet function through G protein-coupled receptors. *Circ Res*. 2006;99(12):1293-1304.

36. Stegner D, Haining EJ, Nieswandt B. Targeting Glycoprotein VI and the Immunoreceptor Tyrosine-Based Activation Motif Signaling Pathway. *Arteriosclerosis, Thrombosis, and Vascular Biology*. 2014;34(8):1615-1620.

37. Whitaker-Azmitia PM. The discovery of serotonin and its role in neuroscience. *Neuropsychopharmacology*. 1999;21(2 Suppl):2S-8S.

38. Whitaker-Azmitia PM. The Discovery of Serotonin and its Role in Neuroscience. *Neuropsychopharmacology*. 1999;21(2, Supplement 1):2S-8S.

39. Herr N, Mauler M, Witsch T, et al. Acute fluoxetine treatment induces slow rolling of leukocytes on endothelium in mice. *PLoS One*. 2014;9(2):e88316.

40. Keszthelyi D, Troost FJ, Masclee AAM. Understanding the role of tryptophan and serotonin metabolism in gastrointestinal function. *Neurogastroenterology & Motility*. 2009;21(12):1239-1249.

41. Berumen LC, Rodr, #237, et al. Serotonin Receptors in Hippocampus. *The Scientific World Journal*. 2012;2012:15.

42. Nowak JZ, Szymanska B, Zawilska JB, Bialek B. Hydroxyindole-O-methyltransferase activity in ocular and brain structures of rabbit and hen. *J Pineal Res*. 1993;15(1):35-42.

43. Berger M, Gray JA, Roth BL. The Expanded Biology of Serotonin. *Annual Review of Medicine*. 2009;60(1):355-366.

44. Charnay Y, Leger L. Brain serotonergic circuitries. *Dialogues in Clinical Neuroscience*. 2010;12(4):471-487.

45. Hickman AB, Klein DC, Dyda F. Melatonin Biosynthesis: The Structure of Serotonin N-Acetyltransferase at 2.5 Å Resolution Suggests a Catalytic Mechanism. *Molecular Cell*. 1999;3(1):23-32.

46. Murphy DL, Lesch KP. Targeting the murine serotonin transporter: insights into human neurobiology. *Nat Rev Neurosci*. 2008;9(2):85-96.

47. Murphy DL, Lerner A, Rudnick G, Lesch KP. Serotonin transporter: gene, genetic disorders, and pharmacogenetics. *Mol Interv*. 2004;4(2):109-123.

48. Hoyer D, Clarke DE, Fozard JR, et al. International Union of Pharmacology classification of receptors for 5-hydroxytryptamine (Serotonin). *Pharmacological Reviews*. 1994;46(2):157-203.

49. Walther DJ, Peter JU, Winter S, et al. Serotonylation of small GTPases is a signal transduction pathway that triggers platelet alpha-granule release. *Cell*. 2003;115(7):851-862.

50. Deneris ES, Wyler SC. Serotonergic transcriptional networks and potential importance to mental health. *Nat Neurosci*. 2012;15(4):519-527.

51. Sangkuhl K, Klein T, Altman R. Selective Serotonin Reuptake Inhibitors (SSRI) Pathway. *Pharmacogenetics and genomics*. 2009;19(11):907-909.

52. Yubero-Lahoz S, Robledo P, Farre M, de laTorre R. Platelet SERT as a peripheral biomarker of serotonergic neurotransmission in the central nervous system. *Curr Med Chem*. 2013;20(11):1382-1396.

53. Mercado CP, Quintero MV, Li Y, et al. A serotonin-induced N-glycan switch regulates platelet aggregation. *Sci Rep*. 2013;3:2795.

54. Kristensen AS, Andersen J, Jørgensen TN, et al. SLC6 Neurotransmitter Transporters: Structure, Function, and Regulation. *Pharmacological Reviews*. 2011;63(3):585-640.

55. Masson J, Sagné C, Hamon M, Mestikawy SE. Neurotransmitter Transporters in the Central Nervous System. *Pharmacological Reviews*. 1999;51(3):439-464.

56. Linder AE, Ni W, Szasz T, et al. A Serotonergic System in Veins: Serotonin Transporter-Independent Uptake. *Journal of Pharmacology and Experimental Therapeutics*. 2008;325(3):714-722.

57. Ahern GP. 5-HT and the Immune System. *Current opinion in pharmacology*. 2011;11(1):29-33.

58. Kessler RC, Aguilar-Gaxiola S, Alonso J, et al. The global burden of mental disorders: An update from the WHO World Mental Health (WMH) Surveys. *Epidemiologia e psichiatria sociale*. 2009;18(1):23-33.

59. Ramachandraih CT, Subramanyam N, Bar KJ, Baker G, Yeragani VK. Antidepressants: From MAOIs to SSRIs and more. *Indian Journal of Psychiatry*. 2011;53(2):180-182.

60. Lopez-Munoz F, Alamo C. Monoaminergic neurotransmission: the history of the discovery of antidepressants from 1950s until today. *Curr Pharm Des*. 2009;15(14):1563-1586.

61. Vaswani M, Linda FK, Ramesh S. Role of selective serotonin reuptake inhibitors in psychiatric disorders: a comprehensive review. *Progress in Neuro-Psychopharmacology and Biological Psychiatry*. 2003;27(1):85-102.

62. Stahl SM. Mechanism of action of serotonin selective reuptake inhibitors: Serotonin receptors and pathways mediate therapeutic effects and side effects. *Journal of Affective Disorders*. 1998;51(3):215-235.

63. Tatsumi M, Groshan K, Blakely RD, Richelson E. Pharmacological profile of antidepressants and related compounds at human monoamine transporters. *Eur J Pharmacol*. 1997;340(2-3):249-258.

64. Maurer-Spurej E. Serotonin reuptake inhibitors and cardiovascular diseases: a platelet connection. *Cell Mol Life Sci*. 2005;62(2):159-170.

65. Anglin R, Yuan Y, Moayyedi P, Tse F, Armstrong D, Leontiadis GI. Risk of upper gastrointestinal bleeding with selective serotonin reuptake inhibitors with or without concurrent nonsteroidal anti-inflammatory use: a systematic review and meta-analysis. *Am J Gastroenterol*. 2014;109(6):811-819.

66. Jiang HY, Chen HZ, Hu XJ, et al. Use of selective serotonin reuptake inhibitors and risk of upper gastrointestinal bleeding: a systematic review and meta-analysis. *Clin Gastroenterol Hepatol*. 2015;13(1):42-50 e43.

67. Parekh AB, Putney JW, Jr. Store-operated calcium channels. *Physiol Rev*. 2005;85(2):757-810.

68. Berridge MJ, Bootman MD, Roderick HL. Calcium signalling: dynamics, homeostasis and remodelling. *Nat Rev Mol Cell Biol*. 2003;4(7):517-529.

69. Carafoli E. Calcium signaling: A tale for all seasons. *Proceedings of the National Academy of Sciences*. 2002;99(3):1115-1122.

70. Pozzan T, Rizzuto R, Volpe P, Meldolesi J. Molecular and cellular physiology of intracellular calcium stores. *Physiol Rev*. 1994;74(3):595-636.

71. Sorrentino V, Rizzuto R. Molecular genetics of Ca(2+) stores and intracellular Ca(2+) signalling. *Trends Pharmacol Sci*. 2001;22(9):459-464.

72. Locke EG, Bonilla M, Liang L, Takita Y, Cunningham KW. A homolog of voltage-gated Ca(2+) channels stimulated by depletion of secretory Ca(2+) in yeast. *Mol Cell Biol*. 2000;20(18):6686-6694.

73. Partiseti M, Le Deist F, Hivroz C, Fischer A, Korn H, Choquet D. The calcium current activated by T cell receptor and store depletion in human lymphocytes is absent in a primary immunodeficiency. *J Biol Chem*. 1994;269(51):32327-32335.

74. Varga-Szabo D, Braun A, Nieswandt B. Calcium signaling in platelets. *J Thromb Haemost*. 2009;7(7):1057-1066.

75. Taylor CW, da Fonseca PCA, Morris EP. IP3 receptors: the search for structure. *Trends in Biochemical Sciences*. 2004;29(4):210-219.

76. Mountian II, Baba-Aissa F, Jonas JC, Humbert De S, Wuytack F, Parys JB. Expression of Ca(2+) Transport Genes in Platelets and Endothelial Cells in Hypertension. *Hypertension*. 2001;37(1):135-141.

77. Ramanathan G, Gupta S, Thielmann I, et al. Defective diacylglycerol-induced Ca2+ entry but normal agonist-induced activation responses in TRPC6-deficient mouse platelets. *J Thromb Haemost*. 2012;10(3):419-429.

78. Feske S, Skolnik EY, Prakriya M. Ion channels and transporters in lymphocyte function and immunity. *Nat Rev Immunol*. 2012;12(7):532-547.

79. Yoshimura M, Oshima T, Hiraga H, et al. Increased cytosolic free Mg2+ and Ca2+ in platelets of patients with vasospastic angina. *Am J Physiol*. 1998;274(2 Pt 2):R548-554.

80. Takaya J, Kaneko K. Small for Gestational Age and Magnesium in Cord Blood Platelets: Intrauterine Magnesium Deficiency May Induce Metabolic Syndrome in Later Life. *Journal of Pregnancy*. 2011;2011:270474.

81. Rink TJ, Sage SO. Calcium signaling in human platelets. *Annu Rev Physiol*. 1990;52:431-449.

82. Turetta L, Bazzan E, Bertagno K, Musacchio E, Deana R. Role of Ca2+ and protein kinase C in the serotonin (5-HT) transport in human platelets. *Cell Calcium*. 2002;31(5):235-244.

83. Turetta L, Bazzan E, Bertagno K, Musacchio E, Deana R. Role of Ca(2+) and protein kinase C in the serotonin (5-HT) transport in human platelets. *Cell Calcium*. 2002;31(5):235-244.

84. Nishio H, Nezasa K, Nakata Y. Role of calcium ion in platelet serotonin uptake regulation. *Eur J Pharmacol*. 1995;288(2):149-155.

85. Ramamoorthy S, Giovanetti E, Qian Y, Blakely RD. Phosphorylation and regulation of antidepressant-sensitive serotonin transporters. *J Biol Chem*. 1998;273(4):2458-2466.

86. Qian Y, Galli A, Ramamoorthy S, Risso S, DeFelice LJ, Blakely RD. Protein kinase C activation regulates human serotonin transporters in HEK-293 cells via altered cell surface expression. *J Neurosci*. 1997;17(1):45-57.

87. Anderson GM, Horne WC. Activators of protein kinase C decrease serotonin transport in human platelets. *Biochim Biophys Acta*. 1992;1137(3):331-337.

88. Myers CL, Lazo JS, Pitt BR. Translocation of protein kinase C is associated with inhibition of 5-HT uptake by cultured endothelial cells. *Am J Physiol*. 1989;257(4 Pt 1):L253-258.

89. Go AS, Mozaffarian D, Roger VL, et al. Heart disease and stroke statistics--2014 update: a report from the American Heart Association. *Circulation*. 2014;129(3):e28-e292.

90. Dorffler-Melly J, Schwarte LA, Ince C, Levi M. Mouse models of focal arterial and venous thrombosis. *Basic Res Cardiol*. 2000;95(6):503-509.

91. Farrehi PM, Ozaki CK, Carmeliet P, Fay WP. Regulation of arterial thrombolysis by plasminogen activator inhibitor-1 in mice. *Circulation*. 1998;97(10):1002-1008.

92. Hechler B, Gachet C. Comparison of two murine models of thrombosis induced by atherosclerotic plaque injury. *Thrombosis and Haemostasis*. 2011;105(99):S3-S12.

93. Li W, McIntyre TM, Silverstein RL. Ferric chloride-induced murine carotid arterial injury: A model of redox pathology. *Redox Biology*. 2013;1(1):50-55.

94. Eckly A, Hechler B, Freund M, et al. Mechanisms underlying FeCl3-induced arterial thrombosis. *Journal of Thrombosis and Haemostasis*. 2011;9(4):779-789.

95. Barr JD, Chauhan AK, Schaeffer GV, Hansen JK, Motto DG. Red blood cells mediate the onset of thrombosis in the ferric chloride murine model. *Blood*. 2013;121(18):3733-3741.

96. Massberg S, Gawaz M, Grüner S, et al. A Crucial Role of Glycoprotein VI for Platelet Recruitment to the Injured Arterial Wall In Vivo. *The Journal of Experimental Medicine*. 2003;197(1):41-49.

97. Renné T, Pozgajová M, Grüner S, et al. Defective thrombus formation in mice lacking coagulation factor XII. *The Journal of Experimental Medicine*. 2005;202(2):271-281.

98. Sachs UJH, Nieswandt B. In Vivo Thrombus Formation in Murine Models. *Circulation Research*. 2007;100(7):979-991.

99. Walther DJ, Peter JU, Bashammakh S, et al. Synthesis of serotonin by a second tryptophan hydroxylase isoform. *Science*. 2003;299(5603):76.

100. New AS, Gelernter J, Yovell Y, et al. Tryptophan hydroxylase genotype is associated with impulsive-aggression measures: a preliminary study. *American Journal of Medical Genetics*. 1998;81(1):13-17.

101. Jun SE, Kohen R, Cain KC, Jarrett ME, Heitkemper MM. TPH gene polymorphisms are associated with disease perception and quality of life in women with irritable bowel syndrome. *Biol Res Nurs*. 2014;16(1):95-104.

102. Paterson DS, Hilaire G, Weese-Mayer DE. Medullary Serotonin Defects and Respiratory Dysfunction in Sudden Infant Death Syndrome. *Respiratory physiology & neurobiology*. 2009;168(1-2):133-143.

103. Fehr C, Schleicher A, Szegedi A, et al. Serotonergic polymorphisms in patients suffering from alcoholism, anxiety disorders and narcolepsy. *Prog Neuropsychopharmacol Biol Psychiatry*. 2001;25(5):965-982.

104. Duerschmied D, Suidan GL, Demers M, et al. Platelet serotonin promotes the recruitment of neutrophils to sites of acute inflammation in mice. *Blood*. 2013;121(6):1008-1015.

105. Suidan GL, Duerschmied D, Dillon GM, et al. Lack of tryptophan hydroxylase-1 in mice results in gait abnormalities. *PLoS One*. 2013;8(3):e59032.

106. Savage JS, Williams CM, Konopatskaya O, Hers I, Harper MT, Poole AW. Munc13-4 is critical for thrombosis through regulating release of ADP from platelets. *Journal of Thrombosis and Haemostasis*. 2013;11(4):771-775.

107. Stegner D, Deppermann C, Kraft P, et al. Munc13-4-mediated secretion is essential for infarct progression but not intracranial hemostasis in acute stroke. *Journal of Thrombosis and Haemostasis*. 2013;11(7):1430-1433.

108. Deppermann C, Cherpokova D, Nurden P, et al. Gray platelet syndrome and defective thrombo-inflammation in Nbeal2-deficient mice. *The Journal of Clinical Investigation*. 2013;123(8):3331-3342.

109. Golebiewska EM, Poole AW. Platelet secretion: From haemostasis to wound healing and beyond. *Blood Rev*. 2015;29(3):153-162.

110. Guerrero JA, Bennett C, van der Weyden L, et al. Gray platelet syndrome: proinflammatory megakaryocytes and alpha-granule loss cause myelofibrosis and confer metastasis resistance in mice. *Blood*. 2014;124(24):3624-3635.

111. Visser D, Middelbeek J, van Leeuwen FN, Jalink K. Function and regulation of the channel-kinase TRPM7 in health and disease. *European Journal of Cell Biology*. 2014;93(10–12):455-465.

112. Kaitsuka T, Katagiri C, Beesetty P, et al. Inactivation of TRPM7 kinase activity does not impair its channel function in mice. *Scientific Reports*. 2014;4:5718.

113. Jin J, Desai BN, Navarro B, Donovan A, Andrews NC, Clapham DE. Deletion of Trpm7 Disrupts Embryonic Development and Thymopoiesis Without Altering Mg(2+) Homeostasis. *Science (New York, NY)*. 2008;322(5902):756-760.

114. Ryazanova LV, Rondon LJ, Zierler S, et al. TRPM7 is essential for Mg2+ homeostasis in mammals. *Nat Commun*. 2010;1:109.

115. Middelbeek J, Clark K, Venselaar H, Huynen MA, van Leeuwen FN. The alpha-kinase family: an exceptional branch on the protein kinase tree. *Cellular and Molecular Life Sciences*. 2010;67(6):875-890.

116. Clark K, Langeslag M, van Leeuwen B, et al. TRPM7, a novel regulator of actomyosin contractility and cell adhesion. *Embo j*. 2006;25(2):290-301.

117. Ryazanova LV, Hu Z, Suzuki S, Chubanov V, Fleig A, Ryazanov AG. Elucidating the role of the TRPM7 alpha-kinase: TRPM7 kinase inactivation leads to magnesium deprivation resistance phenotype in mice. *Scientific Reports*. 2014;4:7599.

118. Matsushita M, Kozak JA, Shimizu Y, et al. Channel function is dissociated from the intrinsic kinase activity and autophosphorylation of TRPM7/ChaK1. *J Biol Chem*. 2005;280(21):20793-20803.

119. Li F-Y, Chaigne-Delalande B, Su H, Uzel G, Matthews H, Lenardo MJ. XMEN disease: a new primary immunodeficiency affecting Mg(2+) regulation of immunity against Epstein-Barr virus. *Blood*. 2014;123(14):2148-2152.

120. Trapani V, Shomer N, Rajcan-Separovic E. The role of MAGT1 in genetic syndromes. *Magnesium research*. 2015;28(2):46-55.

121. Li F-Y, Lenardo MJ, Chaigne-Delalande B. Loss of MAGT1 abrogates a Mg(2+) flux required for T cell signaling and leads to a novel human primary immunodeficiency. *Magnesium research : official organ of the International Society for the Development of Research on Magnesium*. 2011;24(3):S109-S114.

122. Zhou H, Clapham DE. Mammalian MagT1 and TUSC3 are required for cellular magnesium uptake and vertebrate embryonic development. *Proceedings of the National Academy of Sciences*. 2009;106(37):15750-15755.

123. Shattil SJ, Kim C, Ginsberg MH. The final steps of integrin activation: the end game. *Nat Rev Mol Cell Biol*. 2010;11(4):288-300.

124. Stritt S, Wolf K, Lorenz V, et al. Rap1-GTP-interacting adaptor molecule (RIAM) is dispensable for platelet integrin activation and function in mice. *Blood*. 2015;125(2):219-222.

125. Watanabe N, Bodin L, Pandey M, et al. Mechanisms and consequences of agonist-induced talin recruitment to platelet integrin alphaIIbbeta3. *J Cell Biol*. 2008;181(7):1211-1222.

126. Han J, Lim CJ, Watanabe N, et al. Reconstructing and Deconstructing Agonist-Induced Activation of Integrin αIIbβ3. *Current Biology*. 2006;16(18):1796-1806.

127. Bergmeier W, Rackebrandt K, Schroder W, Zirngibl H, Nieswandt B. Structural and functional characterization of the mouse von Willebrand factor receptor GPIb-IX with novel monoclonal antibodies. *Blood*. 2000;95(3):886-893.

128. Nieswandt B, Echtenacher B, Wachs FP, et al. Acute systemic reaction and lung alterations induced by an antiplatelet integrin gpIIb/IIIa antibody in mice. *Blood*. 1999;94(2):684-693.

129. Nieswandt B, Bergmeier W, Rackebrandt K, Gessner JE, Zirngibl H. Identification of critical antigen-specific mechanisms in the development of immune thrombocytopenic purpura in mice. *Blood*. 2000;96(7):2520-2527.

130. May F, Hagedorn I, Pleines I, et al. CLEC-2 is an essential platelet-activating receptor in hemostasis and thrombosis. *Blood*. 2009;114(16):3464-3472.

131. Nieswandt B, Bergmeier W, Schulte V, Rackebrandt K, Gessner JE, Zirngibl H. Expression and function of the mouse collagen receptor glycoprotein VI is strictly dependent on its association with the FcRgamma chain. *J Biol Chem*. 2000;275(31):23998-24002.

132. Bergmeier W, Schulte V, Brockhoff G, Bier U, Zirngibl H, Nieswandt B. Flow cytometric detection of activated mouse integrin alphaIIbbeta3 with a novel monoclonal antibody. *Cytometry*. 2002;48(2):80-86.

133. Kuijpers MJ, Schulte V, Bergmeier W, et al. Complementary roles of glycoprotein VI and alpha2beta1 integrin in collagen-induced thrombus formation in flowing whole blood ex vivo. *FASEB J*. 2003;17(6):685-687.

134. Schulte V, Rabie T, Prostredna M, Aktas B, Gruner S, Nieswandt B. Targeting of the collagen-binding site on glycoprotein VI is not essential for in vivo depletion of the receptor. *Blood*. 2003;101(10):3948-3952.

135. Bergmeier W, Bouvard D, Eble JA, et al. Rhodocytin (aggretin) activates platelets lacking alpha(2)beta(1) integrin, glycoprotein VI, and the ligand-binding domain of glycoprotein Ibalpha. *J Biol Chem*. 2001;276(27):25121-25126.

136. Bengel D, Murphy DL, Andrews AM, et al. Altered brain serotonin homeostasis and locomotor insensitivity to 3, 4-methylenedioxymethamphetamine ("Ecstasy") in serotonin transporter-deficient mice. *Mol Pharmacol*. 1998;53(4):649-655.

137. Walther DJ, Peter J-U, Bashammakh S, et al. Synthesis of Serotonin by a Second Tryptophan Hydroxylase Isoform. *Science*. 2003;299(5603):76.

138. Vanschoonbeek K, Feijge MA, Van Kampen RJ, et al. Initiating and potentiating role of platelets in tissue factor-induced thrombin generation in the presence of plasma: subject-dependent variation in thrombogram characteristics. *J Thromb Haemost*. 2004;2(3):476-484.

139. Hemker HC, Giesen P, Al Dieri R, et al. Calibrated automated thrombin generation measurement in clotting plasma. *Pathophysiol Haemost Thromb*. 2003;33(1):4-15.

140. Schuhmann MK, Kraft P, Stoll G, et al. CD28 superagonist-mediated boost of regulatory T cells increases thrombo-inflammation and ischemic neurodegeneration during the acute phase of experimental stroke. *Journal of Cerebral Blood Flow and Metabolism*. 2015;35(1):6-10.

141. Kleinschnitz C, Pozgajova M, Pham M, Bendszus M, Nieswandt B, Stoll G. Targeting platelets in acute experimental stroke: impact of glycoprotein Ib, VI, and IIb/IIIa blockade on infarct size, functional outcome, and intracranial bleeding. *Circulation*. 2007;115(17):2323-2330.

142. Bederson JB, Pitts LH, Tsuji M, Nishimura MC, Davis RL, Bartkowski H. Rat middle cerebral artery occlusion: evaluation of the model and development of a neurologic examination. *Stroke*. 1986;17(3):472-476.

143. Wolf K, Braun A, Haining EJ, et al. Partially Defective Store Operated Calcium Entry and Hem(ITAM) Signaling in Platelets of Serotonin Transporter Deficient Mice. *PLoS One*. 2016;11(1):e0147664.

144. Qi R, Ozaki Y, Satoh K, et al. Quantitative measurement of various 5-HT receptor antagonists on platelet activation induced by serotonin. *Thromb Res*. 1996;81(1):43-54.

145. Carneiro AM, Cook EH, Murphy DL, Blakely RD. Interactions between integrin alphaIIbbeta3 and the serotonin transporter regulate serotonin transport and platelet aggregation in mice and humans. *J Clin Invest*. 2008;118(4):1544-1552.

146. Serebruany VL, Glassman AH, Malinin AI, et al. Selective serotonin reuptake inhibitors yield additional antiplatelet protection in patients with congestive heart failure treated with antecedent aspirin. *European Journal of Heart Failure*. 2003;5(4):517-521.

147. Dale GL, Friese P, Batar P, et al. Stimulated platelets use serotonin to enhance their retention of procoagulant proteins on the cell surface. *Nature*. 2002;415(6868):175-179.

148. Mazepa M, Hoffman M, Monroe D. Superactivated platelets: thrombus regulators, thrombin generators, and potential clinical targets. *Arterioscler Thromb Vasc Biol*. 2013;33(8):1747-1752.

149. Dale GL. Coated-platelets: an emerging component of the procoagulant response. *J Thromb Haemost*. 2005;3(10):2185-2192.

150. Prodan CI, Joseph PM, Vincent AS, Dale GL. Coated-platelets in ischemic stroke: differences between lacunar and cortical stroke. *J Thromb Haemost*. 2008;6(4):609-614.

151. Szasz R, Dale GL. Thrombospondin and fibrinogen bind serotonin-derivatized proteins on COAT-platelets. *Blood*. 2002;100(8):2827-2831.

152. de Aguiar Matos JA, Borges FP, Tasca T, et al. Characterisation of an ATP diphosphohydrolase (Apyrase, EC 3.6.1.5) activity in Trichomonas vaginalis. *Int J Parasitol*. 2001;31(8):770-775.

153. Richardson A, Taylor CW. Effects of Ca2+ chelators on purified inositol 1,4,5-trisphosphate (InsP3) receptors and InsP3-stimulated Ca2+ mobilization. *Journal of Biological Chemistry*. 1993;268(16):11528-11533.

154. Weigert G, Berisha F, Resch H, Karl K, Schmetterer L, Garhofer G. Effect of unspecific inhibition of cyclooxygenase by indomethacin on retinal and choroidal blood flow. *Invest Ophthalmol Vis Sci*. 2008;49(3):1065-1070.

155. Tucker KL, Sage T, Gibbins JM. Clot retraction. *Methods Mol Biol*. 2012;788:101-107.

156. Mackman N, Tilley RE, Key NS. Role of the extrinsic pathway of blood coagulation in hemostasis and thrombosis. *Arterioscler Thromb Vasc Biol*. 2007;27(8):1687-1693.

157. Davie EW, Ratnoff OD. Waterfall Sequence for Intrinsic Blood Clotting. *Science*. 1964;145(3638):1310-1312.

158. Macfarlane RG. An Enzyme Cascade in the Blood Clotting Mechanism, and Its Function as a Biochemical Amplifier. *Nature*. 1964;202:498-499.

159. Heemskerk JWM, Mattheij NJA, Cosemans JMEM. Platelet-based coagulation: different populations, different functions. *Journal of Thrombosis and Haemostasis*. 2013;11(1):2-16.

160. Bender M, Hagedorn I, Nieswandt B. Genetic and antibody-induced glycoprotein VI deficiency equally protects mice from mechanically and FeCl3-induced thrombosis. *Journal of Thrombosis and Haemostasis*. 2011;9(7):1423-1426.

161. Espinera AR, Ogle ME, Gu X, Wei L. Citalopram enhances neurovascular regeneration and sensorimotor functional recovery after ischemic stroke in mice. *Neuroscience*. 2013;247:1-11.

162. McFarlane A, Kamath MV, Fallen EL, Malcolm V, Cherian F, Norman G. Effect of sertraline on the recovery rate of cardiac autonomic function in depressed patients after acute myocardial infarction. *Am Heart J*. 2001;142(4):617-623.

163. Mead GE, Hsieh CF, Lee R, et al. Selective serotonin reuptake inhibitors (SSRIs) for stroke recovery. *Cochrane Database Syst Rev*. 2012;11:Cd009286.

164. Eming SA, Krieg T, Davidson JM. Inflammation in Wound Repair: Molecular and Cellular Mechanisms. *J Invest Dermatol*. 2006;127(3):514-525.

165. Pamuklar Z, Federico L, Liu S, et al. Autotaxin/lysopholipase D and lysophosphatidic acid regulate murine hemostasis and thrombosis. *J Biol Chem*. 2009;284(11):7385-7394.

166. Goytain A, Quamme G. Identification and characterization of a novel mammalian Mg2+ transporter with channel-like properties. *BMC Genomics*. 2005;6(1):1-18.

167. Lafuente EM, van Puijenbroek AA, Krause M, et al. RIAM, an Ena/VASP and Profilin ligand, interacts with Rap1-GTP and mediates Rap1-induced adhesion. *Dev Cell*. 2004;7(4):585-595.

168. Lee HS, Lim CJ, Puzon-McLaughlin W, Shattil SJ, Ginsberg MH. RIAM activates integrins by linking talin to ras GTPase membrane-targeting sequences. *J Biol Chem*. 2009;284(8):5119-5127.

169. Calverley DC, Roth GJ. ANTIPLATELET THERAPY: Aspirin, Ticlopidine/Clopidogrel, and Anti-Integrin Agents. *Hematology/Oncology Clinics of North America*. 1998;12(6):1231-1249.

170. Estevez B, Shen B, Du X. Targeting integrin and integrin signaling in treating thrombosis. *Arterioscler Thromb Vasc Biol*. 2015;35(1):24-29.

171. Ziu E, Mercado CP, Li Y, et al. Down-regulation of the serotonin transporter in hyperreactive platelets counteracts the pro-thrombotic effect of serotonin. *J Mol Cell Cardiol*. 2012;52(5):1112-1121.

172. Sauer WH, Berlin JA, Kimmel SE. Selective Serotonin Reuptake Inhibitors and Myocardial Infarction. *Circulation*. 2001;104(16):1894-1898.

173. Frankhauser P, Grimmer Y, Bugert P, Deuschle M, Schmidt M, Schloss P. Characterization of the neuronal dopamine transporter DAT in human blood platelets. *Neurosci Lett*. 2006;399(3):197-201.

174. Schmitt A, Benninghoff J, Moessner R, et al. Adult neurogenesis in serotonin transporter deficient mice. *Journal of neural transmission*. 2007;114(9):1107-1119.

175. Tseng YL, Chiang ML, Huang TF, Su KP, Lane HY, Lai YC. A selective serotonin reuptake inhibitor, citalopram, inhibits collagen-induced platelet aggregation and activation. *Thromb Res*. 2010;126(6):517-523.

176. Pavanetto M, Zarpellon A, Borgo C, Donella-Deana A, Deana R. Regulation of serotonin transport in human platelets by tyrosine kinase Syk. *Cell Physiol Biochem*. 2011;27(2):139-148.

177. Pavanetto M, Zarpellon A, Borgo C, Donella-Deana A, Deana R. Regulation of Serotonin Transport in Human Platelets by Tyrosine Kinase Syk. *Cellular Physiology and Biochemistry*. 2011;27(2):139-148.

178. Braun A, Vogtle T, Varga-Szabo D, Nieswandt B. STIM and Orai in hemostasis and thrombosis. *Front Biosci (Landmark Ed)*. 2011;16:2144-2160.

179. Offermanns S, Toombs CF, Hu YH, Simon MI. Defective platelet activation in G alpha(q)-deficient mice. *Nature*. 1997;389(6647):183-186.

180. Stegner D, Deppermann C, Kraft P, et al. Munc13-4-mediated secretion is essential for infarct progression but not intracranial hemostasis in acute stroke. *Journal of thrombosis and haemostasis : JTH*. 2013;11(7):1430-1433.

181. Watts SW. Serotonin-induced contraction in mesenteric resistance arteries: signaling and changes in deoxycorticosterone acetate-salt hypertension. *Hypertension*. 2002;39(3):825-829.

182. Watts SW, Morrison SF, Davis RP, Barman SM. Serotonin and blood pressure regulation. *Pharmacol Rev*. 2012;64(2):359-388.

183. Canan F, Ataoglu A. The effect of escitalopram on platelet activity. *Thromb Res*. 2011;127(1):57.

184. Hallback I, Hagg S, Eriksson AC, Whiss PA. In vitro effects of serotonin and noradrenaline reuptake inhibitors on human platelet adhesion and coagulation. *Pharmacol Rep*. 2012;64(4):979-983.

185. Wester P, Dietrich WD, Prado R, Watson BD, Globus MY. Serotonin release into plasma during common carotid artery thrombosis in rats. *Stroke*. 1992;23(6):870-875.

186. Asada M, Ebihara S, Yamanda S, et al. Depletion of serotonin and selective inhibition of 2B receptor suppressed tumor angiogenesis by inhibiting endothelial nitric oxide synthase and extracellular signal-regulated kinase 1/2 phosphorylation. *Neoplasia*. 2009;11(4):408-417.

187. Hankey GJ. Selective serotonin reuptake inhibitors and risk of cerebral bleeding. *Stroke*. 2014;45(7):1917-1918.

188. Ziu E, Mercado CP, Li Y, et al. Down-regulation of the serotonin transporter in hyperreactive platelets counteracts the pro-thrombotic effect of serotonin. *Journal of molecular and cellular cardiology*. 2012;52(5):1112-1121.

189. Sander K. SD. Depression and psychological distress as risk factors for stroke and worse stroke recovery: clinical implications and therapeutic options. *EMJ Neurol*. 2014;1:53-58.

190. Ungerer M, Rosport K, Bultmann A, et al. Novel antiplatelet drug revacept (Dimeric Glycoprotein VI-Fc) specifically and efficiently inhibited collagen-induced platelet aggregation without affecting general hemostasis in humans. *Circulation*. 2011;123(17):1891-1899.

191. Linder AE, Diaz J, Ni W, Szasz T, Burnett R, Watts SW. Vascular reactivity, 5-HT uptake, and blood pressure in the serotonin transporter knockout rat. *Am J Physiol Heart Circ Physiol*. 2008;294(4):H1745-1752.

192. Calama E, Fernandez MM, Moran A, Martin ML, San Roman L. Vasodilator and vasoconstrictor responses induced by 5-hydroxytryptamine in the in situ blood autoperfused hindquarters of the anaesthetized rat. *Naunyn Schmiedebergs Arch Pharmacol*. 2002;366(2):110-116.

193. Vanhoutte PM. Platelet-derived serotonin, the endothelium, and cardiovascular disease. *J Cardiovasc Pharmacol*. 1991;17 Suppl 5:S6-12.

194. Van Nueten JM. Serotonin and the blood vessel wall. *J Cardiovasc Pharmacol*. 1985;7 Suppl 7:S49-51.

195. Vanhoutte PM. Serotonin and the vascular wall. *Int J Cardiol*. 1987;14(2):189-203.

196. Vanhoutte PM. Serotonin and the blood-vessel wall. *J Hypertens Suppl*. 1986;4(5):S112-115.

197. Welsh JD, Stalker TJ, Voronov R, et al. A systems approach to hemostasis: 1. The interdependence of thrombus architecture and agonist movements in the gaps between platelets. *Blood*. 2014;124(11):1808-1815.

198. Kawut SM, Horn EM, Berekashvili KK, et al. Selective serotonin reuptake inhibitor use and outcomes in pulmonary arterial hypertension. *Pulmonary Pharmacology & Therapeutics*. 2006;19(5):370-374.

199. Toh S, Mitchell AA, Louik C, Werler MM, Chambers CD, Hernández-Díaz S. Selective Serotonin Reuptake Inhibitor Use and Risk of Gestational Hypertension. *American Journal of Psychiatry*. 2009;166(3):320-328.

200. Soll C, Jang JH, Riener MO, et al. Serotonin promotes tumor growth in human hepatocellular cancer. *Hepatology*. 2010;51(4):1244-1254.

201. Shajib MS, Khan WI. The role of serotonin and its receptors in activation of immune responses and inflammation. *Acta Physiol (Oxf)*. 2015;213(3):561-574.

202. Mann DA, Oakley F. Serotonin paracrine signaling in tissue fibrosis. *Biochim Biophys Acta*. 2013;1832(7):905-910.

203. Deppermann C. The role of platelet granules in thrombosis, hemostasis, stroke and inflammation. Biomedicine. Vol. Doctoral degree: University Würzburg; 2015:117.

204. Nieswandt B, Watson SP. Platelet-collagen interaction: is GPVI the central receptor? Vol. 102; 2003.

205. Shechter M, Merz CN, Rude RK, et al. Low intracellular magnesium levels promote platelet-dependent thrombosis in patients with coronary artery disease. *Am Heart J*. 2000;140(2):212-218.

206. Hornyak M, Voderholzer U, Hohagen F, Berger M, Riemann D. Magnesium therapy for periodic leg movements-related insomnia and restless legs syndrome: an open pilot study. *Sleep*. 1998;21(5):501-505.

207. Sinniah D. Magnesium deficiency: a possible cause of restless leg syndrome in haemodialysis patients. *Internal Medicine Journal*. 2015;45(4):467-468.

208. Altura BM, Altura BT. Tension headaches and muscle tension: is there a role for magnesium? *Med Hypotheses*. 2001;57(6):705-713.

209. Durlach J, Collery P. Magnesium and potassium in diabetes and carbohydrate metabolism. Review of the present status and recent results. *Magnesium*. 1984;3(4-6):315-323.

210. Vormann J, Magdorf K, Gunther T, Wahn U. Increased Na+/Mg2+ antiport in erythrocytes of patients with cystic fibrosis. *Eur J Clin Chem Clin Biochem*. 1994;32(11):833-836.

211. Kisters K, Korner J, Louwen F, et al. Plasma and membrane Ca2+ and Mg2+ concentrations in normal pregnancy and in preeclampsia. *Gynecol Obstet Invest*. 1998;46(3):158-163.

212. Welch KM, D'Andrea G, Tepley N, Barkley G, Ramadan NM. The concept of migraine as a state of central neuronal hyperexcitability. *Neurologic clinics*. 1990;8(4):817-828.

213. Westermaier T, Stetter C, Vince GH, et al. Prophylactic intravenous magnesium sulfate for treatment of aneurysmal subarachnoid hemorrhage: A randomized,

placebo-controlled, clinical study*. *Critical Care Medicine*. 2010;38(5):1284-1290.

214. Roden DM. Magnesium treatment of ventricular arrhythmias. *The American Journal of Cardiology*. 1989;63(14):G43-G46.

215. Deason-Towne F, Perraud A-L, Schmitz C. The Mg(2+) transporter MagT1 partially rescues cell-growth and Mg(2+) uptake in cells lacking the channel-kinase TRPM7. *FEBS letters*. 2011;585(14):2275-2278.

216. Deason-Towne F, Perraud AL, Schmitz C. Identification of Ser/Thr phosphorylation sites in the C2-domain of phospholipase C gamma2 (PLCgamma2) using TRPM7-kinase. *Cell Signal*. 2012;24(11):2070-2075.

217. Runnels LW, Yue L, Clapham DE. The TRPM7 channel is inactivated by PIP(2) hydrolysis. *Nat Cell Biol*. 2002;4(5):329-336.

218. Schmitz C, Perraud A-L, Johnson CO, et al. Regulation of Vertebrate Cellular Mg2+ Homeostasis by TRPM7. *Cell*;114(2):191-200.

219. Chen W. Studies on the role of calcium channels and the kinase domain of transient receptor potential melastatin-like 7 (TRPM7) in platelet function Biomedicine. Vol. Doctoral degree: University Würzburg; 2014:117.

220. Sheu JR, Hsiao G, Shen MY, et al. Mechanisms involved in the antiplatelet activity of magnesium in human platelets. *Br J Haematol*. 2002;119(4):1033-1041.

221. Stefanini L, Ye F, Snider AK, et al. A talin mutant that impairs talin-integrin binding in platelets decelerates alphaIIbbeta3 activation without pathological bleeding. *Blood*. 2014;123(17):2722-2731.

222. Klapproth S, Sperandio M, Pinheiro EM, et al. Loss of the Rap1 effector RIAM results in leukocyte adhesion deficiency due to impaired β2 integrin function in mice. *Blood*. 2015;126(25):2704-2712.

223. Calderwood DA. The Rap1-RIAM pathway prefers β2 integrins. *Blood*. 2015;126(25):2658-2659.

7. Appendix

List of figures

List of tables

Abbreviations

abbreviation	name
(hem)ITAM	(hem)Immunoreceptor tyrosine-based activation motif
$[Ca^{2+}]_i$	Intracellular calcium concentration
°C	Degree Celsius
5-HIAA	5-hydroxyindole acetic acid
5-HIAL	5-hydroxyindole acetaldehyde
5-HT	5-hydroxytryptamine, Serotonin
$5\text{-}HT_{2A}$	Serotonin receptor
5-HTP	5-hydroxytryptophan
5Htt/SERT	Serotonin transporter
AA	Arachidonic acid
AC	Adenylate cyclase
ADP	Adenosine diphosphate
ALDH	Aldehyde dehydrogenase
APS	Ammonium persulfate
AT	Antithrombin
ATP	Adenosine triphosphate
BCR	B cell receptor
BM	Bone marrow
BSA	Bovine serum albumin
CalDAG-GEFI	Calcium diacylglycerol guanine nucleotide exchange factor I
CaM	Calmodulin
cAMP	Cyclic adenosine monophosphate
CLEC-2	C-type lectin-like receptor-2
COAT	Collagen and thrombin activated platelets
CRAC	Calcium release-activated channel
CRP	Collagen-related peptide
CVX	Convulxin
DAG	Diacylglycerol
DAT	Dopamine receptor
DDC	L-aromatic amino acid decarboxylase
ddH_2O	Double-distilled water

DIC	Differential interference contrast
Dko	Double knock-out
DMSO	Dimethylsulfoxide
DNA	Deoxyribonucleic acid
DTS	Dense tubular system
EA	Ellagic acid
EBV	Epstein Barr virus
ECL	Enhanced chemiluminescence
ECM	Extracellular matrix
EDRF	Endothelium-derived relaxing factors
ELISA	Enzyme-linked immune absorbance assay
ER	Endoplasmatic reticulum
et al.	*et alteri*
FACS	Fluorescence-activated cell sorting
FcR	Fc-receptor
$FeCl_3$	Ferric(III)chloride
Fg	Fibrinogen
FITC	Fluorescein isothiocynate
FSC	Forward scatter
GAP	GTPase-activating protein
GDP	Guanosine diphosphate
GEF	Guanine nucleotide exchange factor
GI	Gastrointestinal tract
GP	Glycoprotein
GPCR(s)	G protein-coupled receptor(s)
GPS	Gray platelet syndrome
GTP	Guanosine triphosphate
h	Hour
HCT	Hematocrit value
HE	Hematoxylin-eosin
Het	*Heterozygous*
HGB	Hemoglobin
HRP	Horse radish peroxidase

i.p.	intraperitoneally
i.v.	Intravenously
IFI	Integrated fluorescence intensity
Ig	Immunoglobulin
IP_1	Inositol-mono-phosphate
IP_3	Inositol-1,4,5-triphosphate
IP_3R	Inositol-1,4,5-triphosphate receptor
ITAM	Immunoreceptor tyrosine-based activation motif
ITIM	Immunoreceptor tyrosine-inhibition motif
kbp	Kilo base pair
kDa	Kilo Dalton
Ko	*Knock-out*
Lat	Linker for activation of T cells
mAb	Monoclonal antibody
MAO	Monoamine oxidase
MAOI	Monoamine oxidase inhibitor
MFI	Mean fluorescence intensity
MI	Myocardial infarction
MK(s)	Megakaryocyte(s)
MP	Microparticle
MPV	Mean platelet volume
mRNA	messenger RNA
n.d.	not detectable
n.s.	not significant
NaCl	Sodium chloride
NBEAL2	Neurobeachin-like 2
NET	Norepinephrine receptor
OCS	Open canalicular system
OCT	Organic cation transporter
PAR	Protease-activated receptor
PBS	Phosphate buffered saline
PCR	Polymerase chain reaction
PE	Phycoerythrin

PFA	Paraformaldehyde
PGI_2	Prostacyclin
PH	phosphadydrolase enzyme
PI_3K	Phosphatidylinositol-3-kinase
PIP_2	Phosphatidylinositol-4,5-bisphsphate
PIP_3	Phosphatidylinositol-3,4,5-trisphosphate
PKC	Protein kinase C
PLC	Phospholipase C
PLT	Platelet
PM	Plasma membrane
PPP	Platelet-poor plasma
PRP	Platelet-rich plasma
PS	Phosphatidylserine
PTP	Protein-tyrosine phosphatases
PTT	Partial thromboplastin time
PVDF	Polyvinylidene fluoride
RBC	Red blood cell
Rest.	Resting
Rhd	Rhodocytin
RhoA	Ras homolog gene family member A
RIAM	Rap1-interaction adapter molecule
RNA	Ribonucleic acid
ROC	Receptor-operated Ca^{2+}
ROCE	Receptor-operated calcium entry
rpm	Revolutions per minute
RT	Room temperature
SD	Standard deviation
SDS	Sodium dodecylsulfate
SFK	Src family kinase
SNARE	soluble N-ethylmaleimide-sensitive-factor attachment receptor
SOC	Store-operated Ca^{2+}
SOCE	Store-operated calcium entry
SSC	Side scatter

SSRI	Selective serotonin reuptake inhibitors
STIM	Stromal interaction molecule
Syk	Spleen tyrosine kinase
TAE	TRIS acetate EDTA buffer
TBS	TRIS-buffered saline
TCA	Tricyclic antidepressants
TCR	T cell receptor
TE	TRIS EDTA buffer
TF	Tissue factor
TG	Thapsigargin/ transgluataminase
Thr	Thrombin
tMCAO	Transient middle cerebral artery occlusion
TP	thromboxane-prostanoid
TPH	L-tryptophan hydroxylase
TRIS	Tris (hydroxymethyl) aminomethane
TRPC	Canonical transient receptor potential channel
TRPM	Transient receptor potential cation channel superfamily M
TTC	Triphenyltetrazolium chloride
TxA_2	Thromboxane A_2
U46	U46619
VMAT	Vesicular monoamine transporter
vWF	von Willebrand factor
WBC	White blood cells
Wt	*Wild-type*
XMEN	X linked immunodeficiency with magnesium defect, Epstein Barr virus and neoplasia disease

7.1. Publications

7.1.1. Articles

Stritt S., **K. Wolf**, V. Lorenz, T. Vogtle, S. Gupta, M. R. Bosl, and B. Nieswandt, 2015, Rap1-GTP-interacting adaptor molecule (RIAM) is dispensable for platelet integrin activation and function in mice: Blood, v. 125, p. 219-22.

Wolf K., A. Braun, E. J. Haining, Y. L. Tseng, P. Kraft, M. K. Schuhmann, S. K. Gotru, W. Chen, H. M. Hermanns, G. Stoll, K. P. Lesch, and B. Nieswandt, 2016, Partially Defective Store Operated Calcium Entry and Hem(ITAM) Signaling in Platelets of Serotonin Transporter Deficient Mice: PLoS One, v. 11, p. e0147664.

7.1.1. Oral presentation

GTH, 59th Annual Meeting of the Society of Thrombosis and Hemostasis Research, Düsseldorf, Feb. 2015	The role of platelet serotonin in thrombosis and ischemic stroke

7.1.2. Poster presentations

GSLS, 9th International PhD Symposia EUREKA 2014, Würzburg, Oct. 2014	The physiological role of platelet serotonin in thrombosis and hemostasis
GSLS, 10th International PhD Symposia EUREKA 2014, Würzburg, Oct. 2015	Partially defective SOCE and hem(ITAM) signaling in platelets of *5Htt*$^{-/-}$ mice

7.2. Curriculum Vitae

7.3. Acknowledgements

This thesis was accomplished in the group of Prof. Dr. Bernhard Nieswandt at the Department of Experimental Biomedicine-Vascular Medicine, University Hospital and Rudolf Virchow Center for Experimental Biomedicine, University Würzburg. I would like to thank all the people, who helped and supported me during my PhD work (July 2013-February 2016):

Prof. Dr. Bernhard Nieswandt for giving me the opportunity to perform my PhD in his laboratory and for the opportunity to present my work at international conferences and symposia.

Prof. Dr. Alma Zernecke-Madsen and Prof. Dr. Christoph Kleinschnitz for helpful scientific discussions and for reviewing my thesis.

Prof. Dr. Guido Stoll, Dr. Peter Kraft, Dr. Michael Schuhmann and their team of the Department of Neurology for performing of the tMCAO experiment.

Dr. Attila Braun for his support and help to finish my PhD project.

Dr. Elizabeth Haining for her great help during the submission process of the paper, the constant support, the encouragement during the whole time and proofreading of my thesis.

Birgit Midloch for her technical assistance and genotyping of the genetically modified mice used for the thesis. A great thanks to all technical assistance for the good environment and the help, whenever needed.

Sarah Beck and Tano Marth for the thrombin generation assay.

Dr. Yu-Lun Tseng for starting the analysis of the mouse line (*5Htt*$^{-/-}$) and the citalopram experiments.

A great thanks to Dr. Elizabeth Haining, Dr. Attila Braun, Ayesha Baig, Dominic Faber, Kiran Sanjeev Gotru, Dr. Simon Stritt and Dr. Deya Cherpokowa for carefully proofreading my thesis.

Dr. Sabine Herterich for the measurements of the coagulation factors.

Dr. Heike Hermanns and Donata Dorbath for the experiment of the expression levels of coagulation factors in liver samples.

Dr. Klaus-Peter Lesch for providing the *5Htt*$^{-/-}$ mice. Dr. Daniel Dürschmied for supplying the *Tph1*$^{-/-}$ mice. Prof. Dr. T. Gudermann and Dr. V. Chubanov for the *Trpm7*$^{fl/fl\text{-}Pf4Cre}$ and *Trpm7*^{KI} mice.

The animal caretakers, who kept the animal facility running.

All current and former members of the laboratory for the support, the discussions and the enjoyable working atmosphere.

Finally, I would like to thank my life partner, who was always on my side and supported me in good and especially in bad times. My family, as well as my “parents-in-law” and my friends for the continuous encouragement and patience.

Affidavit

I hereby confirm that my thesis entitled „ Studies on the role of platelet serotonin in platelet function, hemostasis, thrombosis and stroke“, is the result of my own work. I did not receive any help or support from commercial consultants. All sources and/or materials applied are listed and specified in the thesis.

Furthermore, I confirm that this thesis has not yet been submitted as part of another examination process neither in identical nor in similar form.

Eidesstattliche Erklärung

Hiermit erkläre ich an Eides statt, die Dissertation „Studien zur Rolle des Serotonins aus Thrombozyten für die Thrombozytenfunktion, Hämostase, Thrombose und Schlaganfall“ eigenhändig, d.h. insbesondere selbstständig und ohne Hilfe eines professionellen Promotionsberaters, angefertigt und keine anderen als die von mir angegebenen Quellen und Hilfsmittel verwendet zu haben.

Ich erkläre außerdem, dass die Dissertation weder in gleicher noch in ähnlicher Form bereits in einem anderen Prüfungsverfahren vorgelegen hat.

Würzburg, _____ _____

Unterschrift/signature